

Digital Electronic Predistortion for Optical Communications

Robert Waegemans

*Submitted to University College London for the degree of
Doctor of Philosophy*

*Department of Electronic and Electrical Engineering
University College London
October 2009*

I, Robert Waagemans, confirm that the work presented in this thesis is my own. Where information has been derived from other sources, I confirm that this has been indicated in the thesis.

Acknowledgements

Above all I have to thank my primary supervisor Dr. Robert Killey, firstly for making it possible for me to do the studies related to this thesis. He accepted me being aware of my limited academic background. In addition he secured the necessary funds and assignments giving me the option to interrupt my industrial career. But foremost for always supporting me in my research and believing in the progress that was made.

I also received much support from the Optical Networks group at UCL. I have to mention by name my second supervisor Prof. Polina Bayvel whose dedication makes it possible to have such an excellent research group at UCL. Special thanks also to Dr. Phil Watts. I was only capable of achieving the goals in this work because I could build upon his earlier research. The same thanks are for everyone who contributed to the ONG simulation toolbox giving me tools for my work and for many interesting discussions in the group.

From industry I need to mention the companies Ericsson and Intel. Both gave me the opportunity to have an intensive experience in industrial based R&D. At Ericsson I thank Dr. Stefan Herbst, for making it possible for me to work with cutting edge tools, and among many other things, for showing me how to differentiate between priorities. Also Ludwig Holbein for his master classes in digital design and all other members of the group for their inspiring discussions and advice, especially because they did spend all these efforts during difficult times at the plant in Backnang. From Micram I thank Dr. Tobias Ellermeyer for giving us access to state of the art digital to analogue converters.

At Intel, Dr. Madeline Glick made it possible for me to work, as one of the last before it closed, at the Intel research facilities in Cambridge.

Maybe less direct but at least as important was the support of my parents who did not see any issue in a son going back to university chasing an old dream.

Abstract

The distortion of optical signals has long been an issue limiting the performance of communication systems. With the increase of transmission speeds the effects of distortion are becoming more prominent. Because of this, the use of methods known from digital signal processing (DSP) are being introduced to compensate for them.

Applying DSP to improve optical signals has been limited by a discrepancy in digital signal processing speeds and optical transmission speeds. However high speed Field Programmable Gate Arrays (FPGA) which are sufficiently fast have now become available making DSP experiments without costly ASIC implementation possible for optical transmission experiments.

This thesis focuses on Look Up Table (LUT) based digital Electronic Predistortion (EPD) for optical transmission. Because it is only one out of many possible implementations of EPD, it has to be placed in context with other EPD techniques and other distortion combating techniques in general, especially since it is possible to combine the different techniques.

Building an actual transmitter means that compromises and decisions have to be made in the design and implementation of an EPD based system. These are based on balancing the desire to achieve optimal performance with technological and economic limitations. This is partly done using optical simulations to assess the performance.

This thesis describes a novel experimental transmitter that has been built as part of this research applying LUT based EPD to an optical signal. The experimental transmitter consists of a digital design (using a hardware description language) for a pair of FPGAs and an analogue optical/electronic setup including two standard DAC integrated circuits. The DSP in the transmitter compensated for both chromatic dispersion and self phase modulation.

We achieved transmission of 10.7 Gb/s non-return-to-zero (NRZ) signals with a +4 dBm launch power over 450 km keeping the required optical-signal-to-noise-ratio (OSNR) for a bit-error-rate of 2×10^{-3} below 11 dB. In doing so we showed experimentally, for the first time, that nonlinear effects can be compensated with this approach and that the combination of FPGA-DAC is a viable approach for an experimental setup.

Table of Contents

Acknowledgements.....	3
Abstract.....	4
List of Figures	9
List of Tables	11
Abbreviations and Acronyms.....	12
1 Introduction	18
1.1 An overview of this thesis.....	19
1.2 Original contributions	19
1.3 Publications related to this thesis.....	20
2 Overview of distortion and distortion compensation	22
2.1 Distortion of optical signals	22
2.1.1 Attenuation.....	23
2.1.2 Chromatic dispersion	24
2.1.3 Nonlinear effects.....	25
2.1.4 Polarization effects	26
2.1.5 Intermodal effects.....	27
2.1.6 Other effects	27
2.1.7 Combined effects	27
2.2 Where to counteract distortion.....	28
2.3 Distortion in non-optical transmission	30
2.4 Distortion in Radio over Fibre applications	31
2.5 Counteracting distortion in optical transmission	32
2.5.1 Coding techniques.....	32
2.5.2 Use of alternative fibre types.....	33
2.5.3 Optimised modulation formats.....	34
2.5.3.1 Intensity based modulation	36
2.5.3.2 Differential phase modulation	38
2.5.3.3 Intensity shaping.....	39
2.5.3.4 Single sideband (intensity shaping in frequency domain)	40
2.5.3.5 Phase shaping	41

2.5.3.6	Non-binary symbol coding	41
2.5.3.7	Multiplexing	42
2.5.4	Soliton pulses	43
2.5.5	Channel assignment in DWDM	43
2.5.6	Optical correction of the distortion	44
2.5.6.1	Dispersion Compensating Fibre	44
2.5.6.2	Distortion Compensating Devices	45
2.5.6.3	All-Optical Regeneration	45
2.5.6.4	Optical Phase Conjugation	46
2.5.7	Electrical Distortion Compensation	47
2.5.7.1	Electric-optical and optical-electrical conversion	47
2.5.7.2	Analog versus Digital Electronic techniques	52
2.5.7.3	FPGA versus ASIC	55
2.5.7.4	Tx versus Rx based electronic signal processing	60
2.5.7.5	Proposed digital signal processing blocks	63
2.5.7.6	Performance of electronic distortion compensation	64
2.5.7.7	Electronic regeneration	65
2.5.8	Combined approached	66
2.6	Summary	66
3	Digital Electronic Predistortion	67
3.1	Principle	67
3.2	Overview of published research	68
3.2.1	Proposing phase and intensity based predistortion	70
3.2.2	Non-linear effects in combination with EPD	70
3.2.3	Expanding EPD for other scenarios	71
3.2.4	Additional Implementation issues of EPD	72
3.3	Deterministic distortion	73
3.4	Offline versus real time signal processing	76
3.5	Defining the predistorted transmission signal	77
3.6	Inverse of the simplified NLSE function	79
3.7	Limited influence window and LUT build-up	81
3.8	Digitisation of predistorted signals	84
3.9	Selecting predistortion method (LUT versus FIR)	87
3.10	Controllable parameters and choice of modulator	92

3.11	Published expected performance of EPD	95
3.11.1	Fundamental limits of EPD systems.....	98
3.11.2	Implementation penalties.....	101
3.11.2.1	Penalties originating from numerical modelling.....	101
3.11.2.2	Penalties originating from the DSP	102
3.11.2.3	Penalties originating from the DAC.....	103
3.11.2.4	Penalties originating in the analogue part of transmitter	104
3.11.3	Other performance reports	104
3.12	Summary	105
4	Transmission simulation	106
4.1	Introduction to optical simulation	106
4.2	Simulation setup	107
4.3	Simulation results	112
4.3.1	Transmission without EPD	112
4.3.2	Non-Linear versus Dispersion only EPD	112
4.3.3	Deviation in power to detect NL compensation	114
4.3.4	Influence of sampling method to calculate LUT	115
4.4	Summary	117
5	An FPGA-based EPD Transmitter	118
5.1	Introduction	118
5.2	The Field Programmable Gate Array.....	121
5.3	DAC/MUX.....	123
5.4	Other components.....	124
5.5	Clocking.....	125
5.6	Operating principles.....	127
5.6.1	Parallel processing of data	130
5.6.2	Synchronisation.....	133
5.6.2.1	Port synchronisation	135
5.6.2.2	Arm synchronization	141
5.6.3	Conditioning of the analogue signals.....	144
5.7	FPGA Design.....	146
5.7.1	Design Overview	146
5.7.2	Details on HDL implementation.....	148
5.7.3	Resource utilisation.....	152

5.7.4	Timing Closure.....	156
5.8	Calculation of predistorted pulse shape.....	157
5.8.1	Calculating ideal optical predistorted signal.....	158
5.8.2	Calculating LUT entries & predistorted signal.....	159
5.9	Summary.....	162
6	Transmission results and analysis.....	163
6.1	Method.....	163
6.2	Linear transmission.....	165
6.3	Effects of suboptimal control parameters.....	170
6.4	Nonlinear transmission.....	174
6.5	Summary.....	177
7	Conclusions and future work.....	178
	Appendix A : An introduction to FPGAs.....	182
	Appendix B : Introduction to FPGA design.....	186
	References.....	191

List of Figures

Figure 1 : Dispersion effects on pulse train.	25
Figure 2 : General optical transmission link.....	29
Figure 3: Characteristics of NRZ-OOK.	37
Figure 4: Characteristics of DPSK	38
Figure 5: Characteristics of RZ.....	39
Figure 6: Spectrum of SSB or VSB signal.	40
Figure 7: Modulation techniques using phase shapping.	41
Figure 8: Modulation techniques using non-binary symbol coding.	42
Figure 9: Principle of Optical Phase Conjugation (OPC).....	46
Figure 10: Block diagrams of modulation setups for an optical transmitter.	49
Figure 11: Block diagrams of optical recievers.	51
Figure 12: Signal in optical reciever.	52
Figure 13: Principle of predistortion.	68
Figure 14: Performance versus distance.....	74
Figure 15: OPC as method to calculate predistorted signal.....	78
Figure 16: Split-Step-Fourier method for back propagation.....	80
Figure 17: Spreading of optical pulse.....	81
Figure 18: Principle of the LUT table.....	82
Figure 19: Principle of integration of a LUT in a Tx design.	83
Figure 20: Characteristics of weak versus heavy predistorted signal.....	85
Figure 21: Block diagram of a FIR filter.	87
Figure 22: Modulators for EPD transmitter.	93
Figure 23 : Achievable IQ modulation space for MZs.	94
Figure 24 : NRZ versus predistorted NRZ signal.....	98
Figure 25 : Penalties due to DAC parameters	103
Figure 26: Operation of Block Mode simulator.	107
Figure 27: Block diagram of simulation.	109
Figure 28 : Simulation results of transmission without EPD.....	112
Figure 29: Simulation results of ideal and realistic EPD.....	113
Figure 30: Simulation results of transmission at incorrect launch power.	114
Figure 31: Impact of quantization method of EPD signal on performance.	116
Figure 32 : The physical setup of the transmitter and the transmission system used.	118
Figure 33 : Top level schematic representation of the transmitter.....	119
Figure 34 : Clock distribution and timing parameters	126
Figure 35 : Block diagram of transmission setup.	127
Figure 36: Noise addition in transmission setup.....	129
Figure 37 : Block diagram of FPGA and DAC/MUX internal working.	129
Figure 38 : Parallel processing of data	131
Figure 39 : Points where signals merge in the design.....	133
Figure 40 : Delays of different High Speed IO ports.	135

Figure 41 : Principles of port alignment.....	136
Figure 42 : Distribution of the delays set in the variable delay block.....	139
Figure 43 : Eye diagram of misaligned DAC/MUX ports.	140
Figure 44 : Arm synchronization process.....	142
Figure 45 : Analogue conditioning of drive signals in the transmitter.....	144
Figure 46: Hierarchical view of VHDL source files instantiation of entities.....	147
Figure 47: dsp_rocketio input/output nets.	148
Figure 48: Internal signal diagram of architecture of dsp_rocketio entity.....	149
Figure 49 : Desired signal at the receiver generated by pulse generator in model.....	158
Figure 50 : Block diagram of simulation calculation ideal predistorted signal.....	159
Figure 51: Ideal predistorted signal as calculated by simulation tool.	159
Figure 52: Conversion optical field to electrical drive signal samples.....	160
Figure 53: Averaging 4 sampled bit for each 11 bit combination.....	161
Figure 54: Resampling in time to 2 samples per bit.....	161
Figure 55: Resampling from real to integer.	162
Figure 56: Diagram of transmission setup.	163
Figure 57: BER versus OSNR for an 11 bit LUT at 0 dBm launch power [1].....	165
Figure 58: Eye diagrams of 11 bit LUT EPD with an OSNR of 18 dB at the receiver	165
Figure 59: BER versus OSNR for a 7 bit LUT at 0 dBm launch power.	166
Figure 60: Performance comparison 7 bit, 11 bit LUT and uncompensated NRZ.	167
Figure 61: Analysis of NRZ LUT contents.	168
Figure 62: Analysis of EPD BtoB LUT contents.....	168
Figure 63: Analysis of EPD +4dBm 552km LUT contents.	168
Figure 64: Influence of suboptimal control signals [1].	170
Figure 65: Influence of misalignment in time between I and Q arm [1].....	171
Figure 66: Effect of non-optimal PkPk levels of the signal driving the MZ arms [1].....	172
Figure 67: Performance at +4 dBm and +8 dBm launch power.....	174
Figure 68: Performance for different launch powers.	175
Figure 69: Performance of LUTs being used at different launch powers	176
Figure 70: Transmission results showing compensation of nonlinear effects [1].	176
Figure 71 : A block diagram explaining basic principles of an FPGA.....	183
Figure 72 : Workflow for creating an FPGA design.	187

List of Tables

Table 1 : Fibre types and relation to distortion effects.	34
Table 2: Analogue versus digital signal processing.	54
Table 3 : Chronological overview of major publications on predistortion.	69
Table 4 : Digitisation parameters.	84
Table 5 : Overview of investigated EPD systems in publications.	96
Table 6 : Specifications of used FPGA.	121
Table 7 : Specifications of used DAC/MUX.	123
Table 8 : Overview of components used.	124
Table 9: FPGA resources used by the design.	152
Table 10: Usage of RAMB16 blocks by instances.	153
Table 11: Block RAM used for different LUT depths.	155
Table 12: Timing analysis results.	156

Abbreviations and Acronyms

3R	Retime Reshape Reamplify
8B/10B	8 bit into 10 bit encoding
ACE™	Advanced Configuration Environment
A/D	Analogue/Digital
ADC	Analogue to Digital Conversion (Converter)
AIS	Alarm Indication Signal
ASE	Amplified Spontaneous Emission
ASIC	Application Specific Integrated Circuit
ATT	Attenuator
AT&T	American Telephone & Telegraph Inc.
AU	Austria
BER	Bit Error Rate
BiCMOS	Bipolar junction transistors in CMOS
BRAM	Block RAM
BS	Base Station
BtoB	Back to Back
BUFG	Global buffer (as used by Xilinx Inc.)
CD	Chromatic Dispersion
CDR	Clock and Data Recovery
CF	Compact Flash
CMOS	Complementary Metal–Oxide–Semiconductor
COIN	International Conference on the Optical Internet
CORDIC	Coordinate Rotation Digital Compute
CPU	Central Processing Unit
CS	Control Station
CS-RZ	Carrier Suppressed Return to Zero
CW	Continuous Wave
DAC	Digital to Analogue Conversion (Converter)
dBm	decibels milliwatt
DC	Direct Current
DCF	Dispersion Compensating Fibre

DFB	Distributed Feedback
DFB-LD	Decision Feedback Laser Diode
DFE	Decision Feedback Equalizer
DFT	Discrete Fourier Transform
DML	Direct Modulated Laser
DP-QPSK	Dual Polarization – Quadrature Phase Shift Keying
DPSK	Differential Phase Shift Keying
DQPSK	Differential Quadrature Phase Shift Keying
DS	Dual Stage (Optical Amplifier)
DSF	Dispersion Shifted Fibre
DSP	Digital Signal Processing
DWDM	Dense Wavelength Division Multiplexing
EAM	Electro Absorption Modulator
ECOC	European Conference and Exhibition on Optical Communication
eDCO	electronic Dynamically Compensating Optics (product name of an EPD system by Nortel)
ENOB	Effective Number Of Bits
EDFA	Erbium Doped Fibre Amplifier
EDIF	Electronic Design Interchange Format
ENOB	Effective Number of Bits (of a DAC or ADC)
E-O	Electrical to Optical
E-O-E	Electrical-Optical-Electrical
EPD	Electronic Predistortion
f	frequency
f	analysis in frequency domain (spectrum analyser)
FEC	Forward Error Correction
FFE	Feed Forward Equalizer
FFT	Fast Fourier Transform
FIR	Finite Impulse Response (Filter)
FPGA	Field Programmable Gate Array
FR	France
FWHM	Full Width Half Maximum
FWM	Four-Wave Mixing
Gb	Gigabit

GE	Germany
GmbH	Gesellschaft mit beschränkter Haftung (company with limited liability)
GVD	Group Velocity Dispersion
HDL	Hardware Description Language
HPA	High Power Amplifier
I	In-phase Signal Component
IC	Integrated circuit
ICTON	International Conference on Transparent Optical Networks
IEE	Institution of Electrical Engineers
IEEE	Institute of Electrical and Electronics Engineers
IFFT	Inverse Fast Fourier Transform
IFWM	Intra-Channel Four Wave Mixing
IIR	Infinite Impulse Response (Filter)
IMD3	Intermodulation Distortion third harmonic
I/O	Input Output (ports)
IP	Intellectual Property
IP	Internet Protocol
IQ	Intensity-Quadrature (diagram)
ISI	Inter Symbol Interference
ITU	International Telecommunication Union
IXPM	Intra-Channel Cross Phase Modulation
JLT	Journal of Lightwave Technology
JTAG	Joint Test Action Group (common name used for Standard Test Access Port and Boundary-Scan Architecture or IEEE 1149.1)
LDPC	Low-density parity-check code
LEAF	Large Effective Area Fibre
LED	Light Emitting Diode
LEOS	Lasers & Electro-optics Society
LSB	Least Significant Bit
LUT	Look Up Table
MGT	Multi-Gigabit Transceiver
MLSE	Maximum Likelihood Sequence Estimator
MSB	Most Significant Bit
MUX	Multiplexer

MZ	Mach-Zehnder
NCD	Native Circuit Description
NDSF	Non Dispersion Shifted Fibre (known as G652)
NGC	undisclosed acronym used by Xilinx Inc. to indicate a proprietary netlist format
NL	Nonlinear
NLSE	Nonlinear Schrödinger Equation
n-QAM	N-Quadrature Amplitude Modulation
NRE	Non-Recurring Cost
NRZ	Non Return to Zero
NRZ-OOK	Non Return to Zero On Off Keying
NZDSF	Non Zero Dispersion Shifted Fibre
O-E	Optical to Electrical
O-E-O	Optical-Electrical-Optical
OEQ	Optical Equalizers
OFC	Optical Fiber Communication Conference and Exposition
OFDM	Orthogonal Frequency Division Multiplexing
OIF	Optical Internetworking Forum
ONG	Optical Networks Group (of the Electronic and Electrical Department at University College London)
OOK	On Off Keying
OPC	Optical Phase Conjugation
Opt. Exp.	Optics Express
OSA	Optical Society of America
OSNR	Optical Signal to Noise Ratio
OTDR	Optical Time Domain Reflectometer
OTN	Optical Transport Network (Transmission protocol standardized by the ITU)
P	optical power
PCB	Printed Circuit Board
PkPk	Peak to Peak
PLD	Programmable Logic Device
PMD	Polarization Mode Dispersion
PMDC	Polarization Mode Dispersion Compensator

POF	Plastic Optical Fibre
POP	Point Of Presence
PPG	Pulse Pattern Generator
PRBS	Pseudo Random Bit Sequence
PTL	Photonics Technology Letters
Q	Q-factor: parameter reflecting opening of eye diagram
Q	Quadrature Signal Component
QAM	Quadrature Amplitude Modulation
QPSK	Quadrature Phase Shift Keying
RAM	Random Access Memory
RF	Radio Frequency
RoF	Radio over Fibre
ROM	Read Only Memory
RTL	Register Transfer Level
RX	Receiver
R&D	Research and Development
RZ	Return to Zero
SBS	Stimulated Brillouin Scattering
SDH	Synchronous Digital Hierarchy
SiGe	Silicon Germanium
SPM	Self-Phase Modulation
SRS	Stimulated Raman Scattering
SS	Single Stage (Optical Amplifier)
SSB	Single Side Band
t	Time
t	Analysis in time domain (oscilloscope)
TDC	Tuneable Dispersion Compensators
TE	Transverse Electric
TM	Transverse Magnetic
TU	Technische Universität (Technical University)
TX	Transmitter
UCL	University College London
V	Volt
VHDL	VHSIC Hardware Language Description

VHSIC	Very High Speed Integrated Circuits
VOA	Variable Optical Amplifier
VPI	VPIsystems (company name)
VSB	Vestigial Sideband
W	Watt
WDM	Wavelength Division Multiplexing
XPM	Cross-Phase Modulation
XST	Xilinx Synthesis Technology/Tool
ZDSF	Zero Dispersion shifted Fibre
φ	Phase

1 Introduction

The target of the research presented in this thesis was to investigate the possibility of achieving electronic predistortion (EPD) of optical transmission with the use of Look Up Tables (LUT) implemented in a Field Programmable Gate Array (FPGA).

When optical signals travel through an optical fibre they are distorted. The received signal is not only weaker in strength, but other parameters also change. The pulse shape (intensity, phase and polarisation) changes as the pulse travels along the fibre. Instead of trying to limit or undo this distortion of the travelling signal, we can anticipate it at the transmitter. We now send a signal that appears very distorted at the transmitter but after travelling along the fibre, a good quality signal arrives at the receiver. This technique is described by the term predistortion.

In links employing direct detection in the receiver, the advantage of carrying out the compensation at the transmitter is that both the intensity and phase of the signal can be controlled (using, for example, a Mach-Zehnder modulator), hence allowing effective distortion compensation. In contrast, information about the phase is lost during the detection process, limiting the effectiveness of electronic distortion compensation at the receiver.

Because of the recent (around 2005) availability of high speed programmable electronics in the form of field programmable gate arrays (FPGAs) and digital to analogue converters (DAC) with interface speeds of the same order as the optical signals (multiple Gb/s), we can now consider creating these predistorted signal by electronic processing instead of optical means.

The research presented in this thesis shows how such a predistorting transmitter can be realised. As such, it tackles the main implementation issues encountered. This transmitter is then used to transmit a 10 Gb/s predistorted signal and measurements are carried out demonstrating that the compensation of non-linear effects in addition to chromatic dispersion is achievable, as predicted by theory.

1.1 An overview of this thesis

Chapter 2 presents an overview on optical distortion and distortion compensation, focusing on aspects which are used as a basis for EPD or which are important to place EPD within a broader context.

In chapter 3 the method of EPD is presented, together with a literature overview of publications on it and a synopsis of the conclusions reached in them, including a discussion on topics important for the understanding of EPD and the implementation choices.

Chapter 4 is dedicated to the mathematical modelling carried out to assess if the transmitter we planned to build would be capable of effective EPD compensation.

Chapter 5 presents in detail the experimental EPD transmitter that was built with the implementation issues encountered and their solutions.

In chapter 6 the experimental transmission results achieved with the transmitter are presented and analysed.

Finally we present the conclusions from this research in chapter 7 including some details on how the work of this research is being used for newer projects.

A word on references: in chapters where issues related to the design of the EPD transmitter are discussed, much of the knowledge and cited facts are derived from personal discussions and points of view of electrical and optical design engineers at UCL and Ericsson Germany. I did not always find formal academic references to back them up.

1.2 Original contributions

In addition to this thesis, the project also resulted in the following:

A physical EPD transmitter at Ericsson Germany. This transmitter contains:

- A first implementation of an interface module of an integrated circuit (IC) with a Micram Vega DAC
- An original port alignment algorithm between Field Programmable Gate Array (FPGA) and digital to analogue converter (DAC)
- A semi-automated arm alignment method
- A look-up-table (LUT) based predistortion method

- Documentation for its use by other researchers

A fully detailed design for this transmitter was passed on to Ericsson Germany.

This transmitter was used for the first demonstration of real time EPD compensating chromatic distortion (CD) and non-linear (NL) effects. Results of this have been published.

In addition this work also resulted in new components and models for the Photos and the ONG simulation tools.

1.3 Publications related to this thesis

Main publication of the results of the transmitter with the author of the thesis as first publication author:

[1] R. Waegemans, S. Herbst, L. Holbein, P. Watts, P. Bayvel, C. Fürst and R.I. Killey "10.7 Gb/s electronic predistortion transmitter using commercial FPGAs and D/A converters implementing real-time DSP for chromatic dispersion and SPM compensation" *Optics Express* (2009), Vol.17 Iss.10 pp.8630-8640.

Publications and conference proceedings related to this thesis with the author of this thesis as second or subsequent author of the publication.

[2] P. Watts, R. Waegemans, M. Glick, P. Bayvel and R. Killey "An FPGA-based Optical Transmitter Using Real-Time DSP for Implementation of Advanced Signal Formats and Signal Predisortion" in *Proc. of European Conference on Optical Communication* (2006) in Cannes, Vol.3 pp.315-316, We3_P_97.

[3] M. Glick, P. Watts, R. Waegemans, P. Bayvel and R.I. Killey "Electronic Signal Processing to Improve System Performance of Optical Interconnects" at 9th International Conference on Transparent Optical Networks (2007) in Rome, Vol.1 pp.298-301.

[4] P. Watts, S. Savory, Y. Banlachtar, R. Waegemans, V. Mikhailov, R. Killey and P. Bayvel "Compensation of Chromatic Dispersion using Coherent Modulation and Demodulation" in *Proc. of European Conference on Optical Communication* (2007) in Berlin, Vol.1 pp.11, Workshop 5 Hall 4/5.

- [5] P. Watts, R. Waegemans, M. Glick, P. Bayvel and R. Killey "An FPGA-Based Optical Transmitter Design Using Real-Time DSP for Advanced Signal Formats and Electronic Predistortion" *Journal of Lightwave Technology* (2007), Vol.25 Iss.10 pp.3089-3099.
- [6] P. Watts, M. Glick, R. Waegemans, Y. Benlachtar, V. Mikhailov, S. Savory, P. Bayvel and R.I. Killey "Experimental demonstration of real-time DSP with FPGA-based optical transmitter" in *Proc. of 10th International Conference on Transparent Optical Networks* (2008) in Athens, Vol.1 pp.202-205.
- [7] P.M. Watts, R. Waegemans, Y. Benlachtar, V. Mikhailov, P. Bayvel and R.I. Killey "10.7 Gb/s transmission over 1200 km of standard single-mode fiber by electronic predistortion using FPGA-based real-time digital signal processing" *Optics Express* (2008), Vol.16 Iss.16 pp.12171-12180.
- [8] P.M. Watts, R. Waegemans, Y. Benlachtar, V. Mikhailov, M. Glick, P. Bayvel and R.I. Killey "10.7 Gb/s electronically predistorted transmission over 800 km standard single mode fibre using FPGA-based real-time processing" in *Proc. of European Conference on Optical Communication* (2008) in Brussels, Vol.3 pp.121-122.
- [9] P.M. Watts, R. Waegemans, Y. Benlachtar, P. Bayvel and R.I. Killey "Real-time FPGA Implementation of Transmitter Based DSP" in *Proc. of European Conference on Optical Communication* (2009) in Vienna, Vol.1 pp.449-452, 5.4.2.

2 Overview of distortion and distortion compensation

In this chapter I will briefly discuss the model used to describe distortion in optical communications and give an overview of known methods to counter the distortion. Because this is an overview of documented techniques, a major part contains references to other publications explaining them in detail. I will focus on aspects which are used as a basis for the electronic predistortion method that will be investigated in the following chapters.

The use of fibre optics for communication purposes, proposed in 1966 in [10] and [11] is growing steadily. It has replaced most copper cabling in the backbone networks and is starting to show up at an increasing pace in the local access networks [12] [13] [14]. While fibre optic cabling has multiple advantages over copper cabling, for example the possibility of realising longer links because of lower loss and higher capacity due to higher frequency of operation to name the most important ones, it is not a perfect transmission medium and signals are distorted.

2.1 Distortion of optical signals

During transmission over the fibre optic cable, the signal is influenced by multiple effects. For long haul optical transmission a common way¹ to divide the effects that influence the pulse while it travels along a fibre is into the following categories:

- Attenuation: the loss of optical power of the pulse while travelling along the fibre.
- Dispersion: components of the signal (which can be frequency components, polarisation components or different modes) experience different refractive indices and, as a consequence, differences in propagation speeds.
- Non-Linear effects due to stimulated scattering (Raman and Brillouin effects), which can often be neglected when describing distortion of the telecommunication signal.

¹ Another way to categorize and examine them would be from a physical point view as processes between particles or quanta.

- Non-Linear effects related to the fact that the response of the dielectric of the medium (the fibre) is dependent on the electromagnetic field generated by the signal (Kerr nonlinearity).

These effects are documented in detail in most courses and handbooks on optical telecommunication such as [15] [16] [17] [18].

A way to work with these effects without going into the physical processes underlying them is to accept that the propagation of a pulse along a fibre can be expressed by the Nonlinear Schrödinger Equation (NLSE). This equation is derived from the more general description of electromagnetic waves, Maxwell's equations. A good reference for the NLSE is [19]. Defining these effects using the NLSE has the advantage that is closely related to a popular method of modelling of transmission links as used in chapter 4

The simplified version of the NLSE we present here, with only lower order effects, is based on the assumptions that we are using pulses of width > 5 ps (otherwise the expression would become more complicated expressing effects not contributing significantly at larger pulse widths), that the reference frame is moving along with the pulse so that z (a positional dimension along the length of the fibre) and t (the time dimension) are referenced against the middle of the pulse travelling along the fibre, and that A is the signal amplitude normalised so that the optical power is $|A|^2$.

$$\frac{\partial A}{\partial z} + \frac{i}{2} \beta_2 \frac{\partial^2 A}{\partial t^2} + \frac{\alpha}{2} A = i\gamma |A|^2 A \quad (1)$$

The effects modifying a pulse travelling along a fibre can now be defined as being specific terms of this expression.

2.1.1 Attenuation

Attenuation is the loss of power from the optical signal due to absorption and scattering. It is represented by the term:

$$\frac{\alpha}{2} A \quad (2)$$

In the model used the attenuation factor α is not frequency dependent. Because of the definition of distortion² used, it is not assumed that attenuation results in distortion. The

² The word distortion means according to [20] 'change the form of an electrical signal during transmission or amplification'. It is assumed that this means the shape of the pulse shown in a

absolute level of the signal will reduce, but it will not change the shape of the pulse in time or frequency domain. It can be counteracted by perfect amplification. In reality the attenuation is frequency dependent. If the different frequency components experience a different attenuation then the combined signal will distort. However the variation in loss over the frequency range occupied by a single DWDM wavelength channel (25 to 100 GHz) is considered too low to give a significant contribution to the distortion of the signal.

2.1.2 Chromatic dispersion³

Chromatic dispersion is the effect of signal components with different frequencies travelling at different speeds along the fibre. It results in a frequency dependent phase shift or a broadening of the pulse in the time domain. It is represented by the term

$$\frac{i}{2} \beta_2 \frac{\partial^2 A}{\partial t^2} \quad (3)$$

in equation (1). If a higher accuracy is needed or the wavelength is very close to the zero-dispersion point of the fibre, inclusion of the third and higher order dispersion parameters may be necessary. The term (3) is frequency dependent resulting in optical phase shifts. A normal signal will contain many frequency components and so the phase shifts need to be calculated for each frequency present in the signal. All components can then be grouped to obtain the combined result of the dispersion on the full signal. The parameter(s) β_n is (are) temperature dependent but in our models we assume the temperature to be constant.

The result of chromatic dispersion (CD) on a single pulse and a pulse train is represented in Figure 1, (Figure generated using OptSim 4.6 100km NDSF⁴, NRZ modulation 10Gb/s, 0.5mW peak power, fibre loss perfectly balanced by ideal amplifier). Note that in the case of a pulse train, the neighbouring pulses start to overlap and result in deformation that is less intuitive to understand. When neighbouring pulses start to influence each other,

power-time diagram. A wider definition is given in [21], 'The difference in values between two measurements of the signal' For this thesis I use the word distortion as any change in a measurable parameter of a signal except a constant attenuation which only depends on the distance travelled and is not frequency dependent.

³ Also termed Group-Velocity Dispersion (GVD)

⁴ NDSF being Non Dispersion Shifted Fibre as defined in ITU standard G652 assumed to have, at 1546nm, an α of 0.2dB/km, a β_2 of -20.9 ps²/km, a γ of 1.32 (W km)⁻¹.

because of chromatic dispersion or other effects, we describe it as Inter Symbol Interference (ISI)

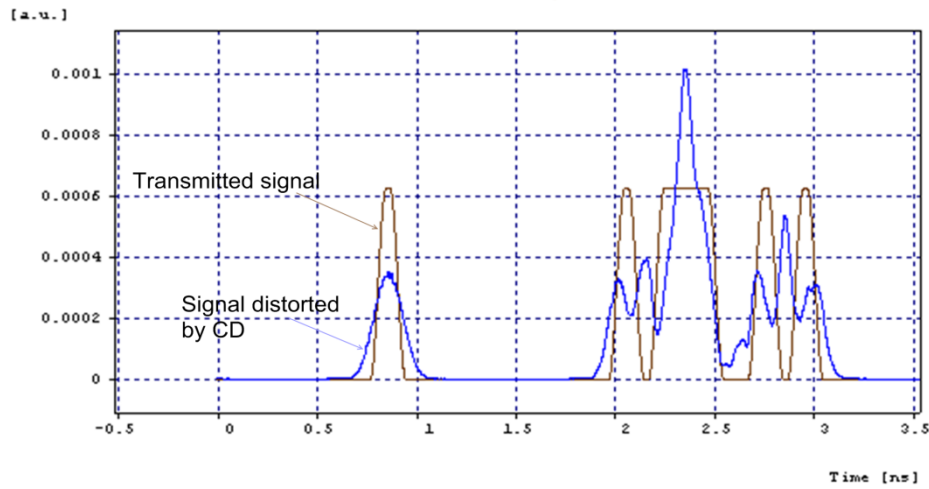


Figure 1 : Dispersion effects on pulse train.
Brown: Transmitted signal; Blue: Signal distorted by CD.

2.1.3 Nonlinear effects

Nonlinear effects for LH transmission result from interactions between the signal and the material, and are commonly divided up into:

- Self-phase modulation (SPM) (first observation [22])
- Cross-phase modulation (XPM)
- Four-wave mixing (FWM)
- Stimulated Brillouin Scattering (SBS)
- Stimulated Raman Scattering (SRS)

The origin of SPM, XPM and FWM is the Kerr effect that states that the intensity of the signal leads to changes in the propagation of the signal. It is expressed in equation (1) by the factor:

$$i\gamma|A|^2 A \quad (4)$$

with

$$\gamma = \frac{n_2 \omega_0}{c A_{eff}} \quad (5)$$

In numerical calculations, n_2 is in most cases handled as a constant⁵.

While the term (4) makes it possible to model some of the listed nonlinear effects it does not account for all these effects. (4) reflects that the signal undergoes a small delay depending on the intensity of the signal (not frequency dependent) The pulse undergoes a phase shift depending on the square of the amplitude of the electromagnetic field. This means that expression (4) can be used to represent the most prominent aspects of SPM and XPM depending on the meaning of the expression $|A|^2$. If $|A|^2$ represents only the power in a single channel, the total expression only reflects SPM effects. If $|A|^2$ represents the total power over all channels then (4) will also include XPM effects.

To include the effects of SBS, SRS and FWM, or more accurate SPM and XPM effects, a more complex version of equation (1) is needed with factors additional to (4) and (5).

XPM and FWM are mostly considered effects between multiple channels in a DWDM setup. However in systems operating at 40 Gb/s/channel and higher these effects become significant as intrachannel effects as explained in [23]. These are then referred to as intrachannel XPM and FWM (IXPM and IFWM).

A more detailed description of these effects through the NLSE can be found in [24]

2.1.4 Polarization effects

Polarization can be represented in single mode fibre by assuming that the pulse can be divided up into two orthogonal polarization states, each state experiencing a slightly different refractive index due to birefringence. The two signal components in the different states arrive with a time difference at the receiver which is termed polarization mode dispersion (PMD)[25].

During propagation along the fibre⁶ the signal will move between the two polarization modes so that the proportion of the signal in a certain polarization state is varying. In

⁵ This constant is published in tables in function of the medium (fibre type), the characteristics of the pulse travelling along it (frequency, width) and the method of measurement. It is not an absolute constant. Values in the range of $2-4 \times 10^{-2} \text{m}^2/\text{W}$ are typical.

⁶ This depends on the fibre type. Here we assume we are using standard NDSF. There exist fibres with special characteristics in relation to polarization effects.

addition the polarization effects change over time (the order can be smaller than seconds) [26] and the changes are stochastic [27].

2.1.5 Intermodal effects

Most long haul communication systems use single mode fibre which allows only a single TE/TM mode⁷ to travel along the fibre. In the case of multimode fibre the presence of multiple modes of the same frequency component of the signal would introduce additional effects and require more complicated expressions to model the travelling of signals along this type of fibre.

2.1.6 Other effects

There are other distortions in a transmission system. In addition to the fibre we need additional components to construct a system. These discrete components can introduce distortions. An example is the effect of amplifiers operating at their saturation point.

The effects mentioned in this chapter result in a distortion of the signal. These distortions will result in degradation of the signal quality and, if severe enough, can increase the likelihood that errors appear in the received signal after transmission (or higher inaccuracy in analogue systems). These distortions are not the only cause of errors. Other factors, for example the presence of noise in a telecommunication system, also contribute to having imperfect communication with errors. A remark to make is that if we split the total signal up into desired signal and noise, then not only the desired signal but also the noise in a system is a source for the distortion effects discussed.

2.1.7 Combined effects

All these effects do not influence the signal independently, but occur simultaneously and influence each other. The most relevant for this thesis is the interworking of chromatic dispersion (CD) and Self Phase Modulation (SPM). The phase changes because of SPM will, through CD, result in intensity changes. These intensity changes will also occur outside the bit slot and so SPM will contribute to Inter Symbol Interference (ISI).

⁷ Or two if you consider the two orthogonal polarisation states modes.

2.2 Where to counteract distortion

When attempting to improve the performance of a telecommunication system, one possibility is to try to counteract the distortions of the signal that negatively impact the transmission system. This can be achieved in different ways.

- The transmission medium can be adapted so that the distortions are acceptable (for example using a Dispersion Shifted Fibre (DSF) instead of standard fibre to avoid distortion due to dispersion)
- The properties of the signal can be changed so that distortion is limited (an example is using signals with a lower power so they have lower non-linear distortions) or so that multiple distortions balance each other out (an example is the use of soliton pulses)
- Devices can be introduced in the transmission system that counteract these distortions. These devices can be placed at different places and be of different types (an example is the use of dispersion compensators to overcome the dispersion along the fibre).

If devices are placed along the transmission path then this can be done at multiple positions in an optical transmission system as represented in

Figure 2 (Red blocks: signal conversion between formats, green blocks signal in certain format where additional processing including distortion mitigation might take place, blue arrows electrical signal, red arrows optical signal):

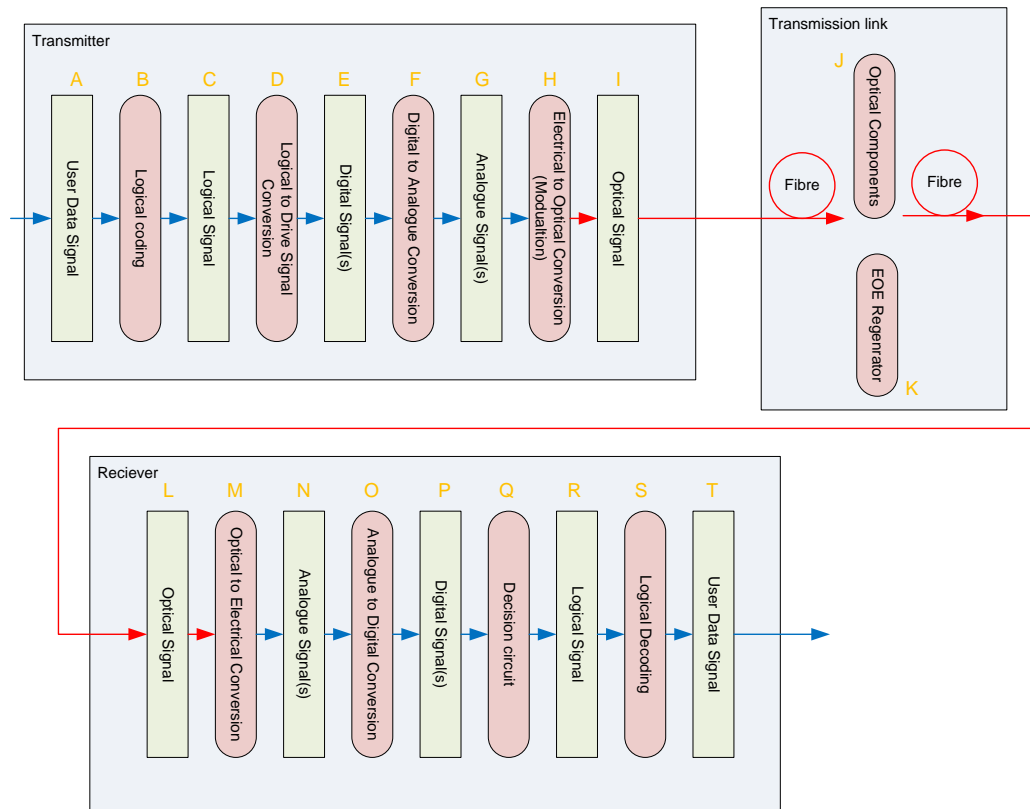


Figure 2 : General optical transmission link.

- K) The optical link can be divided up in two and the optical pulse can be regenerated, recreating the optical pulse without distortions.
- I,J,L) Optical devices can be inserted along the optical path that mitigate part of the distortion.
- G,N) Analogue components can operate on the analogue signals or
- E,P) digital techniques can be applied in the transmitter or receiver on the sampled signals.
- C,R) In addition coding techniques can work on the logical signal in a way that makes it more robust against distortion.

The prepositions pre-, post- are used to indicate that the compensation occurs before or after the transmission medium (the fibre). It is of course possible, rather than concentrating the compensation in one place along the fibre to apply it at multiple positions along the fibre. This is termed distributed compensation.

The blocks logical and digital signals both refer to signals in digital form. The difference between them is that with digital signals we refer to digitized version of the analogue signals in the analogue signal block.

If distortion effects are compensated in the optical part of the transmission link, an important commercial consideration for WDM systems is whether a device applies the compensation across all channels (large bandwidth required) or on a per channel basis (smaller bandwidth is sufficient), since this makes a difference to the number of compensating devices needed and hence has a major effect on the cost of a system.

Some of the methods proposed in the next chapters in a transmission system can be combined; if multiple methods are used then they do not all need to be applied at the same location. Different effects can be mitigated at different locations.

2.3 Distortion in non-optical transmission

Distortion of signals and their compensation are not exclusive to optical transmission. Similar effects have been experienced in transmissions using wires, waveguides and radio waves. Major differences between Radio Frequency (RF) engineering and optical engineering are:

- Non-linear transmission line impairments as described in chapter 2.1.3 are not present in RF engineering.
- Higher carrier frequencies and wider bandwidths make much higher bit rates possible than in the RF domain but make it very challenging to design electrical circuits to support optical transmission.
- Components available for RF do not always have equivalent components in the optical domain (such as digital local oscillators for receivers).

The major differences and RF issues with optical transmission are discussed in [28]. Because an extensive amount of research has been carried out on RF communications, it is still useful to use this research as inspiration.

A search of published papers makes it clear that the term predistortion if used in these domains is mainly used to compensate for distortion caused by discrete components along the link, mainly High Power Amplifiers (HPA).

The term equalization is used for compensating techniques for distortion resulting from effects in the transmission medium (mainly due to bandwidth limitations, and fading effects). Distortion is looked upon as a non-linear degradation of amplitude and/or phase response in the frequency domain of the signal [29 p. 150]. Distortion compensation is

then accomplished by applying the inverse response in the frequency domain to the signal, by applying a filter to the signal.

A wide variety of adaptive filters has been proposed including analogue or digital implementations, preset or adaptive [30] [31]. Another approach is to use more statistical inspired ideas such as the use of the Maximum-Likelihood Sequence Estimation (MLSE) at the receiver. A systematic overview of non optical digital communication including distortion can be found in [32].

In addition some papers in this domain are very instructive for the technology and methods used even if the effects they compensate are not relevant to the research in this thesis. (an example is [33]: VHDL/FPGA implementation of predistortion transmitter for radio over fibre which contains interesting examples of use of FPGAs for predistortion).

2.4 Distortion in Radio over Fibre applications

Because of the economic importance of wireless access there are currently many publications on distortion and distortion compensation for Radio over Fibre (RoF) applications. This application was first demonstrated in [34] and an overview can be found in [35 pp. 31-41]. In this technology a combination of a radio link and a fibre link were used to transport a signal from a Control Station (CS) to an end-user while the complexity of the conversion from fibre link to radio antenna at the Base Station (BS) was kept to a minimum. No protocol conversion or regeneration was done at the BS. The predistortion techniques proposed are mainly focused at compensating the distortion generated by the devices (amplifier, laser, photodiode) at this interface. Because of this, this research [example: [36] : Predistortion for linearization of a DFB-LD reducing the distortion due to the IMD3 component] is in most cases not directly applicable to the problem addressed here.

2.5 Counteracting distortion in optical transmission

A first remark to make is that incorporating specific modules in an optical transmission system for counteracting the distortion is not always necessary. An optical link can be designed so that the distortion stays within acceptable limits. The different effects described earlier can be calculated for a given design and the effect on the quality (error rate) of the signal assessed. This is the classical way of designing optical links as explained in [37] and many other network design books and courses.

But because of technological and market evolution there is a demand for higher bit rates. As a consequence distortion effects are becoming more significant and explicit methods for counteracting distortions are needed. Because the chromatic dispersion effects, in most transmission systems, have greater impact on end to end quality of the link than the polarization and nonlinear distortion effects, most distortion combating techniques have focused on chromatic dispersion compensation.

2.5.1 Coding techniques

Coding techniques work on the logical data stream. A sequence of k-bits of user data is mapped into a sequence of n-bits⁸ which are transmitted and reconverted to the k-bit sequence at the receiver. By carefully choosing the process it is possible to make the transmission less prone to error or the system is even able to correct errors. They fit into the blocks B and C at the transmitter and in blocks R and S in of

Figure 2. Important examples of this method of counteracting distortions in optical transmission is the principle of scrambling, the adding of Forward Error Correction (FEC) codes and so called 8B/10B (or similar) encoding.

These methods do not directly influence the distortions experienced on the transmission link but they do improve the overall transmission quality and as such can also reduce errors finding their origin in distortion. To optimize the working of the coding techniques it is necessary to choose the optimal coding technique dependent on the source of the errors. General information can be found in [32] and a recent paper illustrating the focus on a particular distortion is [38] looking at optimizing LDPC-based turbo codes for PMD.

⁸ In general $n > k$ but this is not a necessity.

2.5.2 Use of alternative fibre types

In the NLSE different parameters controlling the effects on the pulse are dependent on the fibre type. Through the choice of the fibre type, we can influence these parameters and so influence the distortion of the signal. While from a scientific point of view the use of the optimal fibre for a particular transmission link is a very attractive solution, in reality this is often a commercially unacceptable solution.

The cost of placing new fibre or replacing existing fibre for fibre deployed in between buildings is very high due to the physical work involved (deployment of personnel, digging, opening manholes, right of way, ...). Also supporting many different types of fibre in one network makes logistical support very difficult. It can be a viable way to reduce distortion effects in case the optical connection is very accessible (an example is inter equipment links in a point of presence (POP)) or when new fibre is required for another reason such as a first deployment (an example might be a brand new Intercontinental submarine link).

Multimode fibre	Allows multiple mode of a signal to travel. Because of this the fibre has mode dispersion effects. This makes this fibre, in general, only suitable for relatively short links at low data speeds.
Non Dispersion Shifted Fibre (NDSF)	Does not have mode dispersion effects because only a single mode ⁹ is allowed to travel. The most common deployed fibre for long haul telecommunications.
Zero Dispersion Shifted Fibre (ZDSF)	By shifting the zero dispersion point to the operating frequency no GVD is present at this exact frequency. This significantly increases non-linear related distortion effects, especially FWM between channels when using DWDM.
Non Zero Dispersion Shifted Fibre (NZDSF)	By moving the zero dispersion point closer to but not exactly at the operating frequency a compromise between low GVD and low FWM for DWDM applications is realised.
Reduced Dispersion Slope Fibre	By reducing the dispersion slope the difference in delay between different frequencies is limited. Originally designed to improve transmission of 1.3 μm and 1.55 μm on the same fibre in WDM applications it also limits difference in dispersion between DWDM channels. This allowed band based dispersion compensation to be used without channel based dispersion

⁹ Single mode fibre does still support two modes with orthogonal polarization. It was called single mode because in ideal fibre both modes propagate under identical conditions and as such does not exhibit multimode dispersion.

	compensation. This fibre has in general a higher nonlinear coefficient.
Single Polarisation Fibre	By allowing only one polarization mode, polarization mode dispersion is not present.
Polarization Maintaining Fibre	By not allowing the two polarization modes to interact it is possible to handle both modes independently and so counter polarization mode dispersion. If both modes are transported they can still experience different propagation constants in the fibre.
Large Effective Area Fibre (LEAF)	This fibre has a lower non-linear coefficient than dispersion shifted fibre (but still less than NDSF) because of the size of A_{eff} . It has, in general, a higher dispersion slope [39].
Plastic Optical Fibre (POF)	A type of multimode fibre which in addition has a higher loss. The high loss in most cases limits the performance rather than distortion.

Table 1 : Fibre types and relation to distortion effects.

Basic information on fibre types can be found in [18] and more in depth, on speciality fibres, in [40]. Some other types like doped fibre or dispersion compensating fibre are being used but they are generally considered to be discrete components in the network and are in most cases not classified as a transport medium for long haul communication. Dispersion compensating fibre is especially important for distortion compensation and will be discussed in a later chapter. Many other fibres, such as Hollow Fibre, Liquid Core Fibre, etc have been researched but are not commercially available as an alternative for network deployment as can be seen from the catalogue of a fibre producer [39]. Because of the dominance of NDSF in deployments, I will focus on using this fibre for the transmission link in this thesis.

2.5.3 Optimised modulation formats

From a theoretical point of view it is possible to modulate a carrier optical signal manipulating intensity, phase, frequency¹⁰ and polarisation of the carrier in time. In addition to using these parameters as modulation parameter they can be used to make the signal more robust or (in addition to time) as multiplexing parameters. The

¹⁰ Frequency is related to the phase parameters and it can be defended that it should not be presented as an independent parameter in the case of a modulated carrier.

combination of all possibilities makes the theoretically available modulation options almost endless which is a major issue when giving an overview of modulation formats, as so many formats, variations and modifications of them are proposed by different researchers¹¹. An overview on optical modulation formats and more detail, including detailed references, can be found in [41] [42] [43], and performance comparison in [44]

A practical way to summarize this topic is to concentrate on the modulation formats that have been deployed or are considered for deployment by industry while giving some extra attention to methods related to electronic predistortion. This is a pragmatic way to filter out the formats best suited for use, especially because a major element determining the importance of a format or technique has been market readiness of technology and not the theoretical limitations or achieved performance in lab conditions.

Until the rise of 40 Gb/s/channel (around 2007-2008) [45], non-return-to-zero on-off-keying (NRZ-OOK), an intensity based modulation format, has been dominating as the modulation type of choice for commercial deployments of digital optical links¹². This is illustrated by the latest OTN interconnect standard (March 2008) [46] which only describes NRZ formats for signals up to 10 Gb/s/channel and some Return to Zero (RZ) alternatives for 40 Gb/s/channel. These formats could be detected using a photodiode as detector at the receiver. A single photodiode restricts the detection to the power of the signal¹³.

More advanced modulation types were being introduced on the market with the availability of 40 Gb/s/channel transmission systems. RZ was already mentioned but for long haul communication first Duo-Binary formats were deployed with most vendors of transponder modules and telecom systems now offering different types of Differential Phase Shift Keying (DPSK) [47], a differential phase based modulation format. The use of DPSK flavours was made possible by placing a delay interferometer in front of the photodiode(s).

¹¹ Because of this I realise that the next paragraphs are debatable especially on the upcoming technology because a consensus on the importance of the different formats has not yet been reached (there is also no consensus on the naming of many formats). For a more detailed discussion I refer to the many references in this chapter.

¹² Some exceptions are known such as CS-RZ on submarine links.

¹³ In this introduction I will assume the detector technology was key to the technological evolution. The availability of other components was of course also important.

For 100 Gb/s/channel the standardisation bodies and system builders are now favouring Dual Polarisation Quadrature Phase Shift Keying (DP-QPSK) [48] [49]. Academic research focusing on improving 100 Gb/s/channel¹⁴ and longer 40 Gb/s/channel links are considering options like Optical Frequency Division Multiplexing (OFDM) and n-quadrature amplitude modulation (n-QAM). For these modulation formats the possibility of coherent detectors, constructed using a local laser at the receiver instead of the delayed signal as second interference source in the interferometer(s), are being researched.

Newer more complex modulation formats are in general designed to achieve better transmission quality and increase the achievable bit rates. A disadvantage is that they require more complex transmitters and receivers and as such they increase the cost and difficulty in the practical construction and operation of the proposed systems. Figure 10 and Figure 11 in the chapter on O-E and E-O conversion¹⁵ illustrate the increase in complexity of the transmitter and receiver when more advanced modulation formats are used.

2.5.3.1 Intensity based modulation

Intensity based modulation is accomplished by two types of modulators: direct control of the optical source (cheaper) or modulating a CW optical source with an external modulator (more expensive). The main difference, from the point of view of distortion, is that the on-off switching of the drive signal of an optical source does not produce clean on-off switching of the optical intensity but effects such as chirping and overshoot mean that this method, in general, creates pulses that are already more distorted before being transmitted than those generated by external modulation¹⁶. While direct modulation is

¹⁴ A remark to make is the definition of a 100 Gb/s/channel system. In optical research we expect this term to be used when a single carrier signal produced by a laser is modulated in such a way that it transmits 100 Gb/s. In industry the term is used if the client interfaces at both ends are in accordance to a 100 Gb/s standard. This standard might well be accomplished by multiple carriers (such as the use of 10x10 Gb/s optical CWDM channels), using multiple transmission mediums (an example is ribbon cable for the interface) or other techniques, and transmission in between can also be carried out by multiple carriers (so called inverse muxing). This means that the appearance of 100 Gb/s/channel system does not necessarily mean that 100 Gb/s modulation formats are required. For standardised interconnects, as an example, there is currently no 100 Gb/s/carrier proposed at all.

¹⁵ We only show some Tx/Rx designs representing many more possible variations.

¹⁶ External modulation is not free of these effects but they are better controlled.

the preferred method when cost is the major issue I will focus on external modulation techniques because this is the preferred method for long haul communication

Figure 3 gives a simplified graphical representation of the main characteristics of Non Return to Zero-On Off Keying (NRZ-OOK) generated by an externally modulated carrier which I will use as a reference when presenting modulation techniques influencing distortion in the next paragraphs. In Figure 3, P stand for optical power, t for time, φ for phase, f for frequency, I and Q represent two phase-orthogonal signal components of a quadrature graph. Red are signal components related to a 1 bit, blue to a 0 bit and in this and later figures, purple relates to parts of the signal where the 0 or 1 value cannot be distinguished. All axes are arbitrary units. The dots refer to the signal level at the sampling point. The figures assume that the carrier frequency is noiseless in power and frequency, there is a phase drift of the carrier, and the signal is presented directly after modulation, hence without any transmission line effects. The polarisation parameters are not represented. When I use the diagram in the next paragraphs as reference the NRZ-OOK signal will be shown with faded colours and the discussed format/techniques will be in intense colours.

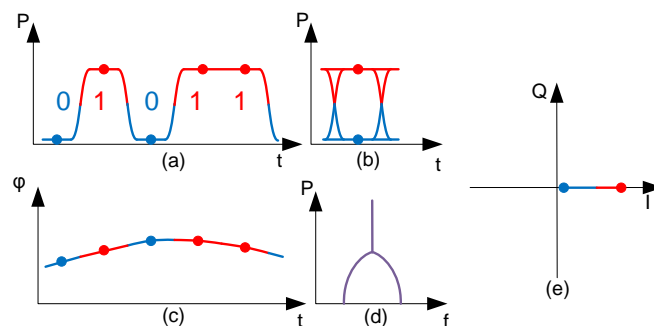


Figure 3: Characteristics of NRZ-OOK.
 (a) Intensity waveform in time domain, (b) eye diagram, (c) optical phase, (d) optical spectrum and (e) constellation diagram.

2.5.3.2 Differential phase modulation

In phase modulation the phase of the underlying carrier signal is modulated. Differential phase modulation means that a change of the phase between two bit slots indicates that a transmitted bit is a 1 (and no change indicates a 0) not the absolute level of the phase. Differential coding is used in phase modulation (compared to absolute coding in most intensity modulation formats) for multiple reasons:

- The phase of a carrier signal generated by commonly used sources drift (represented by the slightly curved line in the phase versus time diagram in Figure 3) making measurement of the absolute phase at the receiver difficult.
- A simple receiver based on a delay line interferometer, optional with a balanced detector, is suited for differential phase decoding.

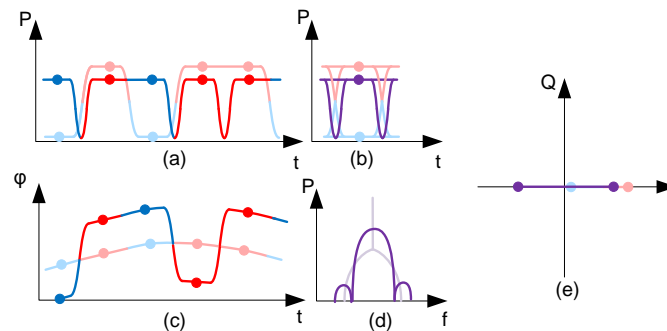


Figure 4: Characteristics of DPSK
(a) Intensity waveform in time domain, (b) eye diagram, (c) optical phase, (d) optical spectrum and (e) constellation diagram.

Other methods of decoding, in particular based on coherent detection where the receiving signal is mixed with a local laser source to detect the phase information, are also possible.

The main advantage of DPSK over OOK¹⁷ is a $\sqrt{2}$ bigger symbol spacing as can be seen in the IQ diagram. Having a more constant power level (depending on the modulation method intensity dips when changing phase may or may not be present) reduces the non linear effects because they are intensity dependent. This is however partly offset by more phase noise.

¹⁷ Assuming a balanced detector and the same average launch power.

2.5.3.3 Intensity shaping¹⁸

Three main techniques based on optimizing the intensity shape of the signal are: adjusting the shape of the pulse, moving from NRZ to Return to Zero (RZ) coding and then further reducing the duty cycle of the pulse.

While manipulating the shape of the pulse is well discussed in telecommunication theory [29 p. 136-149] it is difficult to construct complex and accurate pulse shapes by manipulating the electrical drive signal because of the short bit period and high frequencies in optical transmission. Some proposals have been made to shape the drive current in a complex way mainly to overcome distortions generated by a direct modulated optical source [50, 51].

The limited frequency band of almost all components has a major effect on the pulse shape which in most cases results in reducing the occupied bandwidth and as such can reduce distortion effects. At the transmitter the filters are often placed in the electrical part of the circuit resulting in shaped drive signals, while at the receiver it is usual to reduce distortion with a combination of an optical bandpass filter before and electrical lowpass filters after the OE conversion. The use of these filters is discussed in the literature¹⁹ describing the design of transmitters and receivers of a particular system [52].

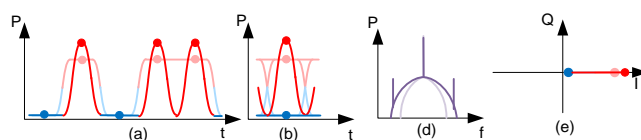


Figure 5: Characteristics of RZ.
(a) Intensity waveform in time domain, (b) eye diagram, (d) optical spectrum and (e) constellation diagram.

With the return to zero (RZ) format the signal power returns to a low intensity in between bit slots. This is shown in Figure 5. This principle can be extended so that the pulse occupies only part of a bit slot. This is known as reduced duty cycle.

¹⁸ Changes applied by devices to the signal intensity in the time domain will also result in changes of the other parameters presented in time or another domain. I classify them here in groups based on where the effects is most prominent.

¹⁹ Often discussed in the first place for the noise reducing effects of these filters.

In Figure 5 two major differences can be noticed compared to NRZ: The peak power of a signal with same average power is higher and the occupied bandwidth is larger. The impact of these on the distortion is complicated. Because we occupy a higher bandwidth there are more signal components with a bigger Δf away from the f_{carrier} and these components result in a higher impact of dispersion. The higher peak power is an issue for the non-linear effects. The net result depends on the bit rate at which the signal is applied. In general it can be said that for >10 Gb/s systems RZ decreases the penalties because of non linear distortion [53], while issues with CD are dealt with through other techniques.

2.5.3.4 Single sideband (intensity shaping in frequency domain)

When a data stream is modulated on a carrier frequency it occupies bandwidth to both sides of the carrier frequency in the frequency domain

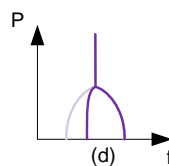


**Figure 6: Spectrum of SSB or VSB signal.
(d) Optical spectrum.**

The data in one sideband contains sufficient information to recreate the data. Removing one sideband by controlling the modulator is called Single Sideband (SSB). When this is achieved by optical filters it is termed Vestigial Sideband (VSB) [54] (Figure 6). Removing one sideband reduces the bandwidth occupied by the signal and so the technique is more often proposed to optimise bandwidth use than for its properties in relation to distortion.

In the framework of electrical distortion compensation SSB is important because it increases the effectiveness of electrical equalization filters (see paragraph 2.5.7.1).

Related to the predistortion transmitter described in this thesis we can remark that the design of this transmitter was used to create and transmit SSB [55]. This has been difficult to achieve with other transmitter designs because of the problems with implementing broadband Hilbert transform functions [41]

2.5.3.5 Phase shaping

A variety of methods of controlling the phase parameter of signals using intensity to carry the information have been proposed to improve the transmission. Three named techniques are chirping, carrier suppression and duobinary.

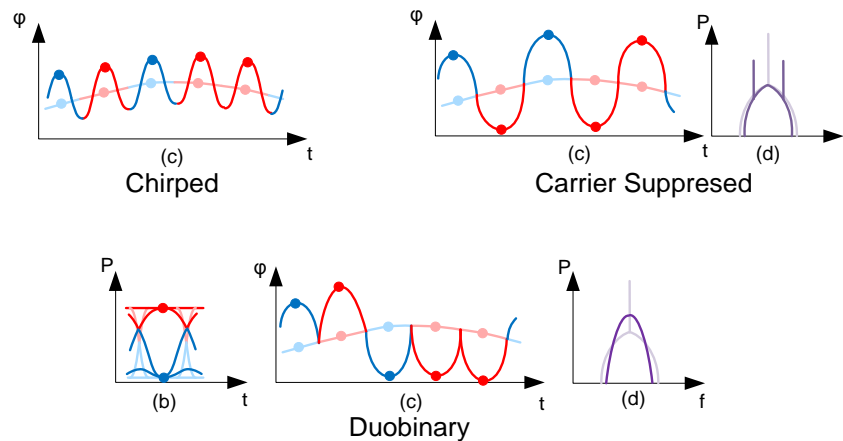


Figure 7: Modulation techniques using phase shaping.
(b) eye diagram, (c) optical phase and (d) optical spectrum.

Chirping is a technique in which the optical phase across each bit slot (see Figure 7) is varied with time in an identical way. It is mainly used to limit the chromatic dispersion effect over short haul transmission distances. By carrier suppression we inverse the phase of alternating bit slots [56] and with duobinary [57] [58] the phase is adjusted with a coded sequence so that the component at the carrier frequency is completely suppressed). These techniques can have positive effects on suppressing non-linear signal distortions in addition to increasing dispersion tolerance.

2.5.3.6 Non-binary symbol coding

The modulation formats presented so far use symbols which have only two states, 0 or 1. It is however possible to make a single symbol represent more states. Modulation formats taking advantage of this are:

- Multilevel coding: multiple signal levels in the intensity domain.
- Quadrature Phase Shift Keying QPSK: more than two phase states²⁰ are used but all states have the same intensity.

²⁰ In this format the phase is now handled as an absolute level and not, as described above, as a differential phase shift between two symbols, though differential QPSK also exists.

- n-Quadrature Amplitude Modulation (n-QAM). States are distributed across intensity and phase domains occupying the full quadrature space.

A major advantage is that for the same data rate, the symbol rate is now lower so the symbol period is longer resulting in lower ISI between symbols. Because we now have more states per symbol, the distance in the modulation space between the states will be reduced. We need to take into account that distortions (and other effects) will also be affecting the determination of the detected state at the receiver, and so increase the likelihood that a state is misinterpreted.

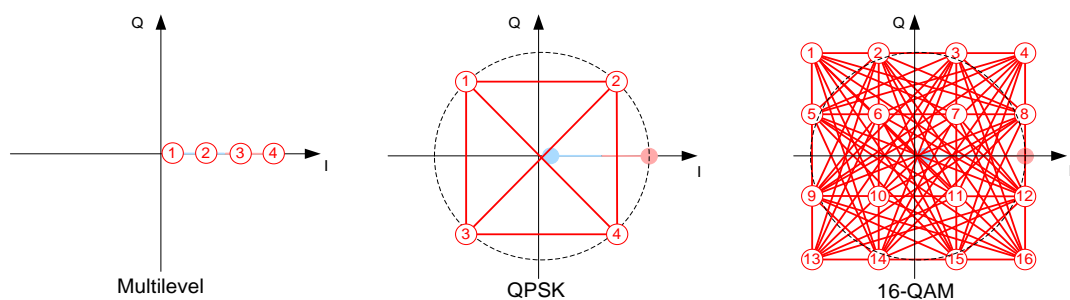


**Figure 8: Modulation techniques using non-binary symbol coding.
All are constellation diagrams.**

2.5.3.7 Multiplexing

Another way to increase the bit rate without increasing the symbol period is through the use of multiplexing techniques across dimensions of the signal space not used for the modulation. We can mention OFDM and polarisation multiplexing.²¹

With OFDM [59] [58] we code a symbol on many orthogonal spaced frequencies. This is achieved not by modulating many closely spaced different optical sources, but by calculating the signal shape of a symbol using an IFFT algorithm and decoding at the receiver using an FFT algorithm. OFDM is an interesting candidate for predistortion because it requires digital signal processing to create the signal, so predistortion can be added by using additional logic on the component performing the IFFT without the requirement for additional components. This advantage can also be present with other modulation formats if DSP is used. The robustness of OFDM versus distortion is related to

²¹ The most well known optical multiplexing techniques are WDM in the frequency space and OTDM. These fall outside the research because we focused on optimising a single WDM channel.

size of prefix inserted in the symbols by increasing the overhead used by the prefix the signal can be made more robust against ISI.

Another option is using the polarisation dimension. In 2.1.4 we explained that in a single mode fibre we can envisage an optical signal as a mix of two orthogonally polarised signals. It is possible to modulate and detect the signal of each polarisation component independently and so achieve a doubling of the bit rate while keeping the symbol period the same.

2.5.4 Soliton pulses

During transmission CD and NL effects both influence a pulse simultaneously. It is possible to make a pulse (in general a high power, short pulse compared to a normal RZ or NRZ signal pulse) in which both effects compensate each other, resulting in a pulse that does not show significant distortion, though it is attenuated and requires amplification. Solitons are described in detail in [19] and an overview paper is [60]. While soliton based systems have been deployed [61] they are not a common solution for telecommunication systems.

2.5.5 Channel assignment in DWDM

Four Wave Mixing (FWM) transfers signals from a certain frequency to other frequencies and this results in distortion. In the case of regularly spaced DWDM this means that the generated components are present at the wavelengths of the other DWDM channels and interfere with them. This can be prevented by placing the DWDM signal at non-regular intervals so that the new signal components generated by FWM do not interfere with the existing channels [62]. An issue with this scheme is that the spectral efficiency is reduced, and the ITU standardised DWDM channel map [63] does not support this.

2.5.6 Optical correction of the distortion

2.5.6.1 Dispersion Compensating Fibre

The dispersion effect in optical fibre is dependent on the type of fibre as mentioned in 2.5.2. Fibre can be made with the opposite sign of dispersion coefficients²² which is termed Dispersion Compensating Fibre²³ (DCF). If a signal travels sequentially through two fibres which are so designed that they have exactly the opposite dispersion effects then the result is that the output signal is free of dispersion induced distortion. An extra bonus is that the signal during transmission still disperses which can be beneficial in reducing some of the non-linear distortion effects. In most case the two fibres balancing each other out are not of equal length. During deployment the first fibre is the real transmission fibre placed in the trench and carrying the signal from hut to hut, while the second fibre is applied to the link on a spool in the telecom hut. This solution is in most cases preferable to using both fibres in the trench because it avoids the need to dig up the fibre if the dispersion design changes or if existing fibre grids are used, in most case created from only NDSF. A disadvantage is that a spool of fibre attenuating and distorting the fibre is present in the telecom huts which is not contributing to carrying the signal a significant distance. In addition the DCF has higher non-linear distortion effects than the transmission fibre and adds a cost to the system. This method of dispersion compensation and distortion compensating is the most commonly deployed one in the field today. Issues arising when applying this method are related to designing the position of the DCF along the transmission link and that in practice the optimal dispersion compensation is only achieved for a single frequency. This method of dispersion compensation was first proposed in [64]. A more recent overview can be found in [65].

²² Opposite sign from the dispersion coefficients in the fibre used as the main transmission fibre.

²³ Or in deployments mostly called Dispersion Compensating Module (DCM)

2.5.6.2 Distortion Compensating Devices

An alternative to using the dispersion compensating fibre mentioned in 2.5.6.1 is using an optical component. The advantages which may be achieved by this compared to using DCF are:

- Lower loss insertion and less other distortion effects generated.
- Higher linearity
- Lower cost.
- Smaller in size and weight.
- Possibility to adjust the distortion (mainly dispersion) controlling parameters without having to replace the spool or device, so giving us a tuneable device²⁴.
- In addition to chromatic dispersion other distortion effects can be targeted.

It is common to divide proposed devices into 3 categories : Optical Equalizers (OEQ), Tunable Dispersion Compensators (TDC), Polarization-Mode Dispersion Compensators (PMDC) [66]. Different physical effects are used as a basis for these devices. Disadvantages of most devices are that they have a smaller bandwidth than other methods and that the promised lower cost compared to fibre based methods has not yet clearly materialised. At present tuneable components are especially important to remove the residual dispersion present on a single channel of a DWDM system (mainly for 40 Gb/s channels) after DCF has been applied to the full DWDM bandwidth along the link to remove most of the CD. An overview on fibre based devices can be found in [67] and on waveguide based designs in [68].

2.5.6.3 All-Optical Regeneration

The term regeneration is, for commercial system, used for systems doing optical-electrical-optical conversion as discussed in chapter 2.5.7.7. Research is ongoing on achieving this in the optical domain without conversion to the electrical domain. An overview on this can be found in [69]. While achievements in the lab have been reported this technique is currently not considered for commercial deployment. Also technology advancements and new products showing higher integration of high speed electronics

²⁴ With two tuneable options possible: tuned once during installation of the link or continually tuned during operation through a feedback system.

with optical components [70] is used as an argument for using O-E-O regeneration instead of moving to optical regeneration.

2.5.6.4 Optical Phase Conjugation

Optical Phase Conjugation (OPC) is based on the principle that the effects adding distortion to the signal during transmission along a fibre have symmetrical properties in relation to central frequency and peak power of a signal. The method was originally published in [71] and more detailed information can be found in [72] and [73]. While OPC is not a significant distortion combating technique in current systems (as far as the author is aware, it has never been deployed) I discuss it in some detail because it is the basis for a method to calculate the predistorted signal.

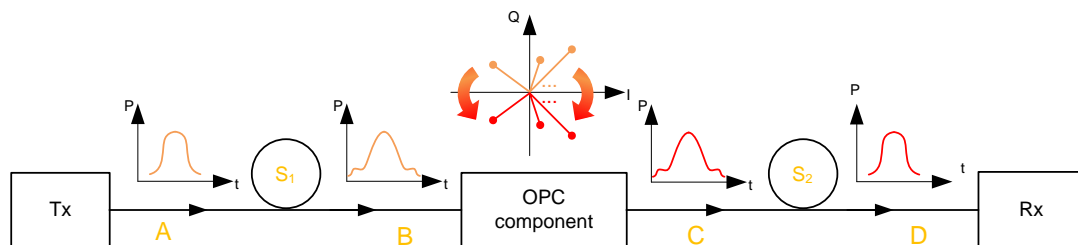


Figure 9: Principle of Optical Phase Conjugation (OPC).

For OPC, the transmission link is divided in two parts, each using the same transmission medium (fibre with the same length and characteristics) represented by the fibre spools S_1 and S_2 in

Figure 9²⁵. An optical pulse is created at the transmitter (A) and travels through the first part (fibre S_1) and becomes distorted (B). The OPC component replaces the different signal components with their phase conjugate (a signal component represented as a complex sample $a+bi$ is transformed into $a-bi$). This signal (C) is now transmitted along the second part of the link (fibre S_2). The distortion effects in S_2 now work on the modified signal and the result is that the resulting pulse (D) has the same shape as at the transmitter (A)²⁶. An

²⁵ It can be shown that theoretically the length of the two parts have to be slightly different and that the compensation only works perfectly for a single wavelength and not the full bandwidth of the signal.

²⁶ For simplicity we assume that we have no signal loss, though when implementing we need to compensate loss by amplification. Effects which cannot be compensated by OPC are considered negligible in this simplified explanation.

issue with OPC is that symmetrical power envelope before and after the OPC component is desired and because of this, Raman amplification is often proposed for OPC solutions.

2.5.7 Electrical Distortion Compensation

The use of electrical circuits to improve optical transmission links can be traced back to the early '70s [74]. Originally the techniques were mainly implemented to compensate for distortions originating in the electrical circuits at the transmitter and/or receiver. The end of the '80s saw an increase in interest in optimising them also for compensating for the distortion originating during the optical transmission [75]. In 2004 an ASIC came on the market capable of applying MLSE to a digitised optical signal (10 Gb/s) at the receiver [76]. Vendors have incorporated electronic signal processing into their telecom system²⁷ and in the R&D community other electronic compensating designs have been investigated and proposed. A review on electrical signal processing can be found in [77], more focused on dispersion compensation in [78] and on long haul in [79] with the latest updates reported during congresses in [80] [81].

2.5.7.1 Electric-optical and optical-electrical conversion

An issue in the use of electrical techniques is that the signals are transported in the optical domain and the correction for impairments is carried out in the electrical domain. So in between where the signal distortion occurs and where the distortion is corrected a conversion takes place between electrical and optical signals.

Ideally we would like to use a transmitter in which the electrical signals can control all parameters of the optical signal: intensity, phase, frequency, and polarisation²⁸ independently of each other and at the receiver a detector that can convert all these aspects of the optical signal into electrical signals.

While lab setups can be built that actually control and measure all these parameters in absolute levels, it is currently commercially unacceptable (because of complexity and cost) to suggest this for a commercial deployment. Because of this only a limited number of optical parameters are translated, describing the optical signal, into electrical signals (or a limited number of optical signal parameters are manipulated with electrical signals). The

²⁷ Most often without disclosing the exact nature of the DSP methods used.

²⁸ With polarisation being a two dimensional parameter in a single mode fibre

available modulation/detection technology will limit which parameters can be translated. Similar arguments have been made in chapter 2.5.3 in relation to the use of modulation formats. Only the parameters converted from optical to electrical (or vice versa) are available for (or can be conditioned by) the electrical signal processing implemented in the device. In addition there are limits on the range of these parameters. In general this discussion boils down to a discussion on the method used for the conversion and its capabilities.

For modulation, electrical to optical conversion, there are two main categories: direct and external. Direct modulation of the drive current of the optical source controls the envelope intensity with considerable distortion effects. External modulation controls parameters of an already created optical carrier and distortion is in general better controlled.

A consequence of external modulation is that the modulator does not control the signal parameters in an absolute way but manipulate them relative to their level generated by the external source. There are two important issues with this:

- Parameters of the signal generated in the optical source may not be constant and can vary. They can vary in two distinct different ways depending on their timescale: a noise-like variation of the level around a centre level and a more constant drift over a longer period.
- The absolute value of certain parameters may be unknown. Taking a laser as an example we can consider that the power of the laser is known in absolute levels (a laser can operate at a constant + 5dBm) but a parameter such as the phase is not absolutely known. Firstly because there is no absolute reference and secondly because there is no system in most CW sources that, once the signal leaves the laser cavity, ensures we always have a signal with the same phase at the modulator.

In addition a modulation technique developed for controlling one parameter of the signal can have an influence on other parameters. An example is the chirping of a direct modulated laser. When we increase the electrical signal driving a laser directly to increase the intensity and the lasing process starts, the laser jumps between different lasing modes. So if we use this method to intensity modulate then in addition to a change in intensity direct modulation will also introduce changes in frequency and phase.

A short overview of the most popular modulators²⁹ will be given, and their major effect in relation to distortion. More detail can be found in [82] [83] [43]. Simplified block diagrams of the use of modulators in transmitters are given in Figure 10 (In Figure 10, polarisation rotators, biasing circuits, amplification and other supporting circuitry are not shown, optical signals in red, electrical signals in blue).

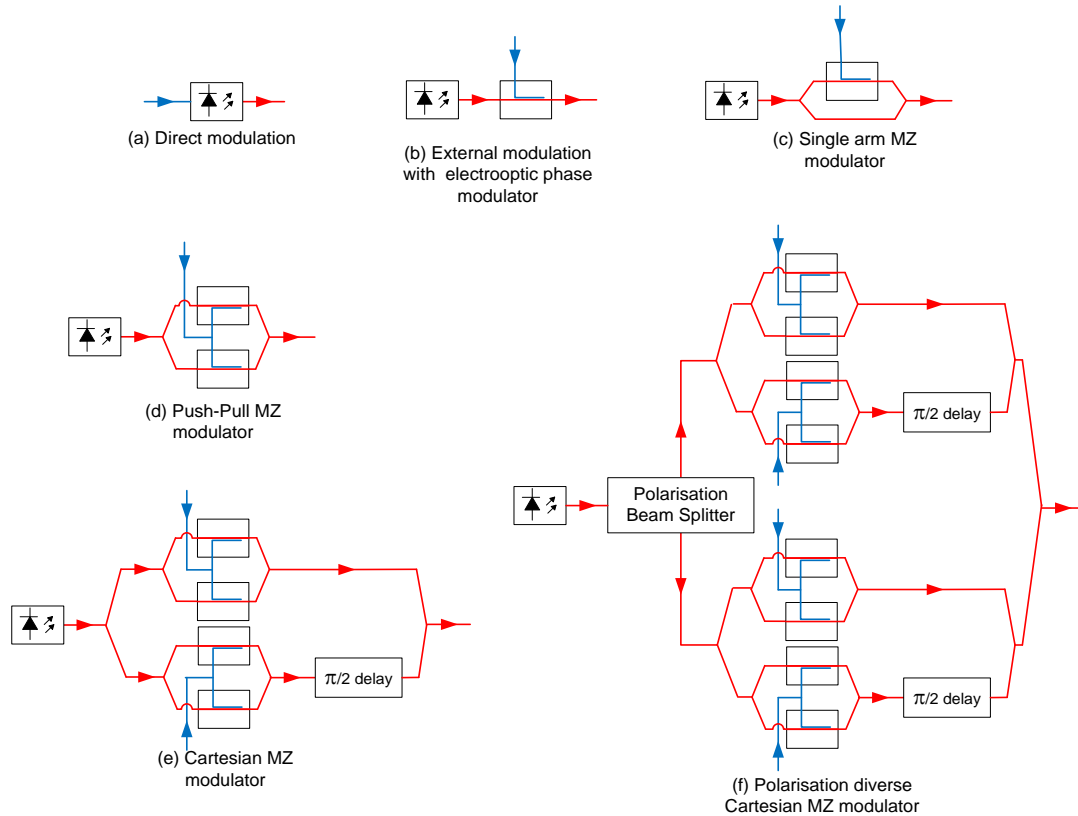


Figure 10: Block diagrams of modulation setups for an optical transmitter.

- Direct modulation: Envelope intensity modulation with considerable distortion effects on the pulse flanks ((a) in Figure 10).
- Electroabsorption modulator (EAM): Intensity modulation based on the Franz-Keldysh effect or the quantum confined Stark effect. Can be made so that the chirp they exhibit is low enough for even 100Gb/s [84] (not shown in Figure 10).
- Electro optic phase modulator: Based on the electro optic effect that the refractive index of some material can be changed by applying a voltage across it.

²⁹ There are many more variations possible I only mention some major types to be able to explain the choice made for the predistortion transmitter, the modulation formats have already been discussed in 2.5.3

This results in a signal delay on order of the wavelength of an optical carrier ((b) in Figure 10).

- Single arm Mach-Zehnder (MZ) modulator: An electro optic phase modulator is placed in one arm of a Mach-Zehnder construction so that destructive and constructive interference create intensity changes. The phase of the signal will also shift depending on the drive signal ((c) in Figure 10) [85].
- Push Pull MZ modulator: Two electro-optic phase modulators are placed in an MZ construction, one in each arm, and the internal waveguides are so placed that they experience inverse electrical fields. The result is that there is intensity modulation without phase shifts ((d) in Figure 10).
- Cartesian MZ modulator: Two Push-Pull MZ modulator are used to modulate two signal components with a 90° phase difference ((e) in Figure 10). The result is full control of phase and intensity parameter.
- Polarisation diverse Cartesian MZ modulator: two Cartesian MZ modulators are used to modulate two orthogonal polarised signal components ((f) in Figure 10). The parameters of each polarisation component can now be controlled independently of each other.

The electro-optic phase modulator is based on the principle that the refractive index of a material depends on the electric field applied to it. A typical material used in optical components for this is Lithium Niobate [86]. The electric field can be varied by changing the voltage applied to two electrodes placed on both sides of a waveguide. A result of the change of refractive index in such a structure is that the delay experienced by an optical signal passing through it changes.

In a Mach Zehnder structure an optical signal is split into two components. A different delay to the two signal components can be applied and the signal recombined. Because of the different delays, constructive or destructive interference will result during the recombination resulting in a change in the intensity of the signal. More detail on optical modulators can be found in [85]. The merits of the Cartesian MZ modulator in relation to predistortion are discussed in chapter 3.10 .

When applying these modulation setups they can be placed in serial configuration to influence multiple parameters of the signal, for example using an intensity modulator followed by a phase modulator. This is often done not only to be able to manipulate multiple parameters of the optical carrier but also to be able to generate the required

optical signal with relatively simple drive signals, such as a clock signal and binary data sequence in combination with bias settings. I mention this issue because an alternative use for the transmitter described in Chapter 5 is to create more complex drive signals, eliminating in some cases the need to place modulation components in series.

The common part in all optical receivers is the photodetector which performs the O-E conversion. The photodetector alone (Figure 11 (a)) works as an intensity envelope detector. A major issue with this detector is that the phase information of the optical signal is lost and that a single frequency component in the baseband at f_{baseband} is related to two frequency components in the passband signal $f_{\text{carrier}-f_{\text{baseband}}}$ and $f_{\text{carrier}+f_{\text{baseband}}}$. This is a major problem for distortion compensation because CD is a frequency dependent phase shift.

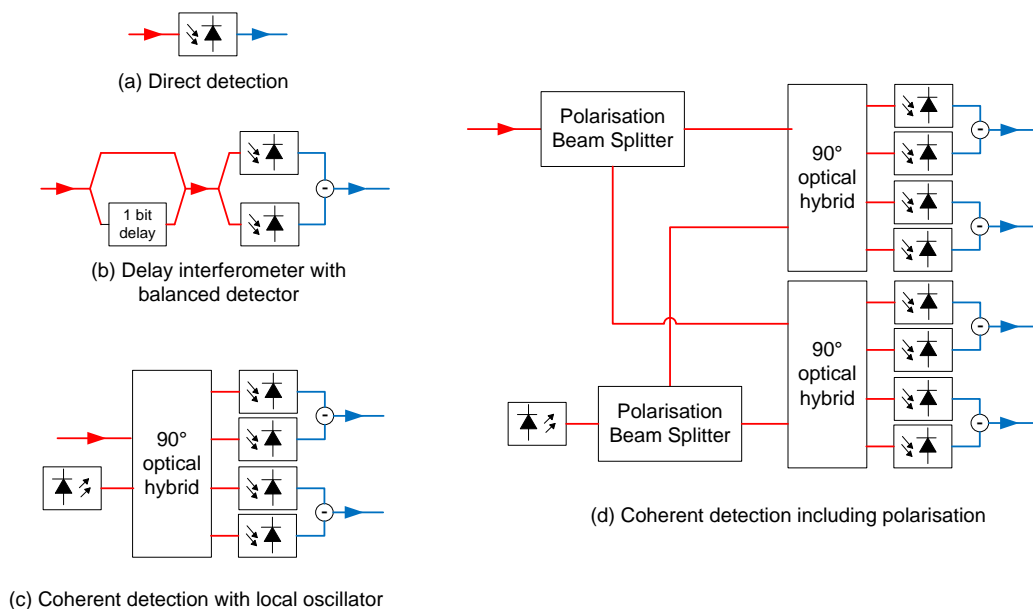


Figure 11: Block diagrams of optical receivers.

Detecting more than the envelope intensity is done in practice by interfering the received signal with another optical signal so that the intensity envelope after the interference is proportional to the other parameters to be measured. There are two major different sources that can be used for the interference: the (delayed) signal itself or a signal generated in the receiver. Interfering the signal with itself is naturally suited for differential phase modulation formats (Figure 11 (b)).

Receivers based on interference with a local source are known under the name of coherent detection (Figure 11 (c) and (d)). The current family of coherent detectors give us

the possibility to pass on phase and polarisation properties to the electrical domain for signal processing. This gives more possibilities for electrical signal processing. More info on coherent detection can be found in [87]. A review on how DSP in the receiver can be used in combination with coherent detection is given in [88]. There is a system combining DSP and coherent detection on the market for 40 Gb/s [49]. Standardisation committees are considering it for 100 Gb/s [48], vendors are showing prototypes and promising availability for end 2009 [49].

An alternative technique to extract the instantaneous signal intensity and frequency not based on a coherent receiver with a local optical source but on interference with a delay line is known under the name passive field detection, and has been published [89] showing simulation work for transmission distances up to 600km. As far as the author is aware, this technique has never been experimentally tested and to date has received little attention in publications.

2.5.7.2 Analog versus Digital Electronic techniques

In Figure 12 (a detail of

Figure 2) the signal flow at the receiver³⁰ end is represented (The discussion in the following paragraphs can also be applied to the transmitter where the components and steps would be presented in reverse order). The optical detection blocks described in 2.5.7.1 are to be placed in block M, Optical to Electrical conversion.

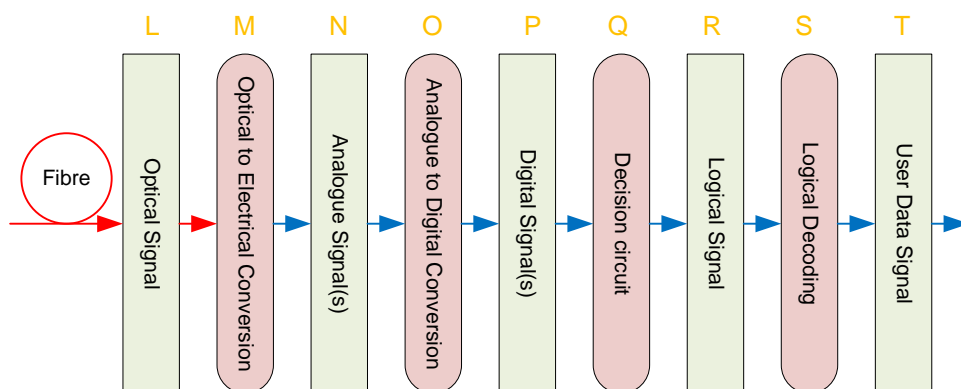


Figure 12: Signal in optical receiver.

³⁰ Not all systems fit exactly in this block diagram.

In current systems the blocks O, P and Q are often conceptually considered to be one step. This is because in on-off keying (OOK) systems there would only be a single analogue signal in block N to convert (a signal related to the intensity) and the A/D converter used would sample at the bit rate and have only 2 levels, directly giving the logical signal.

The analogue signal after the photodiode can be processed by different circuits. Proposals have been made to use passive analogue components, an example being the use of a microstrip with a coherent receiver to compensate chromatic dispersion [90]. More complex systems can be built by combining many active electronic circuits in an IC. Examples of this are SiGe based IC built for 10 Gb/s [91] and 40 Gb/s for binary intensity based formats [92].

In the concept shown in Figure 12 the Digital Signals in block P represent digitised version of the analogue signals present in block N (representing different optical parameters as discussed in 2.5.7.1) and determining the logical data out of them is carried out in block Q. If we now want to use a certain electrical signal processing method working on signals representing the detected parameters, the analogue circuits in block N can now be used or they can be realised with digital electronics in block P. The major advantages and disadvantage of implementing them in analog or digital format are presented in Table 2.

Analog	Digital
No advanced ADC/DAC needed.	Performance of ADC/DAC may limit the performance of the DSP design.
Can operate on continuous or on discrete samples in time.	Can only work on discrete samples in time.
Designs can be made which are in general lower in power consumption than digital.	Can use digital technology, e.g. CMOS, not well suited for analogue circuits
Linearity, reproducibility, precision, testing are issues because of analogue nature of circuits.	Linearity, reproducibility, precision, are limited by number of bits in digital representation.
Analysis, debugging, simulation etc. are difficult.	Analysis, debugging and simulation is easier (register reads and digital simulation methods possible).
Lower noise figures are possible.	Noise is determined by number of levels in ADC/DAC conversion.
Limited flexibility.	Can be defined /controlled by software or

	firmware, can also be implemented with reprogrammable devices (FPGAs).
Susceptible to external noise /interference (power supplies, etc.).	Only the DAC/ADC are susceptible to external noise/inference.
Low complexity because of practicality of design capabilities.	Complexity can be much higher, limited by number of gates available on the IC.

**Table 2: Analogue versus digital signal processing.
Table based on [81, slide 4] with minor modifications.**

Digital techniques to process signals are a very common form of electronic signal processing and an introduction can be found in [93]. Using Digital Signal Processing (DSP) for optical signals is however less common. From the issues presented in Table 2 a key factor for this is the limited availability of ADCs/DACs with sufficient sampling speed and signal levels.

While the minimum sampling speed and signal levels depend on the distortion compensating method applied and the acceptable transmission quality, I start from the point of view that a sample rate of at least 1 to 2 samples per bit³¹ with at least 4 bit resolution are desired.

In terms of the current technology available, 22 GSamples/s 6 bit DAC [94] and 24 Gsamples/s ADC [95] have been presented in papers and the use of these designs for optical telecommunication has been noted in [81]. In [96] a 100 Gsamples/s ADC product was announced (3Q 2009) based on research published in [97] in which 150 Gsamples/s sampling was shown. While this shows the technical possibility to achieve these performances it does not mean that they are available for system design. Issues that may prevent this are:

- The device may not be capable to achieve this performance in a continuous way.
- The design may be built as an unmoveable lab setup.
- The designs may be developed and owned by a private company which may not wish to make the design available to other parties.
- The design may only be available for integration into a bigger ASIC and not as a standalone part and so is not suitable for a project or vice versa.

³¹ Assuming one bit per symbol modulation formats.

- The design may be based on a particular IC technology (CMOS versus BiCMOS discussion) which may not be suited for the rest of the circuit if using the ADC/DAC as part of an ASIC.

For this project I had to focus on a discrete DAC component because the development of an ASIC was not a viable option for reasons discussed in section 2.5.7.3.

The fastest suitable discrete component DAC I knew to be commercial available during this project was a 25 Gsamples/s 6 bit DAC model (ENOB: 5.5 bit, availability since January 2008) and an ADC of 30 Gsamples/s 6 bit (ENOB: 4.5 bit, expected to be available end 2009) [98]. The underlying technology is known as b7hf200 (SiGe) from Infineon [99]. A device from this family was used in this project. Another product that was available achieved 12 GSamples/s (8 bit DAC, 10 bit ADC, SiGe BiCMOS) [100].

With these sample rates, the starting assumption of 2 samples/bit and 4+ bit resolution, and the commercial bit rate intervals of 4x, it became clear that I would have to focus on 10 Gbaud systems.

A note to make is that the four DAC/ADC components mentioned are estimated³² to be currently (2Q 2009) costing well above £10,000 per component and this price is limiting their use for commercial transmitters or receivers. They can be used to demonstrate and assess the feasibility of a proposed design that for commercial deployment would have to be constructed in a more cost effective way.

2.5.7.3 FPGA versus ASIC

The digital electronic circuits used to apply digital electronic processing to the signal can be realised in a number of ways:

Discrete interconnected electrical components can be used. This is only feasible if the circuit consists of a relatively low number of components (and interconnects). The DSP algorithms we propose in this work are implemented with millions of digital gates and so it is impractical to consider building them of discrete components, only representing a single logic function (even if one component combines the functionality of multiple gates). In addition the required data speeds (10Gb/s divided over a parallel bus) and synchronisation issues do not favour discrete components.

³² Exact pricing is confidential commercial information and subject to market conditions.

This leaves two major candidates for building the DSP: the custom Application Specific Integrated Circuit (ASIC) and the Field Programmable Gate Array (FPGA)³³. We will present a more detailed introduction in the capabilities and working of FPGAs in 5.2. Here we will focus on the differences/parallel between them.

The discussion of ASIC versus FPGA for an IC design can be very complex with many difficult to quantify, subjective, and project-dependent arguments on both sides [101] [102] [103] [104]. We will try to summarise, focusing on the ones that were crucial for our project.

For an application designer point of view, the technical difference is that with an ASIC, the design is translated into a physical design of layers of electronic material, and this design is then built at an IC foundry. If the application designer uses an FPGA then the design is translated into a configuration that is loaded onto an existing programmable standardized IC.

We can develop circuits for both with ‘user friendly’³⁴ development tools using the same higher level function descriptive languages (VHDL, Verilog, SystemC,..) and for both, advanced simulation tools exist to test and debug the design before committing to hardware. I will discuss this process for FPGAs in more detail in 5.7.1. The process is similar for ASIC. A consequence of both technologies being designed in the same higher level descriptive languages is that it should, in principle, be possible to develop a design in both technologies without requiring a change in the design (or be migrated from FPGA to ASIC technology, the reverse ASIC to FPGA is less common). This is however only true in principle [105].

- A design will make use of underlying libraries. These libraries available for one technology might very well not be available for another. Specifically, a design carried out for an FPGA will use complex blocks on the FPGA for which the FPGA manufacturer has only disclosed external interfaces and not the internal design. If translating this FPGA design to an ASIC, the designer will have to additionally design these blocks (or, if possible, acquire them from a third party).

³³ There exist other IC products like gate arrays, structured ASIC’s, fuse base FPGAs etc. They were considered and they have very similar pros and cons to FPGAs and custom ASICs.

³⁴ User friendly compared to older design techniques, they still require specialised engineering skills.

- Similarly an ASIC design may make use of design optimisation on a level lower than the descriptive language (like a very high performing DAC/ADC in our case) or having parts which cannot be described in higher level language (such as mixed design using analogue and digital signals on the same substrate. It is unlikely that an FPGA would be available that could combine these for a particular application ³⁵)
- If translating from one technology to the other, an issue might be that the complexity and required performance of one technology (most likely ASIC) design cannot be achieved in the other (most likely FPGA) and that the design tools will never be able to synthesise or achieve timing closure during the design process.
- Thirdly programming styles and techniques for achieving optimal performance for both technologies differ. A good design for an FPGA might well result in a bad design for an ASIC.

Because of these points it is more correct to say that a design for an FPGA or ASIC can be translated by a skilled engineer(ing team) into the other technology, especially if this has been taken into account during the original design.

The design limitations are different for an ASIC and an FPGA designer. An ASIC designer is limited by the limits imposed by the foundry (such as mask size, smallest feature, layers available etc.) and the underlying physical characteristics of the technology (switching time of the used gates etc.).

An application designer for an FPGA is limited by the available FPGAs and their published capabilities (in both cases related to the budget that is available to spend on the device) This is related to the fact that FPGAs are made in large numbers to support many applications. The FPGA designer will design the FPGA chip so that it is an economically acceptable product for the business and not optimise it for one particular application. As a consequence the features and performance implemented on the available 'real estate' of the FPGA have to be balanced. During meetings with FPGA vendors we encountered this issue regularly. An example we discussed with them was the possibility to have an FPGA with 10 Gb/s interfaces (which would have made it possible for us to achieve higher

³⁵ FPGA with analogue circuits do exist and are called mixed-signal FPGAs but they are a very limited and specialized product category.

optical transmission speeds). The vendor confirmed it was possible to build such a device but that with the current market conditions they had no plans to do so. Another supplier offered us an FPGA with internal 2 GHz data crossconnects (making it possible for us to reduce the internal bus width of the data stream) but with insufficient DSP logic blocks for the application we envisioned. This was because the vendor had used the chip's real estate to implement processing blocks for looking at the headers of IP-packets. (In this last case an interesting remark to make was that the product was eventually dismissed not because of its hardware capabilities but because our design team was not familiar with the software tools supporting it).

After choosing the FPGA most suited for the project it did not, however, incorporate all the functionalities required for the complete design, so it required adding additional external discrete components (clock generators, delay lines, DAC, power amplifiers) making the full setup table-top sized. If we had opted to use an ASIC many of these functionalities could have been incorporated, resulting in a design occupying a single PCB. In our case the digital nature and maximum port speed were fundamental limitations that were solved by additional discrete components, and the dimensioning between them will be discussed in 5.1.

Because an ASIC designer can tweak and optimize the design at the physical level, if necessary, the resource utilisation can be optimized and an IC foundry can be selected with the latest and optimal technology for his application. As a consequence he will be capable of system designs which achieve higher performance while consuming less power and have a more compact solution. From this point of view we would prefer to use an ASIC for our design to be able to achieve maximal performance.

The major issue with ASIC design is cost. Firstly there is the financial cost, the payment required to a foundry to build an ASIC from a design you deliver. While exact figures depend highly on the design and market conditions a single ASIC build was estimated to be of different order of magnitude compared to an FPGA. The FPGA used as a list price of approximately £5,000 [106]. Ordering a single ASIC with similar technology and complexity was estimated to be in the £500,000 range [107]. The cost of producing a single ASIC comes down when ordering many units because many production costs, especially the making of the masks, only have to be carried out once when making many ICs, so that at a certain volume the cost of an ASIC becomes lower than that of an FPGA. Break even point is often quoted to be on the order of tens of thousands to hundreds of thousands of units

[108 p. 164]. For the realisation of an experimental transmitter this is not applicable because we did not plan to produce more than a handful of the ICs, but it can be an issue if the design is considered for mass production (although this quantity of production is rather unlikely for a long haul telecom transport product). In addition to the production cost, the cost of tools (including software) and the required support team is in general higher for ASICs than FPGAs. The total Non-Recurring cost (so called NRE in the references) quoted for a single ASIC is in general in the +\$1M range [108 p. 164] [107]

The issue is however not just the financial cost for an ASIC. Ordering an ASIC is a much more complicated process than an FPGA. FPGA are stocked by distributors and can be bought 'off the shelf' (maybe with some months of factory lead time for an uncommon part) and standard development boards do exist for them. When ordering an ASIC, good relations between the application engineering team and the foundry are essential (e.g. if the team regularly orders ASICs from the foundry). This is related to the point that the application designer needs to understand the limitations and possibilities of a particular foundry, that the design needs to be handed over to a foundry team so tools and formats need to be compatible between them (i.e. they use the same software tools). The substrate built by the foundry needs to be packaged so that it is compatible with the test setup of the developer. Because an ASIC is customised the supporting circuitry (power supply, clocking, grounding, RF feed circuits, external lumped components etc.) need to be designed and built. Even with foundries focused on low production, for R&D, all these issues make ordering a ASIC much more complicated if the design group has no experience with this, in comparison to using FPGAs. Some of the statements made here are illustrated in the brochure [99] for the ASIC technology that was used to produce the DAC we used as described in chapter 5.

An additional issue is that once an ASIC has been designed and built, its functionality is fixed. So if a design is made with certain errors (or new improvements are proposed) and they are not included during the design phase before handing the design to the foundry they cannot be corrected on the built IC. The only option is then creating a corrected new design and producing a new IC by forwarding a new design to the foundry, and paying the build fee a second time³⁶. In addition to the financial cost there are also time issues. The time between forwarding a design and having a functional device is often measured in

³⁶ Sometimes foundries quote for a single fee including multiple prototypes.

weeks to months. In contrast an FPGA design can be converted into a program file for an FPGA on a standard PC quickly (for our designs it took, depending on synthesis engine and method, minutes to a couple of hours to obtain program files from design files) and then to programme them on the FPGA (without even removing the IC from the setup).

We can summarize this by saying that, for an application developer, an ASIC delivers better performance, better integration of components and a lower cost of mass production but requires a much higher design effort and much higher budget. Using an FPGA compromises the achievable performance and limits ambitions to the capabilities of the FPGA. Using additional discrete component can be a solution for some limitations, and using FPGAs significantly lowers the required design cost and effort.

Because of these arguments the use of an ASIC was never considered a realistic option for our project, while we understand that for an actual commercial product an ASIC might very well be the only viable option [81] because of required performance, though with a question mark on the issue of whether it is an economical viable option for the given application.

2.5.7.4 Tx versus Rx based electronic signal processing

As mentioned in Chapter 2.2 distortion combating methods can be applied at different positions in the link. If we do not want to introduce additional O-E-O conversion in the system (this option is mentioned in section 2.5.7.7 on electronic regeneration) we have two options: electronic signal processing at the transmitter or at the receiver.

Distortion compensation at the transmitter can only be used for deterministic effects. We will discuss this issue in more detail in chapter 3.3. At the receiver the inserted compensation circuits can also work to improve non-deterministic effects (especially noise).

Another issue is that feedback signals indicating the quality of a terminating layer of the transmission link are present at the receiver. So if we implement the distortion compensation at the receiver we can use this feedback without sending it through the network to the transmitter. Not sending it through the network means that for this feature we do not need inter-node communication and that the delay related to this inter-node communication is not present. Having these feedback signals locally available makes

it easier to design a system where the applied distortion compensation can be tuned so it is optimal.

A technological issue is related to the previously discussed issue of O-E and E-O conversion in combination with the ADC or DAC if we consider digital instead of analogue circuits. As explained in 2.5.7.1 we use different components for E-O O-E the transmitter and receiver and also different components to manipulate/extract the different properties (intensity, phase and polarisation) of the signal.

To structure the discussion, we can divide it up into three categories most often considered in the literature when proposing signal processing:

- intensity
- intensity + phase
- intensity + phase + polarisation

The order and grouping of these three categories is a compromise between achievability and expected performance. Building a circuit using only intensity modulation is the easiest option with the most limited performance improvement. Having all three parameters available is the most costly and complex to build but is expected to give potentially the biggest performance improvement.

The first category with intensity information only is being investigated and the currently achieved results are limited by fundamental issues (the previously discussed issue of frequency dependent phase shift due to CD) or technical issues because of the complexity in case of an MLSE-based filter. The performance of these methods is discussed in more detail in 2.5.7.5 after presenting possible filter blocks. The next logical step to investigate is intensity + phase, while increasing the capacity by also adding polarisation is left for future research.

Ignoring, for the moment, the achievable performance of systems having access to intensity and phase at the transmitter or receiver, we can focus on the complexity to implement them into a device at either location.

As discussed in the previous paragraph, to have these two components available at the receiver, a coherent receiver is required. At the transmitter we will propose to use a Cartesian Mach-Zehnder (with a Push-Pull Mach-Zehnder as alternative). Of these two

components the Cartesian Mach-Zehnder is more commonly available than the coherent receiver (and so is cheaper, quicker to obtain, more compact, etc.)³⁷.

To use electronic digital filters it is required that the signal be converted from the digital to analogue domain by a DAC at the transmitter or from analogue to digital at the receiver as discussed in 2.5.7.1. From the data presented there we recall that for the same IC technology, a DAC was available earlier, (Jan 2008 versus end 2009) than an ADC. It was explained to us by the supplier that designing a DAC is easier than an ADC and the company developed a DAC and then used the experience gained in that project to design the ADC. So the availability of better performing DAC over ADC is not just coincidental. This also had an influence on the choice of transmitter versus receiver.

While this is the current status for this project it might be that in the future, if the sampling rates go up, ADC solutions are preferred over DAC [79], especially for integrated solutions where signal processing and analogue-digital conversion are done on the same substrate. A key point is that it would be easier to create a cost effective ADC on the same substrate as the signal processing logic because CMOS is more suited for an ADC while a DAC would require more expensive BiCMOS technology [81].

The digital circuits applying the digital compensation algorithms to the signal and the DAC/ADC require clock signals. Because we used a small number of samples/symbol (2 in our case) it is important that the processing blocks of the samples are clocked synchronously with the data stream. Having such a synchronous clock is easier to achieve at the transmitter than at the receiver. At the transmitter the bit stream is created so we can use a single oscillator as clock source for all components including bit stream creation, the DSP and the DAC. At the receiver, the source of this common clock has to be retrieved out of the incoming bit stream, because the incoming signal will be the reference with a certain amount of wander that must be tracked. Extracting this clock from a highly distorted signal is not easy. Current commercially available clock recovery modules will not be able to lock onto the signal and recover the signal if significantly distorted. This dilemma can be solved by having a local oscillator with a clock which is close but not exact, and through an iterative algorithm the local clock is adjusted until it runs synchronously with the data. While such systems are very common for modestly distorted

³⁷ In the last 2-3 years, since the start of this research, the availability of coherent receivers has improved.

signals, acquiring or designing one for a signal as heavily distorted as proposed in this work is a major task. When using predistortion at the transmitter the clock recovery at the receiver can be a standard off-the-shelf component making implementation much more feasible.

Some other issues that have been raised in relation of the choice transmitter or receiver DSP are [81]:

- The number of bits required to represent the signal input to the systems is, in general, lower for the transmitter than the receiver leading to fewer gates needed to implement a similar DSP scheme at the transmitter than at the receiver.
- If we concentrate our DSP at just one end of the link (Tx or Rx) we can use a simple standard implementation for the system at the other end of the transmission link.
- If we implement DSP in a chip we could add other functionalities such as soft FEC on the same chip.

In conclusion, we assessed that building real time processing at the transmitter was technically a more straightforward goal than doing it at the receiver, and hence may be an attractive option for future commercial systems for this reason. This approach was investigated in this project.

We will investigate the issues related to predistortion in more detail in chapter 3.

2.5.7.5 Proposed digital signal processing blocks

While in theory we can manipulate the digital sampled signal with the full mathematical toolbox available, in practice only a limited number of components are considered in DSP for high speed telecommunications.

First of all we have the simple function such as addition and multiplication often not even mentioned because considered so 'basic'. In addition we have supporting blocks such as resampling and Discrete Fourier Transform (DFT) which are very important to make DSP possible but which are in most case not designed to actively improve the signal. Three types of signal processing blocks reappear in many studies:

- The Feed Forward Equalizer (FFE) constructed with a Finite Impulse Response Filter (FIR).
- Decision Feedback Equalizer (DFE) constructed with an Infinite Impulse Response Filter (IIR).
- The Maximum Likelihood Sequence Estimation (MLSE) and derivatives in which a (received) signal is compared with possible waveforms and the most likely bit sequence is selected.

These filters are used alone or are combined together with different levels of complexity and methods to optimise the parameter settings. Different transceiver module vendors are now incorporating them in their modules without disclosing the exact setup used.

More complex DSP blocks have been proposed. An example is [109] where the DSP performs real time solution of the NLSE. According to the authors, the complexity of this is, even with further optimisation, still an order of magnitude away from what the most advanced FPGA available can achieve. Another approach is using a Turbo Equalizer in combination with FEC coding which can give a 1 dB required OSNR gain for 40 Gb/s [78].

2.5.7.6 Performance of electronic distortion compensation

The use of electrical filters at the receiver based on FFE and DFE in combination with intensity based modulation formats using direct detection does give a signal improvement but only for lengths up to 100-200km (10Gb/s transmission, NDSF fibre) because of the loss of phase information [110]. MLSE makes transmission lengths of up to 1000 km theoretically possible [111]. To be able to achieve this the number of gates required is so high that the required technology to implement this will probably not be available in the foreseeable future [112]. This is illustrated by [113] where in 2006 a MLSE implementation was shown compensating distortions from dispersion equivalent to that of approximately 250 km of NDSF fibre in combination with the use of duobinary modulation.

When used in combination with SSB/VSB better performing distortion compensation can be achieved. In a specific system employing OOK with filters, a BER of 5×10^{-4} after 240km without SSB was reported, while with SSB modulation transmission over 400 km was achieved [114]. This was for 10Gb/s over NDSF. More detail on SSB with analogue electrical distortion filtering is given in [115] [116] and with digital filters in [55]. It should

be mentioned that this technique was implemented in the past with a transmitter similar to the one described in Chapter 5 [110].

Placing digital filters and DACs in a custom ASIC at the transmitter (predistortion) in combination with a Cartesian modulator has been shown to compensate in real time chromatic distortion up to 1600 km (10 Gb/s DPSK) [117], and a similar setup but with off line calculation was capable of achieving a transmission distance of 5120 km [118].

Applying MLSE to 42.7 Gb/s with DQPSK formats (18 dB OSNR, BER 10^{-3} , 2x4 state MLSE, delay interferometer detection) increased the amount of compensatable dispersion from 230ps/nm (13 km NDSF) to 310 ps/nm (18 km NDSF) [80].

If we combine these DSP blocks with coherent detection better results can be achieved (this is explained in 2.5.7.1.). The compensation of chromatic distortion would be limited by the size of the implemented filters and equalizers, and distance up to 40,000 km (2501 taps FFE filter) of NDSF are considered feasible [88] and distances of 6500km (40.2 Gb/s, BER 3×10^{-3}) have been demonstrated using off line filtering. Research on the maximum achievable distances and the effect of NL distortion on the performance are ongoing.

The possibility of feedback signals optimising the DFE/FFE filter was demonstrated in [119] (40 Gb/s, back to back operation).

2.5.7.7 Electronic regeneration

Electrical Regeneration is a very effective method to clean up distortions. It consists of inserting an additional Optical – Electrical –Optical (OEO) conversion step in the transmission link. In the electrical stage the signal will then be Retimed and Reshaped and because the optical signal is transmitted on a newly modulated carrier it will also have the required power, achieving Reamplification (resulting in so called 3R regeneration) without the necessity of an optical amplifier. It can include termination of protocol layers of the signal (a classic example is the Regeneration Section overhead data of the SDH protocol). It will remove all optical distortions from the signal with the possibility that some are translated into bit errors. You could consider this technique as sectioning a long optical transmission link which induces too much distortion (and other effects) into many smaller links with each complying within the limits set for signal quality.

2.5.8 Combined approached

While to aid understanding of the issues all the compensation techniques have been described as standalone methods, it is important to remark that, except for particular research setups and in links where distortion is not an issue, they do not need to be used standing alone. In practice they would be combined in a telecommunication system and would complement each other to achieve the desired overall system performance

2.6 Summary

The distortion of optical signals during transmission is theoretically well known and can be described very accurately mathematically.

To counter these distortions, a range of methods are available. Out of this range the system designer can choose a combination of methods to achieve the required result. Technical feasibility and economical considerations limit, more than fundamental issues, the methods applied to correct distortion in systems.

The range of methods available and their combined use mean that an almost infinite range of solutions are possible for combating distortion. Only those solutions expected to be the most promising are being investigated by the research community. Because of the complex interaction of the distortion effects, this research does not give an analytical view of the methods in general, but analyses their effectiveness in particular scenarios.

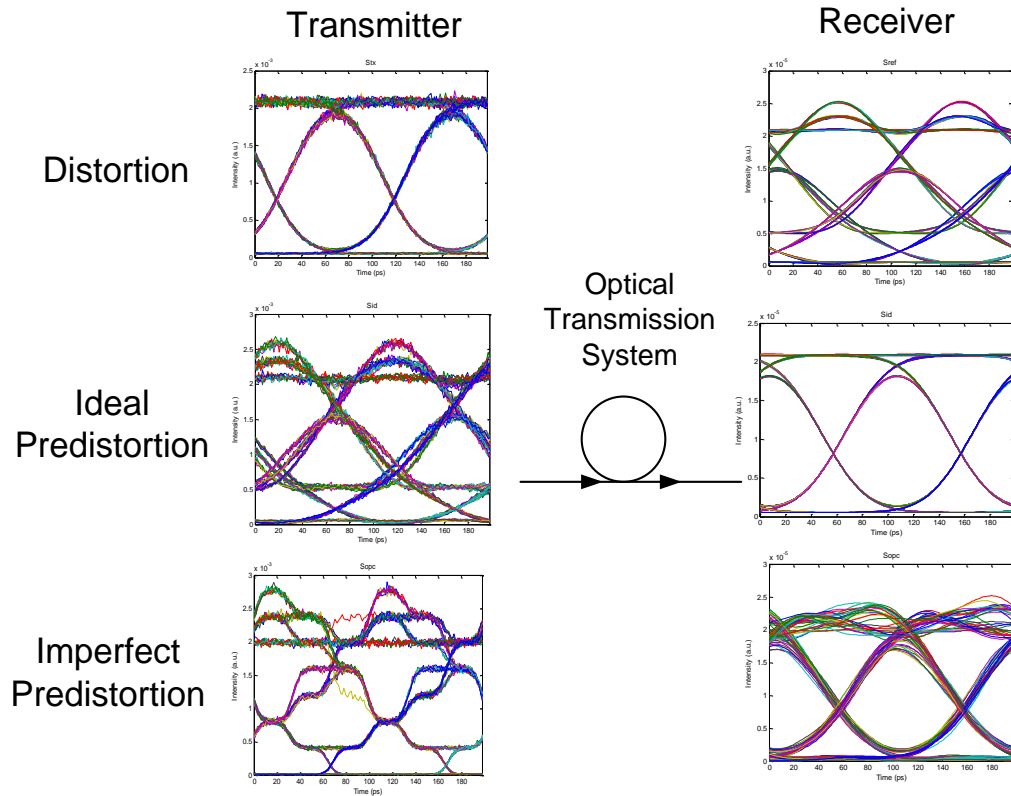
When exploring digital electronic processing for optical systems we mark the importance of selecting a realistic technology. In our particular case this means the use of FPGAs instead of an ASIC to bring the transmitter within practical and financial reach of the researchers. Also, the choice of predistortion instead of electronic filtering at the receiver is partly based on implementation criteria because of the availability of components and to minimize complexity of the system.

3 Digital Electronic Predistortion

In the following sections we will discuss some aspects of EPD mainly to illustrate the working principles and ideas behind EPD. They also show, complemented by simulation results in chapter 4 why certain choices were made during the development of the EPD transmitter described in Chapter 5. Hence they do not always present final conclusions on EPD but act more as the motivated assumptions underlying the design.

3.1 Principle

In relation to the overview of compensation techniques presented in Chapter 2, digital electronic predistortion, the techniques discussed in section 2.5.7, is a form of Electrical Distortion Compensation, with the distortion combating circuits placed at position E in Figure 2. We will use a Cartesian MZ modulator (e) in Figure 10 in combination with direct detection (a) in Figure 11. The underlying principle of predistortion is that if we know how a signal will be distorted during transmission, we can anticipate this distortion when creating the signal at the transmitter. This is illustrated by Figure 13. The figure shows three different signals, all using NRZ modulation, transmitted across the same (simulated) optical transmission system. For the simulation we used the ONG simulator. The signal was represented by 256 bits at 10 Gbit/s with 64 samples per bit and double real for accuracy of the I and Q components. The receiver filter was a 5th order low pass Bessel filter with 10 GHz passband bandwidth. For a more detailed description of the simulations I refer to chapter 4. Polarization modelling was disabled in the fibre code. The six diagrams in Figure 13 plot the optical power versus time with multiple bits overlaid giving the eye diagram of a pulse train. The top two graphs show that if a Gaussian pulse is transmitted over a fibre, the signal at the receiver arrives distorted. In the two middle graphs the signal is shaped so that when it goes through this particular transmission system the received pulses have optimal properties. Because of technological limitations we cannot create this 'ideal' predistorted pulse. In the bottom diagrams we have assumed we are restricted by quantisation in time, amplitude and phase in combination with limited bandwidth components. However, even with the imperfect electronic predistorted signal it can be seen that the eye at the receiver is of a better quality than a signal that has not been predistorted at all.



Simplified representation (eye diagrams generated by simulation, 10 Gb/sec, 100km standard optical fibre, unrealistic low noise level, only chromatic dispersion and self phase modulation simulated, optimal Rx filters)

Figure 13: Principle of predistortion.

3.2 Overview of published research

Predistortion of the optical pulse has been considered at least since the 1980s [120] [121]. It was often limited to intensity shaping (no phase control) and practical implementation was not considered feasible. Interest in it was revived around 2005 when the technological advance of signal processing and modulators made this method possible for transmission at 10 Gb/s.

An overview of publications in table format is presented in Table 3. In Appendix B full standardized references of the publications can be found. For acronyms used see Appendix A Abbreviations and Acronyms. The research group column groups together collaborating researchers based on the author list. It does not imply that the publication, the research or the author is employed or sponsored by the company or organisation

Publication Date	Place of Publication	First Author	Research Group	Title	Comments	Ref.	Related Pub.
Jan 2005	JLT	M. M. El Said	Nortel	An electrically pre-equalized 10-Gb/s duobinary transmission system	Analog implemented FIR filters	[122]	
Mar 2005	PTL	R. I. Killey	UCL	Electronic dispersion compensation by signal predistortion using digital processing and a dual-drive Mach-Zehnder modulator	Principle using LUT for CD and NL EPD incl. simulation results	[123]	[124]
Mar 2005	OFC	J. McNicol	Nortel	Electrical Domain Compensation of Optical Dispersion	Continuous ASIC implementation	[125]	[126]
Mar 2005	OFC	D. McGhan	Nortel	5120 km RZ-DPSK Transmission over G652 Fiber at 10 Gb/s with No Optical Dispersion Compensation	Off line EPD with linear filter with PPG	[118]	[127]
Sept 2005	ECOC	R. I. Killey	UCL	Electronic precompensation techniques to combat dispersion and nonlinearities in optical transmission		[128]	
Sept 2005	ECOC	P. J. Winzer	Bell Labs	Electronic pre-distortion for advanced modulation formats	Focus on CD EPD for OOK, DPSK and QDPSK	[129]	
Sept 2005	ECOC	R. J. Essiambre	Bell Labs	Fibre Nonlinearities in Electronically Pre-Distorted Transmission.		[130]	
Dec 2005	Sem. IEE	P. Watts	UCL	Techniques for long haul transmission without optical dispersion compensation.	Add. details on EPD in combination with SSB.	[131]	
Dec 2005	PTL	D. Walker	Nortel	960-km Transmission Over G.652 Fiber at 10 Gb/s With a Laser/Electroabsorption Modulator and No Optical Dispersion Compensation	Use of Direct modulated Laser for intensity and EAM for phase control instead of MZ	[132]	
Jan 2006	PTL	K. Roberts	Nortel	Electronic precompensation of optical nonlinearity	Experiment, off-line EPD linear + non linear filter	[133]	
Mar 2006	OFC	R. J. Essiambre	Bell Labs	Impact of fiber nonlinearities on advanced modulation formats using electronic pre-distortion		[134]	
Mar 2006	OFC	A. Klekamp	Alcatel	Nonlinear limitations of electronic dispersion pre-compensation by intrachannel effects.		[135]	
Mar 2006	OFC	R. I. Killey	UCL	Electronic dispersion compensation by signal predistortion.	Combination LUT + FIR proposed	[136]	
Mar 2006	OFC	X. Liu	Bell Labs 2	A fast and Reliable Algorithm for Electronic Pre-Equalization of SPM and Chromatic Dispersion		[137]	
Aug 2006	PTL	C. Weber	TU Berlin	Electronic precompensation of intrachannel nonlinearities at 40 Gb/s	CD compensation by DCF, NL by EPD	[138]	
Sept 2006	PTL	R. J. Essiambre	Bell Labs	Electronic predistortion and fiber nonlinearity.		[139]	
Sept 2006	ECOC	P. Watts	UCL	An FPGA-based Optical Transmitter Using Real-Time DSP for Implementation of Advanced Signal Formats and Signal Predistortion	Details on FPGA with discrete DAC design	[2]	
Sept 2006	ECOC	M. Birk	Nortel	WDM Technical trial with complete electronic dispersion compensation	WDM field trial by AT&T of Nortel system.	[117]	
Jul 2007	Opt. Exp.	A.J. Lowery	Monash Univ.	Fiber nonlinearity pre- and post-compensation for long-haul optical links using OFDM		[140]	
Jul 2007	PTL	R. S. Luís	Nokia-Siemens	Dispersion Management of Electrically Precompensated RZ Single-Sideband Signals at 10 Gb/s Without Inline Dispersion Compensation		[141]	
Jul 2007	ICTON	M. Glick	UCL/Intel	Electronic Signal Processing to Improve System Performance of Optical Interconnects.	WDM crosstalk pre and post compensation.	[3]	
Oct 2007	JLT	P. Watts	UCL	An FPGA-Based Optical Transmitter Design Using Real-Time DSP for Advanced Signal Formats and Electronic Predistortion		[5]	
May 2008	PTL	R.S. Luis	Nokia-Siemens	XPM degradation of dispersion-precompensated intensity modulation direct-detection systems without inline dispersion compensation		[142]	
Jul 2008	Opt. Exp.	P. Watts	UCL	10.7 Gb/s transmission over 1200 km of standard single-mode fiber by electronic predistortion using FPGA-based real-time digital signal processing		[7]	[6] [8]
Sept 2008	ECOC	C. Weber	TU Berlin	Impact of fibre nonlinearities in electronic dispersion compensation systems at 40 Gb/s	Single DWDM channel	[143]	
Oct 2008	COIN	Y. Konishi	Mitsubishi	A novel flip-flop based look-up table in digital signal processing for optical communications	Design does not include NL EPD	[144]	
Oct 2008	COIN	T. Sugihara	Mitsubishi	Practical Implementation of Precoding Technologies in High-speed Optical Transmission. in 7th International Conference on the Optical Internet		[145]	
Nov 2008	Ann. Meet. LEOS	D.J. Geisler	Univ. of California	360 Gb/s data modulation with dispersion precompensation using optical arbitrary waveform generation	Carrier is comb signal instead of single f.	[146]	[147]
Mar 2009	OFC	C. Weber	TU Berlin	Fibre Nonlinearities in 10 and 40 Gb/s Electronically Dispersion Precompensated WDM Transmission	Multiple DWDM channels	[148]	
May 2009	Opt. Exp.	R. Waegemans	UCL	10.7 Gb/s electronic predistortion transmitter using commercial FPGAs and D/A converters implementing real-time DSP for chromatic dispersion and SPM compensation.	The work of this thesis	[1]	
Aug 2009	JLT	T. Sugihara	Mitsubishi	Electronic Predistortion by Polar Coordinate Transformation Using the CORDIC Algorithm		[149]	

Table 3 : Chronological overview of major publications on predistortion.

named in this column. The comment column is used to differentiate publications if similar titles are present, not to summarize the publication. Related Pub. column refers to other publications with content closely related to the publication.

3.2.1 Proposing phase and intensity based predistortion

A proposal to apply two FIR filters (in an ASIC using analogue circuitry processing the drive signals) at the transmitter to compensate distortion in a system with duobinary modulation was published in Jan 2005 [122]. This paper focused on using predistortion as part of a general analysis of the use of the duobinary format for transmission.

In March 2005 a paper by R. Killey and co-workers from UCL, proposed predistortion as investigated in this thesis [123]. They described the method of using a MZ modulator in combination with digital filtering to predistort phase and intensity of an optical signal and presented expected single channel system improvements depending on the parameters used for the predistortion.

At the OFC conference in March 2005 material on predistortion was shown by two research groups. Members of the Optical Network Group from University College London (UCL) presented the general principle and theoretical analysis [124]. Researchers from Nortel presented an ASIC implementation applying predistortion in real time in combination with DPSK [125] and showed results for transmission over 5120 km of fibre using an off line calculated predistorted pattern in a post deadline paper [118]. The publication of a full working ASIC suggests that this subject was already under research at this group for a longer period of time without intermediate research being published.

3.2.2 Non-linear effects in combination with EPD

In September 2005, at ECOC, an analysis of compensating non-linear effects was presented [128]. At the same conference researchers from Bell Labs presented papers comparing predistortion for different modulation formats [129] and also providing an analysis of performance related to non-linear (SPM and XPM) transmission effects [130].³⁸

Papers [127] [133] were published in January 2006 by the Nortel researchers, adding experimental result for compensating non-linear effects.

³⁸ This summary does not contain every paper related to predistortion published.

At OFC in March 2006 a more detailed analysis of the limitation imposed by non-linear effects, mainly XPM, were published, this time by researchers from Bell Labs [134] and by researchers from Alcatel [135]. In September 2006 a study focused on comparing NL effects of EPD with in-line compensation was published [139]. Nokia Siemens Portugal researchers published more work on XPM issues in [142].

The conclusion from this series of papers was that NL effects limit the achievable performance gain by predistortion, and that to achieve the best performance gain, distributed distortion compensation methods should be used, rather than lumped distortion compensation at the transmitter.

At OFC in March 2006, UCL researchers presented a paper proposing combining LUT and FIR filters to apply the predistortion [136], making it possible to also predistort for intrachannel NL effects.

At ECOC September 2006 a design for a predistortion transmitter based on FPGAs was presented [2], and experimental verification and performance results of this transmitter were published the following year [5].

Researchers from AT&T presented results from a field trial using the predistortion system developed by Nortel [117]. This trial demonstrated that, while NL effects may impose a limitation on the achievable improvement by EPD, applying EPD to a real world system could still improve its performance significantly.

In May 2009 the results of the work related to this thesis have been published [1], showing experimentally the precompensation of NL effects with real time digital signal processing.

3.2.3 Expanding EPD for other scenarios.

At a seminar of the IEE in London a presentation [131] compared receiver-based electronic compensation (using SSB signals) with predistortion.

During the summer of 2006 a paper analyzing the use of predistortion for NL effects in 40 Gb/s transmission while having DCF for dispersion compensation was published [138]. The same issue of combining the methods of electrical predistortion with optical dispersion correction is analyzed in [141] from Nokia Siemens Portugal. These papers showed that combining both systems is a viable option.

In July 2007 a paper was published which proposed the possibility of using predistortion to compensate NL effects in combination with the OFDM modulation format [140] by A. Lowery from Monash University.

In the same year, at the 9th International Conference on Transparent Optical Networks (ICTON) digital predistortion to compensate for crosstalk between WDM channels was proposed [3].

In Sept 2008 at ECOC a paper was presented comparing NL penalties of predistortion at 10 Gb/s with 40 Gb/s systems [143]. The paper was expanded to include multichannel effects and presented at OFC 2009 [148].

3.2.4 Additional Implementation issues of EPD.

Many implementation issues are discussed in the papers already presented in earlier paragraphs.

In addition in [132] predistortion using direct modulation and a phase modulator was proposed as a possible alternative to the MZ approach.

In 2008 at the 7th International Conference on the Optical Internet (COIN) a Coordinate Rotation Digital Computer (CORDIC) based algorithm as alternative to RAM based LUT was proposed by researchers from Mitsubishi [144, 145]. At the 21st Annual Meeting of the Lasers and Electro-Optics Society (LEOS) 2008 predistortion of a comb of carrier frequencies was described [146] (more details were later published in [147])

Later in August 2009 more implementation details and analysis of the CORDIC algorithm implementation [149] became available.

3.3 Deterministic distortion

An issue of predistortion is that it is carried out on a signal for effects that will happen later in time (even if the distortion is taking place a fraction of a second after the predistortion has been applied to the signal). This means that we need to know the behaviour of the distorting effects in advance. Effects which are not predictable cannot be predistorted.

This does not necessarily mean that the distortions need to have exact analytical descriptions. If certain effects can only be described with a statistical probability it might be possible to predistort for them (maybe imperfectly but still giving an improvement in transmission quality).

An example to illustrate this could be predistortion for polarization mode dispersion. The polarization mode dispersion experienced by a signal along most standard fibre depends on fibre production factors and also varies over time because the stresses on entrenched fibre change [150]. Because these factors are unknown in advance of most system deployments, it is not feasible to predict the polarization distortion of a fibre based on the published parameters and so we cannot calculate this distortion, since the polarization dependent distortion is not deterministic from this point of view. However if we would use standard fibre, install it and then measure the polarisation dispersion, we could then assume that this measured polarization dispersion will stay constant for the following period (be it seconds or even years) and this measured polarization dispersion could be considered a good prediction (how good is a question for debate) for the actual polarization mode dispersion predistortion. This would then be a deterministic system and we could try to find a way to predistort for it.

A consequence of predistorting for a specific set of transmission fibre characteristics is that it is only when these characteristics agree with the assumed ones that the best possible correction of distortion is achieved [129]. If one of the actual parameters deviates from the assumed designed level the performance drops. The most obvious parameter to illustrate this is the fibre length and this is shown with the schematic in Figure 14

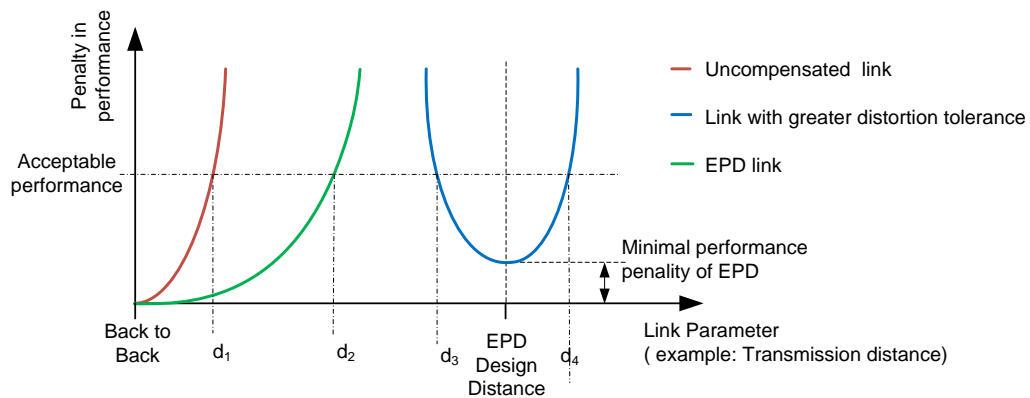


Figure 14: Performance versus distance.

The red curve is the reference performance of a system without dispersion compensation in which it is possible to transmit the signal over a distance d_1 before performance drops below the acceptable level. If we apply certain techniques³⁹ to increase distortion resilience (an example is the use of a modulation format that is more resilient to dispersion), then we can extend the transmission distance up to d_2 (green curve). At shorter distances the link performs at least as well as the reference link. If EPD⁴⁰ is used then we achieve optimal performance at the EPD design distance but the performance will drop if we increase or decrease the distance and acceptable performance will be achieved when the distance is between d_3 and d_4 . If we operate at the EPD design distance, we may experience a performance penalty compared to back to back operation. The performance curve of EPD is not necessarily symmetrical around the EPD design distance or another parameter.

In the predistortion method we use, we assume that the distortion of the signal propagating along a fibre is well described by the simplified Non-Linear-Schrödinger-Equation (NLSE) as discussed in chapter 2. This means that in this work distortion resulting from first order chromatic dispersion and self-phase-modulation are taken into account. A consequence of this approach is that both effects are always treated in a combined way. It is common when designing distortion combating techniques to focus on one of the two effects. We do not do that with the method used here.

³⁹ Not all techniques behave as in the figure especially the conventional used technique of using DCF which has a more complex influence on performance than the simplified representation here.

⁴⁰ Techniques other than EPD also show this behaviour. An example is compensating CD by only placing DCF at the transmitter.

Because crosstalk between different WDM channels is a deterministic effect we could consider predistorting the signal for it [3]. A practical problem is that to determine the expected crosstalk effects on the signal the predistortion algorithm needs to have knowledge of the signals on the other DWDM channels. It needs this information on a time scale equal to the sample period of the samples used to construct the EPD signal. There are two major issues with this:

- The algorithm to apply the XPM predistortion might need to be able to handle more data to calculate the EPD.
- In a DWDM system each channel transmitter is in general implemented on a separate line card and hence the data of the other channels may not be available to the IC handling predistortion. This becomes an even bigger issue for wavelength routed networks in which the transmitter of a neighbouring channel might even be located at a different POP.

As we will see in Section 3.6, defining the predistorted signal is most commonly done by mathematically calculating it. This calculation depends on knowledge of certain parameters of the transmission system. While from a purely scientific point of view, obtaining information such as the length of a fibre, its dispersion parameters, the launch power of the signals etc. poses no problem (they can all be measured) this does not mean that for an operational network, even newly installed, they will be accurately known. Network operators often only know these parameters by estimation and some may vary during the lifetime of a transmission system.

An example is the basic parameter of the length of the fibre between two POPs. Often the operator only knows the route distance, not the length of the actual cable (which is different because the fibre might spiral in its jacket, coils are present at splice points, routing in a POP might be complex). Going into the field and measuring this parameter (with an OTDR or any other technique) may not be acceptable from a cost point of view (interruption of running traffic). If we would be able to measure it by an OTDR, then this requires knowing fibre parameters, specifically the refractive index, which may not be known to the fibre owner.

A method to optimise the predistortion applied to the system would be the use of feedback from the receiver. It can be envisaged that the receiver measures the quality or other parameters of the signal and sends these back to the transmitter via the control plane of the telecommunication system. The amount of feedback data would be much

lower than the actual data rate and a control plane with capacity measured in kb/sec could be used for this. The transmitter could use this feedback to assess whether changes in the settings of the parameters determining the applied predistortion improves or deteriorates the signal, hence optimising the controllable parameters. Because this would require a non-standard receiver and increase the complexity of the systems this has been left for further research.

3.4 Offline versus real time signal processing

It is possible to investigate aspects of the performance of EPD systems without implementing the DSP in real time. Predistortion can be applied to the full block of data using an external system (most commonly a computer) which may take a much longer time (hours) to apply the signal processing to the signal than the time it will take to transmit the block of data (a fraction of a second). We can then store the precalculated signal in a memory and, assuming the memory is fast enough, send this signal as a burst over the link. We might repeat the transmission of the limited sequence of bits so it becomes a continuous data stream of a repeating data sequence⁴¹. The advantage of the offline method is that the designer of this system is less limited by the performance and implementation issues of the algorithm compared to applying it in real time to a continuous data stream.

However, if we want the proposed method to be applied in a commercial system where the data stream is continued for maybe years, it is necessary to implement the signal processing at the same speed as the data stream. For this we need to demonstrate that the proposed digital signal processing can work in real time and can be built with the available technology.

In the solution we use here we combine off line calculation with the requirement of real time processing for operational use.

We split the algorithm for predistortion into two parts: we use an offline method, described in chapter 3.6, to calculate the predistorted shape for a limited number of bits. This is a very computing intensive algorithm and while having been proposed to be

⁴¹ This is a possible solution if certain devices, like clock recovery and BER testsets, in the setup require a data stream longer than the length of the recalculated burst to function.

implemented in real time [109] we do not know of anyone actually demonstrating this with current technology.

We store these precalculated pulse shapes in a memory. We then look at a passing bit stream and apply the most suitable digital processed pulse shape to a bit. This choice of a pulse shape to the data stream works in real time. So from an implementation point of view we ensure that choosing the correct pulse shape and applying it to a bit can be achieved in real time.

A remark on the publications in Table 3 reporting on actual transmission tests is that the papers often do not clearly state whether the predistortion has been achieved with off line or on line real time calculations.

3.5 Defining the predistorted transmission signal

There exist a variety of ways to approach the definition of the ideal predistorted signal for a particular transmission systems.

The method proposed in most papers is termed back-propagation. It consists of finding the inverse of a function describing the signal evolution along the transmission system and applying this inverse function to the desired signal at the receiver. We discuss this method in 3.6

An alternative is based on Optical Phase Conjugation (OPC). OPC was explained in section 2.5.6.4 (and represented by graph (a) in Figure 15). Instead of dividing the transmission fibre into two stages as with OPC, we assume that the full length is present at S_2 . The first half of the transmission link in OPC (so S_1 and the OPC component) we model mathematically (all the green blocks are representing models rather than actual components or fibre). This model starts with the signal shape that is required at the receiver ($A=D$, meaning that at point A in the diagram the signal has the shape required at the receiver in point D of the graph). It is then distorted using the NLSE and the OPC of the signal is calculated.

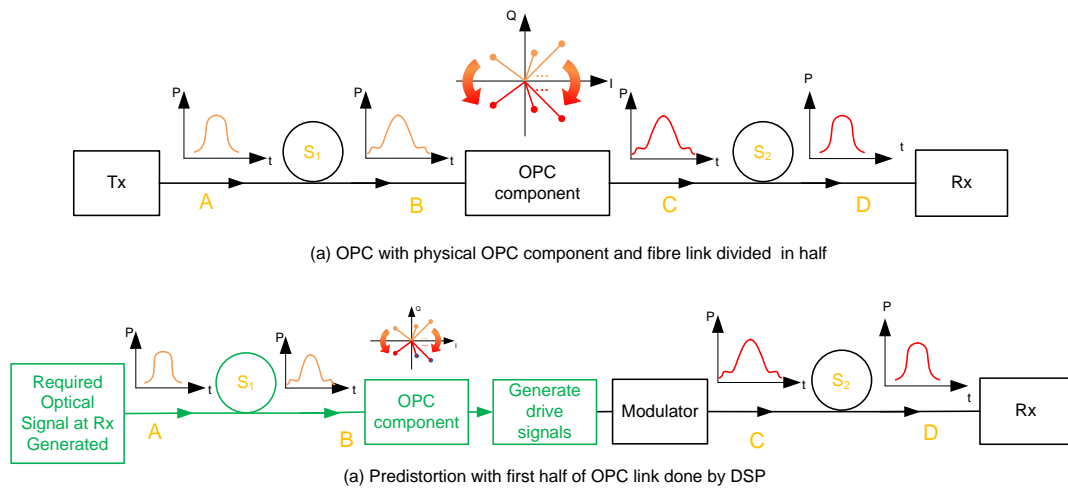


Figure 15: OPC as method to calculate predistorted signal.

An issue complicating the OPC method is that OPC requires symmetry of the power envelope before and after the OPC component. This is achieved by using fibre with negative attenuation and, instead of amplifiers, using attenuators in the link A-B. This can be easily done because this link is not a physical link but a mathematical model.

The result is the predistorted optical signal assuming only the effects described by the simplified NLSE distorting it [73]. The 'Generate drive signals' block is necessary because our model will be describing the signal in the optical domain while our modulator will require to be driven by electrical signals.

Other methods to generate the predistorted signal are conceivable. A method optimising calculation time using a single step to calculate up to 2 spans has been published [151]. Other methods for the case where the parameters of the transmission system are unknown in advance (so called black box transmission link) and where a signal (during actual data transmission or in advance with a physical or mathematical model) is optimised through feedback from the receiver are considered ⁴².

⁴² This method is probably inefficient if not combined with other methods.

3.6 Inverse of the simplified NLSE function

In section 3.5 one of the approaches proposed is to determine the optimal transmitted waveform by applying the inverse transmission function to the desired receiver waveform. As stated earlier we use the simplified NLSE as a description of the distortion applied to a signal. Finding the inverse of this function can be done by using the same equation but replacing the coefficients by their negative values [109]. So equation (1) becomes:

$$\frac{\partial A}{\partial z} = -\frac{i}{2} \beta_2' \frac{\partial^2 A}{\partial t^2} - \frac{\alpha'}{2} A + i\gamma' |A|^2 A \quad (7)$$

With

$$\alpha' = -\alpha \quad \beta_2' = -\beta_2 \quad \gamma' = -\gamma \quad (8)$$

The NLSE is a differential equation which normally is not analytically solved but applied to a signal using numerical methods, a popular one being the Split-Step-Fourier Method [19]. We can apply this method also to the equation with the negative parameters to calculate the predistorted signal. For the Split-Step-Fourier method we rewrite (7) in terms of \widehat{D}' the nonlinear and \widehat{N}' the differential operator as in equation (9)

$$\frac{\partial A}{\partial z} = (\widehat{D}' + \widehat{N}') A \quad (9)$$

$$\widehat{D}' = -\frac{i}{2} \beta_2' \frac{\partial^2}{\partial t^2} - \frac{\alpha'}{2} \quad \widehat{N}' = i\gamma' |A|^2$$

We now assume an optical fibre as a chain of shorter fibres. If we make the fibres sufficiently short we can assume that when the signal transfers through this shorter distance there is no interaction between the \widehat{D}' and \widehat{N}' components distorting the signal and can apply them independently. \widehat{D}' is, in the approach we use, applied to the signal in the frequency domain because it is frequency dependent and \widehat{N}' with the signal in the time domain. So this requires the necessary FFTs and IFFTs in between the steps to convert the signal from one domain to another. If we use this method to calculate the predistorted signal for a system which consists of multiple spans with amplifiers, then the amplifiers are replaced by attenuators, in the calculation.

This process is illustrated in Figure 16.

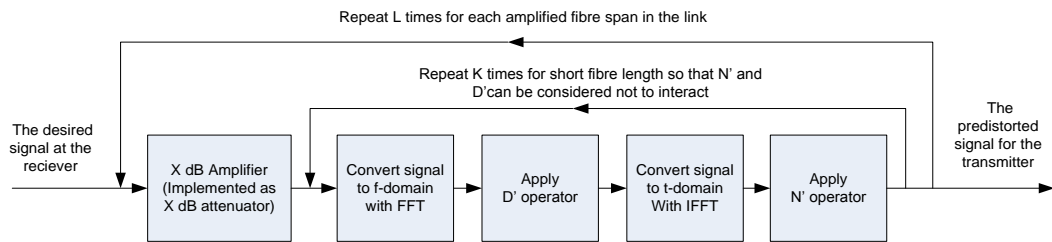


Figure 16: Split-Step-Fourier method for back propagation.

To increase accuracy, we used the symmetrized form of this algorithm, in which application of the D' operator is split before and after applying the N' operator. More detail on the Split Step Fourier method (and the derived more accurate Symmetrical Split-Step Fourier method) can be found in [19], and more on implementation in [43p. 93] or [152].

3.7 Limited influence window and LUT build-up

The two methods explained in sections 3.5 and 3.6 for defining the predistorted signal implicitly require that the signal in the full time domain is known. This can be achieved by the use of the FFT and IFFT in the Split Step Fourier Method in both methods to simulate the transmission along the imaginary fibre. The input/output of these transforms is across the full time domain of the signal.

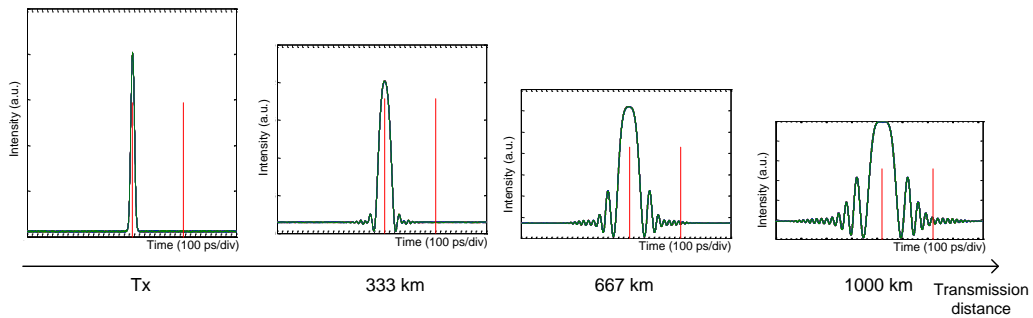


Figure 17: Spreading of optical pulse.

The dispersion effect (as described in the NLSE) causes the different frequency components of the signal to travel at different speeds and so each pulse will spread out into the time slots of the neighbouring bits. The longer the distance the signal travels the wider the pulse spreads out over its neighbours, causing a single pulse to influence more and more other timeslots (illustrated by Figure 17, created by simulation software Photoss, the intensity scales are not uniform between different graphs, red lines are indicating a 10 bit time interval in the pulse train, only CD shown and phase distortion is not illustrated).

If a second pulse is travelling a certain time interval away from this pulse in the pulse train it will experience more interference from pulses travelling closer to it than from pulses travelling further away from it in the pulse train⁴³ (represented by the varying thickness of the red arrows in Figure 18). To be able to calculate in real time the Intersymbol Interference (ISI) for a continuous datastream we limit the pulses contributing to the distortion of a pulse to a limited number of sequential pulses in the pulse train, of which the influenced pulse is positioned in the centre time slot. This limited sequence can be

⁴³ This is a simplified statement because even when we only assume CD is present we can see on the graph that the 'ripple' effect can mean that a nearby pulse causes almost no distortion and a pulse further away more. In addition, we need to take into account effects other than CD.

considered the influence window in the full data stream which is considered to be distorting the central pulse. The size of the window is dependent on the link characteristics (type of fibre, shape of pulse, distance of link, bit rate, etc.) and the required performance.

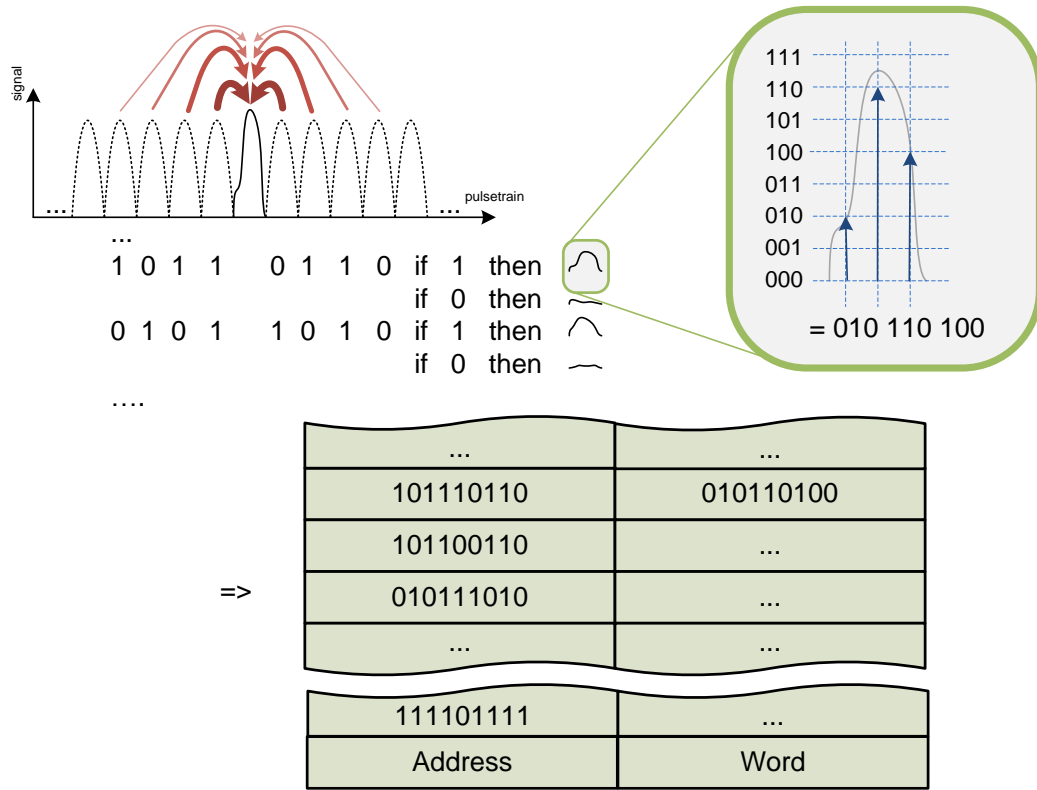


Figure 18: Principle of the LUT table.

Once we limit our window to a finite number of bits we can calculate the predistorted waveform of the central bit using the method described in section 3.5 or 3.6. Figure 18 shows the principle used to obtain the contents of the LUT table used in our EPD implementation⁴⁴. We have limited the influence window to 9 bits and assume our system is capable of processing 3 samples per bit with a 3 bit resolution ($= 2^3 = 8$ levels).

Left top graph in Figure 18 shows a pulse train. The central pulse (solid line) will be influenced by its neighbouring pulses (dotted lines represent undistorted pulse shape, not their actual shape because they will also be distorted, during transmission and when doing the off line calculation of the predistorted signal). With a 9 bit window (8 neighbours + central bit), there are $2^9=512$ possible sequences. Of these only one 101110110, is shown

⁴⁴ But with different parameters in this figure than the actual transmitter built as described in later chapters.

in full detail. We calculate the pulse shape (the I and Q components, not just the power intensity as shown in the graph) for the central bit slot (using methods described in sections 3.5 and 3.6.) if the central bit is a 1. The resulting predistorted shape of the central bit slot is then quantized to fit the used digital representation of the signals, as shown in the top right graph, in this case giving us three samples (010, 110 and 100) out of a possible 8 levels (000 up to 111). The bit sequence and the samples are then stored in a memory, using the bit sequence, including the central bit, as address and the data of the samples as the stored word. This is then repeated, first for the same neighbouring bit sequence but with the central bit a 0, and then for the 255 other possible sequences.

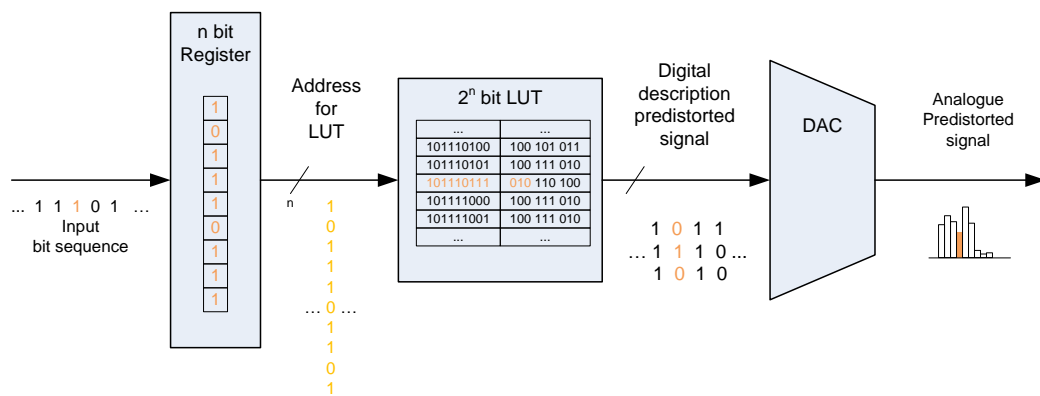


Figure 19: Principle of integration of a LUT in a Tx design.

Figure 19 shows the LUT integrated into the transmitter design. The data needed for generating one sample of one bit is shown in orange. The bit sequence to be transmitted enters the transmitter in a continuous stream. n bits of this data are stored in a register so that the bits related to the window are available as an address for the LUT. In the LUT the sample data at this address is looked up. The sample data is then forwarded to a DAC which generates an analogue sample. The next sample of the same bit is then generated and once all the samples of a bit have been generated by the DAC, the next bit is processed⁴⁵.

⁴⁵ Two clock rates are assumed in this model. The blocks to the left of the LUT are clocked at bit rate and the blocks to the right are clocked at DAC sample rate. In the design presented in this thesis we resolved this by adjusting the width of the parallel processing instead of using different clock rates in the transmitter.

3.8 Digitisation of predistorted signals

Because we use digitised signals, which approximate continuous analogue signals, the parameters of the digitisation will influence the performance of the transmitter. We use digitized signals with different parameters at two points in the EPD method: once to represent the signals in the mathematical models to calculate the predistorted signal as described in 3.5 and 3.6 off line and create the filter parameters (modelling parameters, these are related to the so called simulation samples in later sections), and again in the EPD transmitter to create the predistorted signal in real time (transmitter parameters, related to the quantised samples). The modelling parameters are chosen so that they do not contribute any significant penalty to the system compared to the transmitter parameters. This is illustrated in Table 4, where it can be seen that the difference between them is at least an order of a magnitude. If we had suspected that the Modelling parameters would have had a significant influence (conclusion based on other simulation work in the group and tested by varying them in test runs when calculating the EPD signal) we would have adjusted them.

	Modelling parameters	Transmitter parameters
Sample Rate	640 GSamples/s	20 GSamples/s
Sample Minimum	-1.8e+308	0
Sample Maximum	1.8e+308	64
Sample Resolution at 0	2.2e-308	1
Sample Resolution at 1	2.2e-16	1

Table 4 : Digitisation parameters.^{46 47}

We cannot improve the transmitter parameters because they are limited by the available technology. In our case the components imposing these limits on our design are the DAC and the FPGA and the design loaded onto it chosen so that it achieves the maximal performance of the DAC at its limits (explained in more detail in 0). Based on this, we focus on the transmitter parameters and their effects on the EPD method.

⁴⁶ Resolution varies across the range for Modelling parameters because representation of values by double real format in a computer, typically our signals were in the order of 1e-3.

⁴⁷ With the requirement to have two of these samples to represent an optical signal

General analysis of quantisation parameters has been carried out in detail in many works (see for example [93]) on this subject so we limit ourselves here to its effect on the EPD system. The parameters of the digitization can be divided into two main groups: that related to the time dimension (Sample rate) and those related to the representation of the signal level (Minimum, Maximum, and Resolution).

Based on the theoretical ideal sampling theory [93 p. 23] we expect that the sample speed limits the achievable bandwidth of the digitized signal. A 20 GSamples/s rate limits the system to 20 GHz bandwidth⁴⁸ (symmetrical around the carrier frequency). We used the simulation model we will present in Chapter 4 to calculate the predistorted signal for a weak predistorted signal and a heavily predistorted signal, weak meaning that with the quantisation parameters proposed we will be able to compensate the distortion, and heavy meaning that because of the quantization parameters, the signal will not be able to be decoded at the receiver. We show the eye diagram and the optical spectrum of both signals firstly as calculated for ideal predistortion and then after applying the effects of quantization (using the quantization method described in detail in Chapter 4 with 2 samples per bit and 64 signal levels) to the ideal predistorted signal in Figure 20

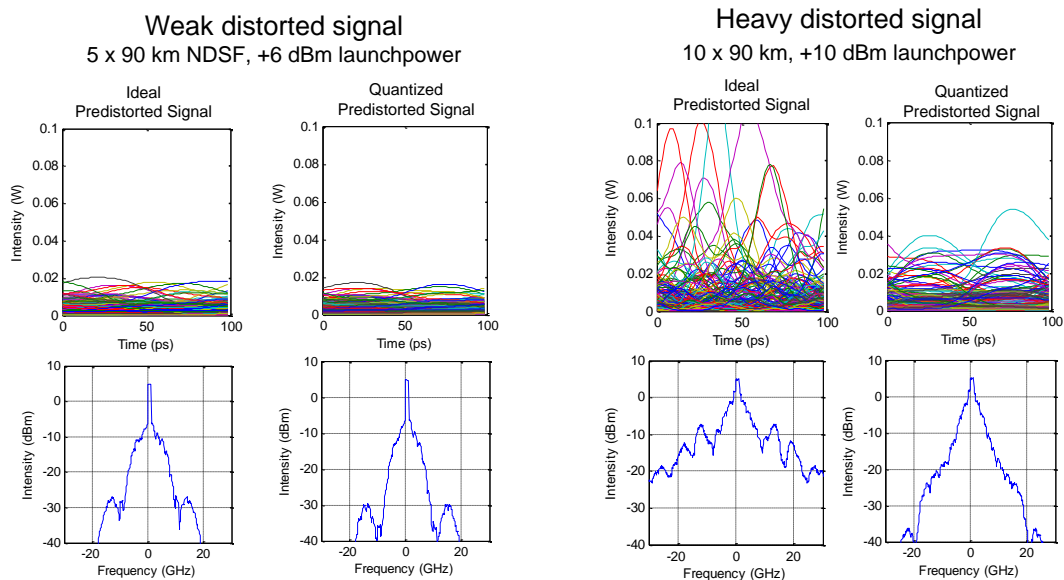


**Figure 20: Characteristics of weak versus heavy predistorted signal.
(Bandwidth of frequency diagrams 1.25GHz)**

⁴⁸ This does not imply that the analogue signal generated by a digital signal through a DAC will not contain frequencies outside this bandwidth, it does imply that we cannot control these components by the samples in the digital representation.

It can be seen that when the distortion of the signal is increased (by increasing launch power and link distance) the occupied bandwidth of the ideal predistorted signal increases and frequency components outside the original bandwidth of the non-predistorted signal appear in the signal. The limited sample rate of the DAC means that these components are not correctly generated when creating the predistorted signal with the proposed EPD transmitter (Figure 20, top right plot). The signal level parameters, especially the limited resolution of the quantised signal, results in quantisation noise. An issue is that we have a limited resolution range and that the calculation of the LUT spreads this resolution out over the full range occupied by the signal. In Figure 20, with the heavily distorted signal with ideal predistortion, we can see that the signal levels occupied by the signal are not uniformly distributed across the full range. The signal mainly occupies levels below 0.03 W and only occasionally peaks up to 0.1 W. If we set the range of our digitised signal to represent the full range of the signal levels present in the ideal predistorted signal and we use a uniform distributed quantization scale, imposed by the DAC design, we increase the amount of quantization noise present on the samples to be able to represent the occasional high power level. A possible way to limit this effect would be to apply clipping to the signal.

In addition to the theoretical limits imposed by the theory of quantised signal, we have to include the fact that the DAC we use to convert the signals from digital to analogue form has a limited frequency response with roll off slopes which is not equal to the frequency response of quantization algorithm that has a frequency response only limited by the underlying signal representation.

We could consider limiting the quantization noise further using dithering techniques. This could reduce errors which are repeating and correlated to the signal. We did not analyse if dithering would improve the final quality of the optical transmission.

So far we have assumed our system can generate signals with unlimited signal levels and with unlimited extinction ratio. This is of course not the case in a realistic system. The use of optical amplifiers after the modulator increases the achievable maximal power significantly. The extinction ratio is in most cases limited by the modulator. Detailed investigation on how these limitations start affecting realistic transmitters is left for further research.

The limitations imposed on the EPD system because of the limitations of the signal’s digital representation are a fundamental limit for the performance that can be achieved by EPD. It means that the fundamental limit of EPD is currently not caused by physical laws but by engineering limits which may be expected to be gradually pushed upwards as the technology evolves.

Because many characteristics of a communication system determine the waveform of the ideal predistorted signal (fibre type, signal parameters, operating point, etc.) it is difficult to give easy relations between these parameters and the achievable performance. Performance has to be assessed on a case by case basis.

3.9 Selecting predistortion method (LUT versus FIR)

In the previous section 3.4 we showed the need for a real time algorithm to apply the predistortion to the signal, mentioned that we proposed to use a Look Up Table (LUT) for this and explained this method in section 3.7. This is however not the only option available. As can be seen from Table 5 (in section 3.11) in addition to LUT, finite impulse response (FIR) filters are regularly used in studies of EPD (the third method in the table, ‘ideal’, is only applicable to offline numerical simulation and not for physical implementation).

A block diagram of a simple FIR filter is shown in Figure 21. In this diagram the green numbers relate to a numerical example I will use to explain its functionality. A sampled signal inputs at the top left (for simplicity we have assumed the samples can only have 2 levels 0 or 10). The sequence shows 5 samples in time. The FIR filter shown has 5 taps (represented by the 5 vertical signal flows in the diagram). The number of taps is only an example; in principle a FIR filter can have any desired number of taps.

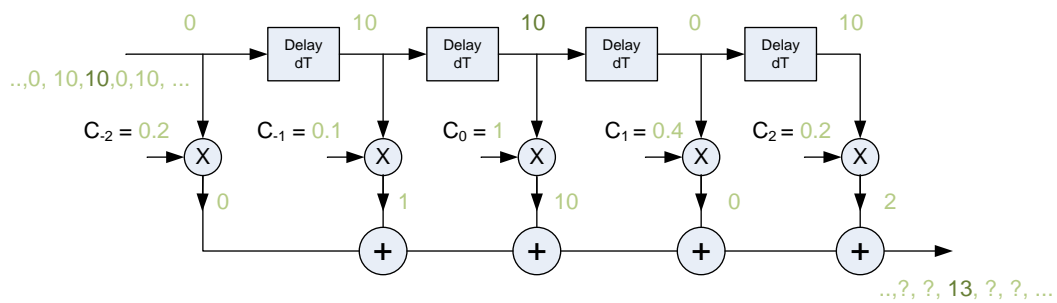


Figure 21: Block diagram of a FIR filter.

The top part of the filter consists of a shift register with a delay dT between the taps equal to the sample period of the incoming samples⁴⁹. So after 5 clock pulses, 5 samples of the continue datastream are loaded in the register, these 5 samples being represented by the green numbers on top. During this clock pulse the FIR filter will calculate a signal level that conceptually can be interpreted as the corrected value for the centre sample (the one in dark green)⁵⁰. It does this by multiplying each sample in the register with a tap weight, the values C_{-2} up to C_2 , adding them all together and forwarding this number (13) out of the filter. During the next clock pulse the next pulse again with value 10 (left from the 10 in the centre) will move into the central position and the filter will now calculate the corrected value for this sample.

To implement distortion the tap coefficients are calculated to generate the I and Q component of the signal. The use of FIR filters has been analyzed and experimentally verified. This has been done in [32] [93] and related to optical EPD in [110].

From these studies we conclude that a LUT is the most general filter possible and so can fully emulated the working of a tap delay FIR filter. The FIR filter is a more limited filter, which can only be used to compensate linear behaviour. In relation to optical transmission we can say a FIR filter can compensate distortion related to the CD but not the distortion related to the NL of the NLSE presented in 2.1.

When looking at the design parameters of both filters there are two we can relate to each other. If we assume that both filters operate on signals with the same sample rate and bit rate than we can compare the address length x (expressed in samples) of the LUT with the tap length of a FIR filter. Both parameters express the window on the data stream (in samples) for which ISI can be compensated. Samples outside this window do not influence the calculation of the predistorted sample.

The advantage of using a FIR filter is related to the use of resources to build the filter, especially how they scale if we want to compensate distortion for larger transmission distances. Assuming we are considering a LUT and a FIR filter for implementation in a

⁴⁹ A sample does not need to equal a logic bit of the transmission.

⁵⁰ From a purely theoretical point of view there is no necessity for a 1-1 relation between samples coming in and going out but it helps in getting a basic understanding of a FIR filter as used for this application.

digital transmitter, from Figure 17 we see that the further a pulse travels along the fibre, the larger the number of bits involved in the ISI will be.

If we implement a LUT we need memory. The amount of memory the LUT filter uses depends on: the number of bits (B) we use as an address, the number of samples per bit (S_b) and the memory required to store 1 sample (S_m). The total required memory is now $2^B S_b S_m$. If we want to express resources in number of gates we need to know the number of gates required to implement a memory capable of storing one sample (G_s). In addition we will most likely need to implement the LUT many times (N_p) on the IC because the internal bit rate on the IC will be lower than the transmission speed and a parallel databus is needed (more detail on this implementation issue is given in paragraph 5.6.1). The number of gates used by a LUT implementation is then:

$$2^B S_b N_p G_s \quad (10)$$

For a FIR filter the required resources depend on the number of taps $T_n (= B S_b)$ and the number of gates needed to implement one tap G_t ⁵¹. We also have the issue of parallel implementation. The total required number of gates to implement a FIR filter is:

$$B S_b N_p G_t \quad (11)$$

There are additional techniques proposed to reduce the number of gates used by a FIR filter. We can try to exploit the fact that a FIR filter for CD has symmetrical properties, and applying the compensation in the frequency domain instead of the time domain also has some possible advantage. These are discussed in [110]. Another proposed way to improve reduce the resources is the CORDIC method [149]. With these methods we might be able to implement a FIR filter with even fewer gates.

If we compare both expressions for the number of gates used as functions of the number of consecutive data bits that are considered for the ISI calculation we notice that the usage of resources for a LUT will increase exponentially while the one for a FIR filter will increase linearly. So for a system with ISI spread out over a large number of bits a FIR filter will always need lower resources than a LUT filter. The size of the window where a FIR

⁵¹ A correction factor can be subtracted from the number of used gates because for n taps we need only $n-1$ adders and delay line instead of n , while needing n coefficient multipliers. We also assume that the resources used to implement a tap do not change when the filter size increases.

filter starts to use fewer resources than a FIR filter depends on the number of gates needed to implement a tap for one sample compared to the number of gates it needs to implement storage for one sample. This can be as low as 1 tap if the required gates for a single tap are less than the required gates for a LUT with only 2 entries.

This is however assuming that we can use the available gates to build memory or to construct taps. If we were proposing to build the circuit on an ASIC then we could investigate this further and analyse if the same amount of 'real estate' on the IC gives more performance increase for a LUT or if used for a FIR filter.

In this work however an ASIC was not considered feasible for the reasons explained in section 2.5.7.3 and instead we used an FPGA. On an FPGA we use different resources for a FIR filter and a LUT table. An FIR filter will use general logic slices⁵² while a LUT table will use memory blocks. While both are made of gates we cannot, because of the characteristics of an FPGA, use the gates which make memory blocks for general logic slices. (The opposite, using general logic slices to build memory structures is possible but this is not advisable for this application because of clocking domains in the FPGA in combination with the number of slices needed. Some experiments we carried out showed that the synthesis engines was not capable of achieving timing closure as soon as LUTs were pushed into general logic blocks instead of block RAM). Consequently the building of LUT based filters does not compromise the capability to implement FIR based filters and vice versa on an FPGA.

If we take an existing FPGA family (the Virtex 4 from Xilinx) we can estimate what size of FIR versus LUT filter would be possible on it based on the available slices compared to available memory on this type of FPGA .

Earlier research in the ONG group [110] showed that a 55 tap FIR filter for the I or Q drive signal⁵³ used 27,836 logic slices (66% of the available 421676 slices) on the Virtex 4 V4FX100. Assuming linear scaling based on formula (7) and assuming an overhead of

⁵² The FPGA terminology used is explained in 0.

⁵³ As will be explained in more detail later we used one FPGA for each arm driving the MZ. The total resources required for a filter processing, in the FIR and LUT case, are twice as high as the cited numbers.

10,000 slices⁵⁴ for other functionalities, this results in a 63 tap FIR filter possible on a V4FX100 (or 90 taps if there is no overhead).

Based on formula (6) we can estimate the maximum address width expressed in samples for a LUT in the available memory (6768 Kb) of a V4FX100 to be 27 samples ($2 \times \log_2(6768k/(64 \times 4 \times 2))$). This is based on formula (6)). Rounded downwards to the nearest full bit because the LUT address is a bit sequence not a sample sequence this gives a 26 sample ISI window. This estimate corresponds with the later measured actual usage in the implementation discussed in section 5.7.3 where 22 samples (11 bit) occupied 2304 Kb (this implementation uses a 6 bit sample so the same formula would estimate $2 \times \log_2(2304000/(64 \times 6 \times 2)) = 23$, rounded to a full bit gives 22 samples).

The conclusion from this estimation is that this FPGA (and other FPGAs of the same Virtex 4 family, which have similar memory/slice ratios) using the same implementation parameters could hold a FIR with an ISI window of 63 samples while a LUT would have an ISI window of 26 samples. So if we are to choose between FIR or LUT then from the point of view of ISI window size, the FIR implementation is preferable. If we look at the effects that can be compensated for, then a LUT filter is preferable over a FIR because it can in addition also compensate NL effects if they are present in the system. Which of the two will deliver the most quality improvement of a link (longest distance, lowest BER, ...) will depend on the link parameters. The important issue in relation to an FPGA is that they use different resources and the ultimate design makes use of both, so their beneficial effects can be added.

Other filter types than LUT or FIR filters, such as IIR filters [153] are possible and could be considered for further research. First indications show however that implementation at the required bit rates and with the width of the databuses required⁵⁵ will make them more complex to implement than LUT or FIR filters [110].

⁵⁴ we used 10106 slices in the implementation in chapter 5 for synchronization and other algorithms. A design with less automated functions used only 2000 slices for this.

⁵⁵ Because of maximum bit rates achievable inside current generation of FPGAs.

3.10 Controllable parameters and choice of modulator

The signal created by the transmitter can be described using multiple parameters (see also chapter 2.5.7.2.) If we assume that the signal is a modulated carrier frequency the common parameters to describe the signal are: intensity, phase, frequency, and polarization. We can only control some of these parameters depending on the type of modulator used. In addition to only being able to manipulate some of the parameters we are also restricted in the range we can manipulate them.

For our setup we decided to control intensity and phase. This can be achieved by different modulator setups.

In the setup proposed in this thesis the Cartesian-Modulator at the transmitter makes it possible to accept and I and Q component of the signal (two signal components placed orthogonally in the quadrature modulation space as an alternative to describing it by phase and intensity). We do not actively control polarization or absolute frequency on a symbol based scale and these are set to be constant over the transmission duration⁵⁶. The major limitation we have is a limited extinction ratio on each of the components of the signal resulting in a limited range we can achieve on the I and Q intensity. The absolute level is more controllable because we can use optical amplifiers to amplify the signal to the required power level.

To achieve this the following modulation methods can be considered:

- (a) Directly Modulated laser followed by phase modulator
- (b) Continuous Wave (CW) source, modulated by an intensity and phase modulator
- (c) CW source and a Dual Arm MZ with individual arm control
- (d) CW source and a Cartesian MZ

We used method (d) in our setup because: Method (a) demonstrated in [132] has the issue that with the direct modulation we introduce chirp on the created pulse. While this chirp could theoretically partly be compensated in the phase modulator (not fully because of limited samples/bit and limited DAC resolution) this would require determining this chirp and incorporating it in the calculation of the LUT tables.

⁵⁶ Polarization and frequency parameters will vary because of other issue such as noise of the CW source but not as a result of a user-controlled parameter.

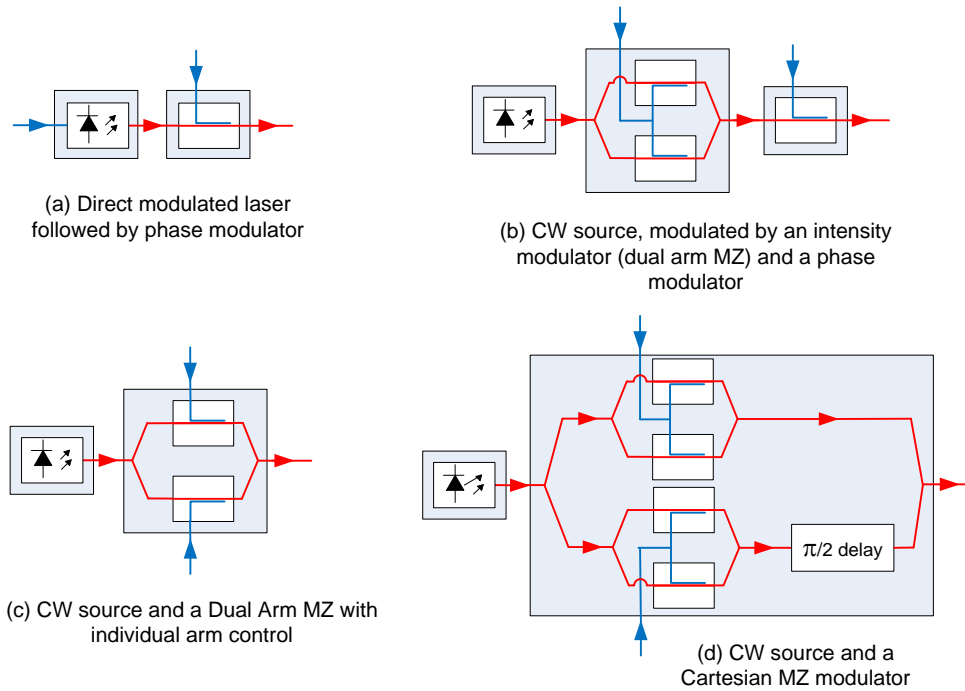


Figure 22: Modulators for EPD transmitter.

In method (b) the intensity and phase modulator could in principle be made on the same substrate. We did not have access to such a component and custom made optical modules were not considered a realistic option. As a result it would have required two separate discrete components, giving a higher insertion loss than a single component. In addition the two drive signals would not be symmetrical and this would require separately designed, calibrated and optimised drive circuits for each signal, complicating the setup. (c) A dual arm MZ can control phase and intensity of a generated signal. This method is patented and described in [123] [154] The issues of using this modulator in comparison to (d) the use of a Cartesian MZ modulator are illustrated in Figure 23.

The graphs in Figure 23 were created by published formulae [123, 138] expressing the output optical field of these modulators in relation to the electrical drive signals. We varied the two drive signals of each MZ model across a range (V_π or $2V_\pi$) in 8 uniform steps ensuring all possible combination ($9 \times 9 = 81$ points) are applied while keeping fixed bias points. The optical signal was separated into I and Q components and the small blue circles are the achieved optical points in the Cartesian IQ optical field and so the surface occupied by these shows the space in the IQ field we can modulate depending on bias, drive sweep and modulator type. At each of these circles we added red and green lines (one for each drive signal controlling one arm of the MZ) with lengths proportional to the

level of the drive signals that were used to generate that particular modulation point. If more than one setting achieves the same point in the IQ space the points are plotted overlapping each other (causing the green/red crosses in graph (b)).

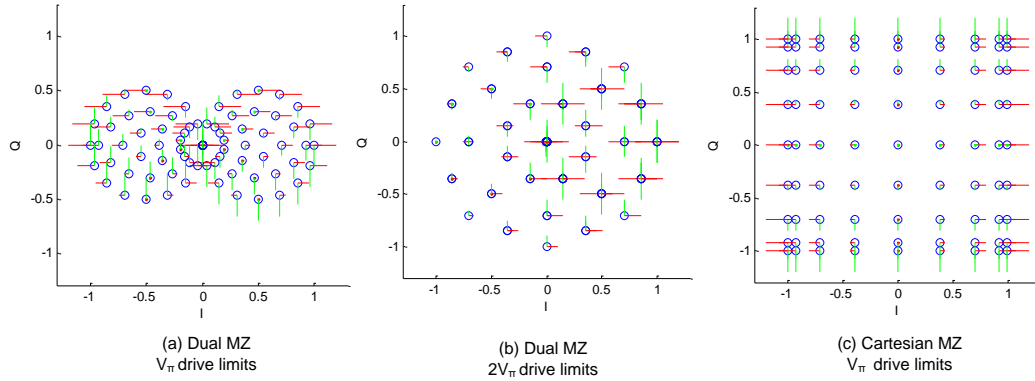


Figure 23 : Achievable IQ modulation space for MZs.

If a dual arm MZ is used and we limit the drive signals to V_π (the voltage required to give a π radians phase shift in a single arm of the MZ) then we cannot modulate a uniform area around the central point (Figure 23 (a)). We can change the achievable modulation area in the IQ space by changing the bias and range. To occupy such a uniform area⁵⁷ we need to increase the allowed drive signal to $2V_\pi$ for each arm, graph (b). If we examine the graph for a Cartesian-MZ modulator (Figure 23 (c)) it can be seen that a more uniform modulation space can be achieved and a simple relation between drive signal and position in IQ space (red drive current in the graph relates to the I component, green drive current the Q component) while keeping the drive signal in a V_π range.

Increasing drive signals to $2V_\pi$ results in greater error in the generated optical signal for a dual arm MZ in comparison to a Cartesian MZ while using an identical DAC. [138]. This is related to a bigger quantization error because the identical number of quantization levels.

The use of higher amplitude signals to drive the Mach-Zehnder also raises technical issues. It requires amplifiers with higher amplification levels without compromising their linear behaviour in the frequency range being used (up to 10 GHz). With a V_π typically around 5V for both types of MZ these amplifiers are not easy to acquire because driver designs for other optical transmitters are in general limited to V_π . The higher drive voltages also result

⁵⁷ While not compromising extinction ratio, central frequency or introducing drive signals requiring non continuous levels.

in more reflections, crosstalk, and interference between the drive signals (RF and DC) at the ports of the MZ.

The less obvious relation between drive signal and occupied space in IQ space complicates troubleshooting, calibration, synchronisation and adjustment of the setup (the simple one to one relation as seen with the Cartesian MZ can be interpreted during operation without needing mathematical analysis).

A dual arm MZ is used for RZ and NRZ setups and hence is a common component. A Cartesian MZ is used for generating DQPSK signals and while less common, it has been commercially deployed, so this component is obtainable from component suppliers.

Because of these arguments we used a Cartesian MZ in the design while understanding that a more cost effective single MZ could be an interesting alternative.

3.11 Published expected performance of EPD

In this section we look at how effective EPD is expected to be in compensating optical distortion effects, and not at how efficient a particular electronic design for EPD is in using resources (gates, power, etc.). We will do this using the publications, mentioned in 3.2, as our source and limit the discussion to the situations described in them.

A remark to make is that when starting this project the question we had was not so much what is the best predistortion method that can be achieved but can we expect to see significant distortion compensation with the technology available to us. Hence we focused on what was most likely currently limiting the achievable performance and on improving that aspect instead of trying to analyse the full interaction of performance limiting issues.

Table 5 gives a summarised overview of which kind of EPD setups have been analysed in these publications. The column 'Method' describes whether the authors analysed the performance using mathematical Simulation (Sim.) or performed a physical experiment (Exp.).

Publication Date	First Author	Ref.	Method	Modulation Format	Filter Type	Bitrate (Gb/s)	Distance (km)	Predistortion of		Modulator	Channels	real time/ off line
								CD	NL			
Jan 2005	M. M. El Said	[122]	Sim.	Duo Binary	FIR	10	800	X		Cart. MZ	1	n.a.
Mar 2005	R. I. Killey	[123]	Sim.	NRZ	LUT	10	800	X		Cart. MZ	1	n.a.
Mar 2005	J. McNicol	[125]	Exp.	RZ-DPSK	FIR + NL stage	10	3840	X	SPM	Cart. MZ.	1	real time
Mar 2005	D. McGhan	[118]	Exp.	RZ-DPSK	FIR	10	5120	X		Cart. MZ	1	off line
Sept 2005	R. I. Killey	[128]	Sim.	NRZ	LUT	10	5000	X	SPM	Cart. MZ	8	n.a.
Sept 2005	P. J. Winzer	[129]	Sim.	NRZ, RZ, DPSK, DQPSK	FIR	10.7	n.a.	X		n.a.	1	n.a.
Sept 2005	R. J. Essiambre	[130]	Sim.	NRZ	ideal ?	10.7	1120	X	SPM	n.a.	8	n.a.
Dec 2005	P. Watts	[131] ⁵⁸	Sim.	SSB	FIR	10 ?	900	X		MZ	1	n.a.
Dec 2005	D. Walker	[132]	Sim. + Exp.	NRZ ?	FIR	10	960	X		DML + EAM	1	off line
Jan 2006	K. Roberts	[133]	Exp.	DPSK	ideal ?	10	1280	X	SPM	Cart. MZ	1	off-line
Mar 2006	R. J. Essiambre	[134]	Sim.	Duo Binary, RZ, RZ-DPSK, NRZ-DPSK	Ideal	10.7	1200	X	SPM ?	n.a.	8	n.a.
Mar 2006	A. Klekamp	[135]	Sim.	NRZ, DPSK	FIR	10	960	X		Cart. MZ	1	n.a.
Mar 2006	R. I. Killey	[136]	Sim.	NRZ	LUT+FIR	10	1200	X	SPM	Cart. MZ.	1?	n.a.
Aug 2006	C. Weber	[138]	Sim.	NRZ	ideal	40	800	(DCF)	SPM	MZ, Cart. MZ.	1	n.a.
Sept 2006	R. J. Essiambre	[139]	Sim.	NRZ	ideal	10.7	1120	X	SPM	n.a.	8	n.a.
Sept 2006	P. Watts	[2]	Sim.	SSB	LUT	10	800	X	SPM	?	1	n.a.
Sept 2006	M. Birk	[117]	Exp.	?	eDCO ⁵⁹	10.7	1600	X		?	7	real time
Jul 2007	A.J. Lowery	[140]	Sim.	OFDM	Mat.	?	2000	X	SPM	Cart. MZ	1	n.a.
Jul 2007	R. S. Luís	[141]	Sim.	SSB	Mat.	10	640	X		MZ	1	n.a.
Jul 2007	M. Glick	[3]	Sim.	NRZ	Mat.	10	<10 m		XPM	Direct Mod.	+3	n.a.
Jul 2008	P. Watts	[7]	Exp.	NRZ	FIR	10.7	1200	X		Cart. MZ	1	real time
Sept 2008	C. Weber	[143]	Sim.	NRZ	ideal	40	800	X		Ideal	1	n.a.
Mar 2009	C. Weber	[148]	Sim.	NRZ	ideal	40	800	X	X	Ideal	5	n.a.
May 2009	R. Waegemans	[1]	Exp.	NRZ	LUT	10.7	737	X	X	Cart. MZ	1	real time

Table 5 : Overview of investigated EPD systems in publications.

⁵⁸ Only new data summarised here, publication also includes results from [112] and [116]⁵⁹ Testing of a commercial product with exact details of the EPD implementation not published.

The abbreviations in 'Modulation Format' and 'Filter Type' are explained in Appendix A with the additional use of Mat. for the use of a mathematical formula not implemented into one of the classical DSP filter types and ideal if the authors did not consider filter based limitations when calculating the predistorted signal. The distance column gives the maximum distance considered in the paper. In the column 'Predistortion of' we note if the authors compensated CD and/or NL effects and not if these effects were considered in the analysis of the performance. The column 'Channels' gives the number of EPD modulated DWDM channels in the system. n.a. is used if an option is not applicable to the work in the publication and we used question marks if we are uncertain of a fact because of limited information in the publication.

From Table 5 a couple of conclusions can be drawn: most analysis of performance has been done by numerical simulation work, experimental work is limited to research at Nortel and UCL. Bitrates have in almost all cases been limited to 10.7 Gb/s. Most analyses are considering distances up to 1000km but actual implementations doing a multiple of this are reported. If a modulator is being considered it is in most cases a Cartesian MZ.

3.11.1 Fundamental limits of EPD systems

The predistortion method based on a signal calculated by backwards propagation and modulation in quadrature space as described in the earlier chapter is proposed for compensation of first order dispersion and SPM effects. The fundamental effect that does limit EPD in DWDM scenarios is XPM [130]. While we can theoretically predistort for XPM the scheme proposed in this work does not do so as explained in section 3.3. We also do not predistort for four wave mixing but this effect is negligible because of the high local dispersion.

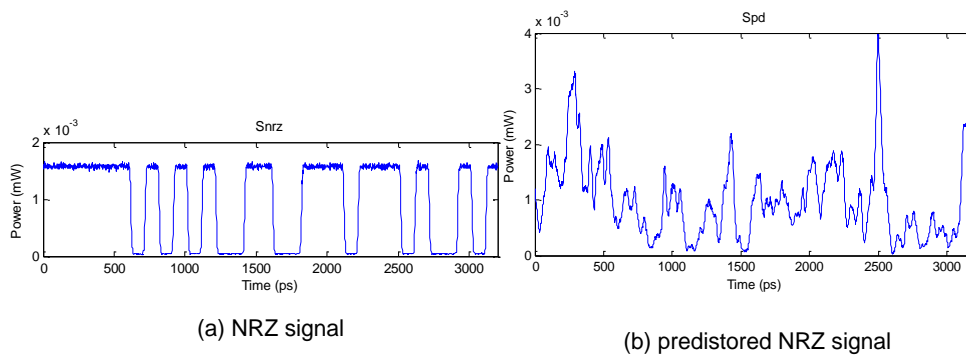


Figure 24 : NRZ versus predistorted NRZ signal.

Figure 24 explains the underlying issue. This figure compares the optical power of a 32 bit sequence of an NRZ signal with an ideal predistorted version of the same signal at the transmitter. Both signals have the same average power.

When we compare both signals we see that the predistorted signal occupies a much larger range of optical powers. The NRZ signal is limited to signals between 0 and 1.7 mW, the EPD signal ranges from 0 to 4 mW. XPM is caused by intensity changes in the sum of all channels in a DWDM system (see section 2.1.3.) Once we have many channels in the system the possible range of the total power is potentially even bigger. For example for a 16 channel system a possible variation of (16×1.7) 27 mW for NRZ is far lower than the (16×4) 64 mW for the EPD system. However this is assuming that the peak power (at around 2500 ps in graph (b) for the example) of all the channels correlate with each other. In Figure 24 it can also be seen that the EPD signal reaches this maximal level only once in the 32 bits, the maximal level for NRZ is present 50% of the time. So the probability that multiple channels achieve this maximal power level at the same time is lower than the probability that all NRZ channels achieve their maximal level. As a result the maximum

possible XPM is much higher than for NRZ but the possibility that this actually happens in a system is lower.

To assess the effects of XPM in simulation or experiment it is necessary that we decorrelate the different WDM signal not only on a bit scale but also in pattern so that the statistical appearance of bit sequences of the signal are similar to independent data on the DWDM channels (as is the case in all known DWDM systems). The use of fixed shifted versions of the same PRBS sequence at the same rate across all channels is not sufficient to assess the XPM effect. A solution is to run the simulation multiple times and shift the patterns each run. Because running through all possible pattern shifts (as many shifts as the total length of the reoccurring pattern in the PRBS test sequence) requires an unrealistic amount of simulation time, all published analyses are limited to a smaller series of random shifts, used as a statistical approximation.

The effect of XPM has been analysed in [128]. In this analysis a central channel of an 8 channel system of 10 Gb/s NRZ using 80 km spans was examined after 3040 km. The EPD system showed a penalty of 2.7 dB OSNR while the system with distributed DCF only showed a penalty of 0.2 dB.

Similar conclusions have been drawn in [130]. The link parameters were a 14 x 80 km link with NRZ modulation format, 10.7 Gb/s in an 8 channel system and 3 dBm launch power per channel. The authors conclude that for a 50 GHz system the OSNR penalty to achieve a BER of 10^{-3} is 1 to 8 dB, and in some cases increasing up to 16 dB depending on the correlation between the channels.

This penalty is not exclusive to EPD but is an issue with all types of predistorted signal, experiments showing these penalties for signals predistorted using optical methods (only CD being precompensated) have been reported in [155, 156]. They show that for a similar setup (10 Gb/s, NRZ). The targeted performance (BER 10^{-3}) was reached by predistortion at launch powers of 3 dBm while distributed DCF allowed launch powers up to 11 dBm.

While this research shows that distributed DCF can potentially achieve better performance, it is important to confirm that a field trial has shown that the performance of EPD is sufficient for many applications. A commercial product consisting of a 72 channel system with 7 adjacent 50 GHz spaced EPD channels over 1600 km of G652 fibre (ITU standardised NDSF). At an optimal launch power between 0 dBm and -1 dBm (depending on the channel), it showed at least 5.5 dB OSNR margin (up to 7.5 dB) compared to the

provisioned OSNR (at start of life). The margin used was 9.5 dB OSNR at which point around 8×10^{10} forward error correction frames ran error free. This led to the conclusion by the customer that this is consistent with practices applied to guarantee link performance in this long reach system over its lifetime.

Recently research has been carried out into the theoretical limit of EPD in combination with 40 Gb/s systems [148], showing that the XPM disadvantage of EPD compared to distributed DCF is not as prominent as at 10 Gb/s. The system considered was an 800km link (10 x 80 km) with NRZ signal format. At 10 Gb/s the EPD signals had to be limited to -3 dBm launch power per channel compared to +8 dBm launch power per channel for optical dispersion compensation for similar performance (1 dB OSNR for BER 10^{-4}). At 40 Gb/s it was 0 dBm launch power for EPD compared to 1 dBm without predistortion.

In earlier work by the ONG group [110 p. 120] the conclusion is drawn that for a typical 10 Gb/s NRZ DWDM system with 50 GHz channel spacing and using standard SMF the maximum achievable distance is around 6000 km if EPD is used rather than DCF in the links.

These analyses are for the theoretical case of perfect predistortion. This means that (among other limitations) there is no maximum signal level set. In a practical system clipping will always be present and in addition we could introduce clipping intentionally when calculating the predistorted signal. This clipping will reduce the accuracy of the generated predistorted signal compared to the ideal predistorted signal and so, in the linear case, decreases the performance of EPD. However because of reduced XPM, performance will benefit in the nonlinear system. The balance between both effects depends on many characteristics of the link. As far as the author is aware no detailed analysis of this has been published.

The overall conclusion drawn is that 10 Gb/s NRZ systems relying only on predistortion for distortion compensation are expected to perform worse than distributed compensation designs. Hence a purely predistorted system is not the best design choice for a design to achieve maximal performance. This depends on system characteristics and if they change, for example an increase in bit rate, this has to be reinvestigated. Field results have shown that 10 Gb/s EPD does deliver acceptable results up to 1600 km distance showing that the fundamental limit of XPM is not the limiting factor for deployment of this type of systems.

While XPM might be the fundamental limit on maximum transmission distance we did not expect our experiments to reach this limit, primarily because we did not carry out DWDM experiments, the reason being that DWDM would require multiple EPD transmitters (we built only one). An alternative setup to realise many channels used in other DWDM experimental setup is the simultaneous modulation of multiple carriers. This could be realized by modulating a comb of carriers and eventually adding channel specific delay to partly decorrelate the signals. The XPM analysis show that this is however insufficient to prevent the statistical issues from invalidating the results.

3.11.2 Implementation penalties

For single channel operation the system performance is limited by implementation issues. The principle of EPD requires us to generate an optical signal predicted by a predistortion algorithm. Because of limited technology we simply cannot generate the optimal predistorted signal as can be described analytically.

There are 4 main sources in the implementation that cause these inaccuracies:

- The numerical calculation of the predistorted signal
- Applying the predistorted signal to the logical data stream
- Limits in digital representing the signal related to the parameters of the DAC-FPGA combination
- Electrical and optical limits in the analogue part of the transmitter.

3.11.2.1 Penalties originating from numerical modelling

The numerical calculations we proposed to use are described in 3.6. The implementation of these methods relies on numerical simulation of optical transmission. The accuracy of these numerical simulations is partly dependent on key approximations (such as limiting calculations to 1st order CD and NL effects). In [128] EPD predistortion based on CD predistortion only and CD and NL predistortion was compared (issue related to the choice of FIR/LUT filter in the implementation). For a 1200 km link using NRZ coding, standard SMF and a 2 samples/bit DAC the analysis shows that with CD predistortion only, the required OSNR (dB) to achieve a BER of 10^{-5} increases from 15 to 20 dB, while at signal launch powers between -4 dBm and 0 dBm if we include NL predistortion this limit now occurs at powers between 4 and 5 dBm launch power. So adding the NL factor to the

system (assuming we use also apply it to the signal so requiring LUT instead of FIR filters for the predistortion) increases the allowed launch power of the system.

In addition to the limited number of effects included in the calculation of the distortion effects, parameter settings of the numerical algorithms in their calculation influence the accuracy. In most published analyses it is assumed that all these parameter settings are chosen so they are not significantly contributing to the inaccuracy of the compensation characteristics. This is possible because these calculations are carried out offline. In [110 p. 115] the effect of the backpropagation step size in the NLSE on the achieved required OSNR is analyzed. It demonstrates that for low launch powers power (<1 dBm) even large steps, in this case 80 km which was equal to the span length, had no effect on the achieved required OSNR. Once the step size was reduced to 2 km no impact could be seen for launch powers up to 6 dBm in this analysis which included SPM compensation.

3.11.2.2 Penalties originating from the DSP

We planned to apply the predistortion to the logic signal by digital signal processing (DSP). Some characteristics of the DSP (samples/bit and the resolution of the signal) were determined by the DAC used in the next stage in the transmitter. In the DSP the signal representation is chosen so they do not add significant additional penalties to those originating from the DAC.

This leaves one main parameter of the DSP to be considered: the size of the memory address in the LUT or the number of taps in the FIR filter (their relation has been discussed in 3.7 and 3.9). In [123 fig 4] the eye-opening penalty versus the size of the lookup table in bits is expressed for 10 Gb/s, 2 samples/bit, NRZ. We notice a dependency of achievable transmission distance versus lookup length. If we take an eye opening penalty of 1.5 dB as an acceptable margin, then a 5 bit table achieves 200 km transmission distance, 9 bit 500 km and 13 bit 700 km.

This has been discussed in even more detail in [129] where other modulation formats are considered and more advanced methods for BER analyses instead of eye penalties are used. Applying the NRZ figure to NDSF ($D = 17$ ps/nm/km) we see that an overall 1.5 dB penalty is reached with 9 bits ISI compensation after 320km, 25 bits ISI compensation results in 1250 km and 95 bits ISI relates to 5000 km. From this research we also learn that the required number of bits for the address space of the LUT to achieve the same

performance depends on the modulation format. Over 1250 km, NRZ required 25 bits, Duobinary (17 bits) and DQPSK (21 bits) use smaller tables, while RZ (29 bits) and DPSK (31 bits) require larger LUTs to achieve the same performance.

3.11.2.3 Penalties originating from the DAC

When using a digitized signal to represent an analogue signal, two main parameters that determine the accuracy are the resolution in time and in intensity of the digitised signal. These two parameters are dictated by the DAC used in the system. The resolution in time is expressed as number of samples/s⁶⁰ and resolution in signal intensity is given as the number of quantization bits (with n quantization bits leading to 2^n levels)⁶¹.

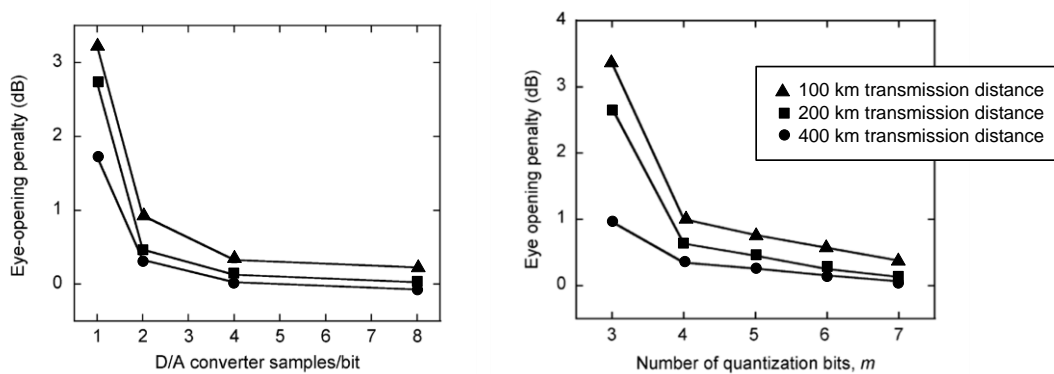


Figure 25 Figure 25 : Penalties due to DAC parameters
(from [123 Fig. 3 & Fig. 5.]

In [123] both these parameters are investigated for a 10 Gb/s NRZ system with a LUT table as predistortion method and for transmission distances of 100 (circles), 200 (squares) and 400 km (triangles) of NDSF. We show them in Figure 25.

It can be seen that the eye opening penalty drops more significantly when moving from 1 to 2 samples/bit than when moving from 2 to 4 samples/bit. This is important once we realize that with current technology at 10 Gb/s we have no possibility to go any further than 2 samples per bit. An increase in the number of quantization bits show a similar drop in penalty when going to only 4 quantization bits. Subsequent implementation of a 4 bit DAC based on these analyses suggested however that an increase to more than 4 bits may

⁶⁰ Main contributor to the parameter bandwidth of the DAC.

⁶¹ Sometimes Effective Number Of Bits (ENOB) is used. This is the number of bits used for the signal corrected by a factor for the noise originating from the device.

be required to achieve the expected results because of issues in the analogue circuitry after the DAC [110].

3.11.2.4 Penalties originating in the analogue part of transmitter

The analogue signals generated by the DACs need to be converted into an optical signal. The components carrying out this function (amplifiers, modulators, bias blocks, cabling) add additional noise to the signal, limit the bandwidth, and do not always have linear responses. A particular issue is that while we can generate optical signals with unlimited power and extinction ratio in models a physical modulator will cap both of these parameters.

Some analysis of these issues can be found in [110]. However because the DAC used in that study is constructed from many discrete components and we used an IC in this work they are not transferable.

As far as the author knows none of this has been analysed in detail in published papers in relation to EPD.

3.11.3 Other performance reports

In [135] EPD based on FIR filters is analytically compared with distributed optical dispersion compensation. It shows that if EPD is used only for CD predistortion (FIR filters used) then distributed optical CD predistortion outperforms it in relation to NL penalties. A 12 span link launch power is reduced from a maximum of 9 dBm to 0 dBm (NRZ) or from 8 dBm to 2 dBm with an additional 1-2 OSNR penalty if applying EPD to DPSK.

We have not discussed DPSK and 40 Gb/s performance analysed in the papers because these did not form part of the project goals and are left for future projects.

3.12 Summary

Theoretical work underpinning electronic predistortion, theoretical evaluation of expected results and first implementations have been described. This area of research is, however, far from being fully explored and many opportunities to improve the systems are possible.

The existing work shows that EPD is not a miracle solution because it cannot counter all distortions in a system. The technology available for implementing this principle limits what can be achieved. A key component is the digital to analogue converter; the converter's finite sampling speed is a key element limiting what can be achieved.

We choose to implement predistortion by applying a LUT table based method to allow predistortion for non-linear effects in addition to chromatic dispersion. For the modulator a Cartesian Mach-Zehnder is chosen to minimise the complexity of the transmitter.

From published material, we can see that improvement can be expected of a NRZ signal with the available technology.

4 Transmission simulation

During the research two major types of simulation were used: digital circuit simulation and optical system simulation. The digital circuit simulation was used to validate the logic design on the FPGA. Digital circuit simulation is not discussed in detail here because it is part of the digital design process discussed in 5.7.1 but simulation of the optical transmission system will be described, including effects from the electrical circuitry (the DAC in particular) on the system. As far as we know the simulation results and conclusion in this chapter are novel and have not been published before. Based on reports seen we do assume that some of the analysis done in this chapter might be available within companies as confidential information.

4.1 Introduction to optical simulation

To assess complex telecommunication systems, including the proposed predistortion techniques, the use of computer assisted simulation techniques is essential [157] [158 pp. 564-610]. This is because numerical simulation with a computer is a more cost and time effective way to assess multiple solutions and scenarios compared to only evaluating with physical lab setups or using a pure mathematical analytical approach. Simulation can also give additional benefits:

- The possibility to increase understanding by running physically impossible setups (an example is assessing all the effects in fibre individually while in reality they will coexist).
- Reuse work done by other authors developing simulations code.
- Practical advantages because no physical setup is needed.

For the work in this chapter I used an optical simulation environment known as the ONG-Simulator [159]. This simulation environment is a collection of Matlab code, a standardised signal representation and a series of guidelines available to the Optical Networks Group (ONG) at UCL. We used it in combination with Matlab 2009a [160]. In addition during the research related to this thesis we used VPI TransmissionMaker 7.0 to assess initial predistortion ideas, Optsim 4.7 from Rsoft Design Group to create graphs for publications and Photoss 4.5 from P.I. Systemtechnik to calculate LUT tables and to carry out simulations while building the system described in Chapter 5. The diversity of systems

used was related to availability of licenses and support at the different locations where the research was done.

The ONG simulator is based on the block mode simulation principle [161]. This means that a telecommunication system is envisaged as a series of submodels each representing a component of the telecommunication system. The signal is modelled as a limited series of samples of the electromagnetic field of the signal. The samples are complex numbers capable of representing intensity and phase of the underlying carrier. The array of samples is passed on as one block of data between the submodels (hence the name block mode simulator)⁶². The blocks pass through each submodel in a unidirectional way. Submodels can have multiple inputs and outputs or require additional information. This functionality is presented in Figure 26.

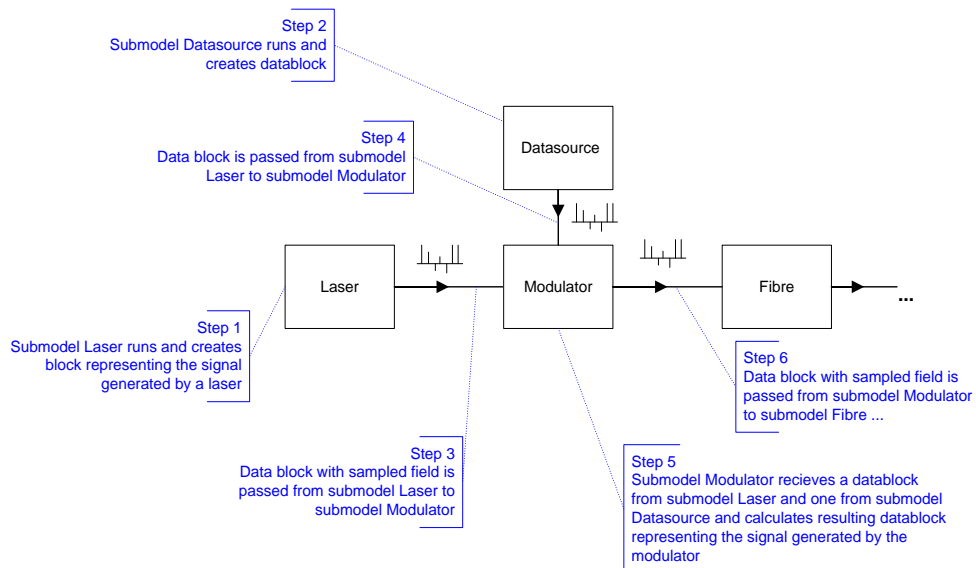


Figure 26: Operation of Block Mode simulator.

A more detailed introduction to optical simulation and the ONG simulator, including underlying details on how it was used for this research can be found in the transfer thesis related to this work [162].

4.2 Simulation setup

A block diagram of the structure of the simulation is given in Figure 27. It includes the default values of the parameters used for the different submodels. The graphs

⁶² In addition to the field sampled there can be additional information stored in the block passed between submodels.

representing eye diagrams and performance at different points in the simulation are not made with these default settings but with settings showing more clearly the functionality of the sub blocks on the signal. The red arrows represent the passing on of the sampled signal between submodels. Signal names used in this thesis are annotated. The submodels Align, Quantize, Adjust Powerlevel, QAnalyser have been purposely written for this simulation and the submodels Fibrepropagation, Eyeanalyser, Errorcount and Monte Carlo are modified versions of the ones present in the ONG simulator. Other submodels are unmodified code from the ONG simulator.

The simulation can be divided up into 5 major steps:

- Transmitter non-EPD: Here we create the signal as we ideally would like it to arrive at the receiver. For practical reasons we shape the pulse using a filter and add a very small amount of noise (60 dB OSNR) so diagrams and measured values are easier to interpret.
- Apply EPD: In this block we calculate a predistorted signal using back propagation. We then align the samples of the simulation with the start of the signal block so that during quantization the quantization samples are at the same positions in the bit period between different simulation scenarios. We use quantization and filtering to apply limitations normally originating from the technology (DAC & electrical circuitry) used to create the EPD signal in a physical system. The quantization reduces the number of levels (across time and intensity of I and Q components) in the signal without changing the number of samples (and their internal representation) used for simulating the signal. Averaging is used to calculate the quantization level across the sample period.
- Transmission link: we simulate propagation of the signal along a fibre system consisting of 90 km NDSF spans using the Split Step NLSE. The amplifiers are modelled as being noiseless.
- Receiver: We add all the noise that would be added to the signal at the different stages in the system in one lump. The receiver has an optical bandpass and electrical lowpass filter with characteristics typical for 10 Gb/s NRZ systems.

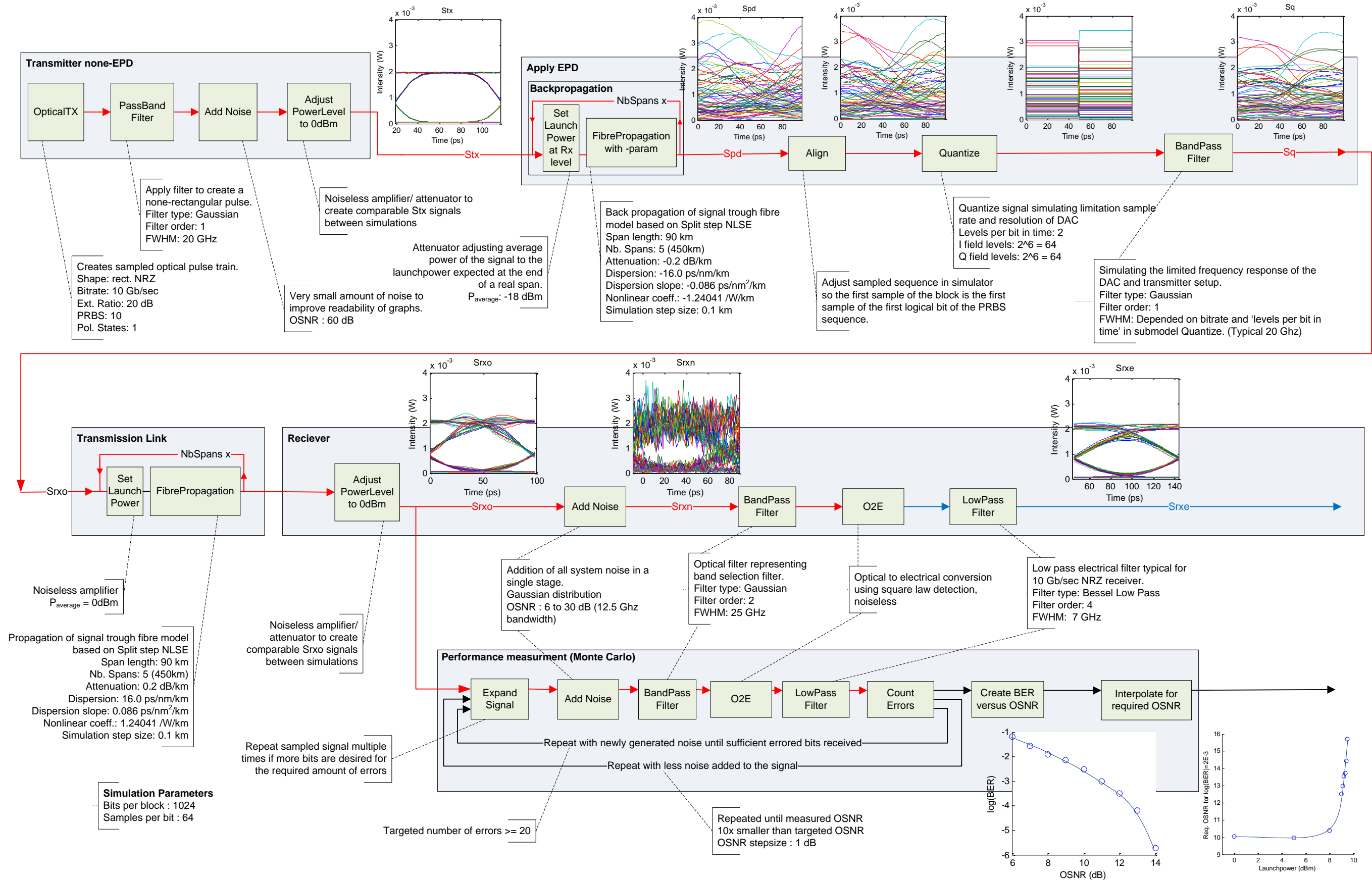


Figure 27: Block diagram of simulation.

- Performance measurement (Monte Carlo): Because of the pattern dependent grouping of signal levels observed in early simulations we chose to use Monte Carlo over Q based performance measurement. If necessary we copy the signal block multiple times to increase the number of bits available to assess performance. We then add noise and sending it through the same submodels at the receiver, we count the errors based on the known logical data sequence with optimised sampling time and decision threshold. We repeated this always adding newly random generated random noise aiming to observe at least 20 errors at the targeted BER. This was repeated for different noise levels including BER levels up to 10x smaller than the desired BER. The OSNR for the targeted BER and confidence intervals were then calculated using interpolation as documented in [157].

The noise is added in a single lump at the receiver. The reason to do so is to allow the Monte Carlo method to be used. If we were to distribute the noise addition along the transmission link, each iterative loop in the Monte Carlo would require the time intensive submodel of the fibre propagation to be executed. However as a consequence the simulations do not model the build-up of noise during transmission and its nonlinear interaction with the signal in the fibre.

The most obvious omission from the simulation in comparison with a real EPD transmitter is that there is no block that simulates the limited address size of the LUT table (or limited number of taps of a FIR filter). This means that the effect of the limited size of the influence window as discussed in paragraph 3.7 is not simulated. As a consequence the results of the simulation are only meaningful for distances for which the penalty, because of the limited size of influence window, is negligible. This penalty has been examined in depth in the works mentioned in section 3.11.2 and with the designed size of an 11 bit LUT we therefore were limited to a distance of 450 km (5 spans of 90 km). This assumption was in later experiments confirmed to be correct. To increase the NL effects, which were a primary target for investigation, we increased the launch power instead of the transmission distance.

An important remark to make is the difference between simulation samples and quantization samples on the model. Simulation samples refer to the sampled optical field or electrical signal (at 640 GSamples/s) used to represent these signals in the ONG simulator. Quantization samples refer to the sampled signal as it is represented in the digital part of the EPD transmitter. These samples have a much lower rate (20 GSamples/s) and 1 quantisation sample is stored in the simulation as 32 simulation samples.

4.3 Simulation results

4.3.1 Transmission without EPD

To benchmark the simulation model, the performance of non EPD NRZ back to back and over a single span was calculated. The average launch power was 0 dBm. The results are presented in Figure 28 and show how transmission without distortion compensation limits NRZ transmission as a benchmark for the EPD results. The solid line is a fitting curve of the performance points reported by the simulation. Some performance points were calculated with fewer than 20 measured errors.

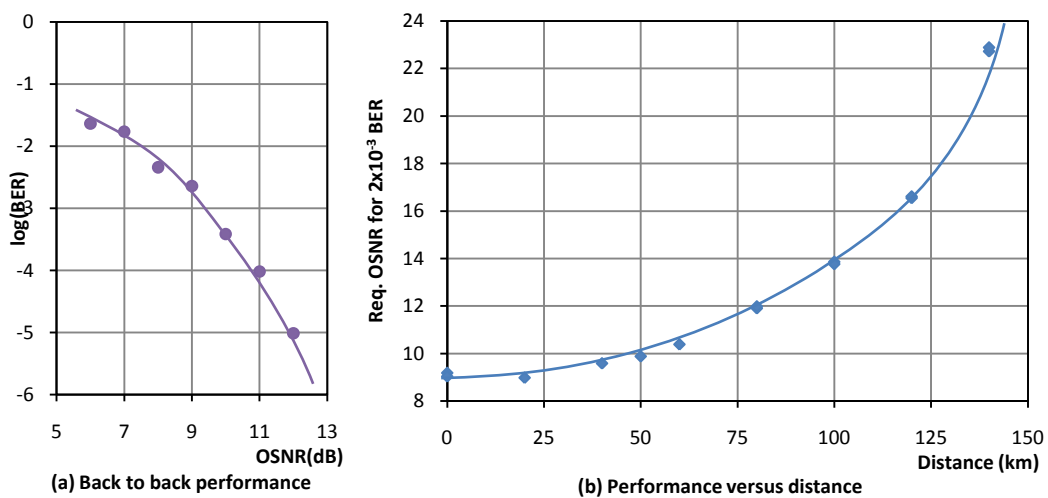


Figure 28 : Simulation results of transmission without EPD.

We did not optimize the NRZ system in the model for optimal performance. The back to back required OSNR for the targeted BER of 2×10^{-3} is approximately 9 dB OSNR, setting the reference for later EPD simulations. The single span results show that NRZ at 10 Gb/s without distortion compensation drops in performance significantly at a distance of around 100 km over standard SMF.

4.3.2 Non-Linear versus Dispersion only EPD

In a first series of simulations we assessed the possible performance gain that could be made by predistorting for NL effects in addition to CD effects. The simulation parameters for each submodel are given in Figure 27.

The red curve for ideal EPD compensating CD and NL effects in Figure 29 shows that in the simulation model no penalty is observed if the launch power is increased. This should not

be interpreted that if we could realise ideal EPD then distortion would be nonexistent, only that the effects that would distort the signal in that case are not simulated in our model. The blue curve shows the performance of a predistorted signal without non-linear effects (simulating the use of a FIR filter instead of a LUT table) We can see that up to power levels of around 2 dBm we see no noticeable degradation of the performance compared to compensating CD and NL effects. NL effects however then degrade the performance significantly making the use of launch powers higher than 6 dBm unrealistic for this type of system.

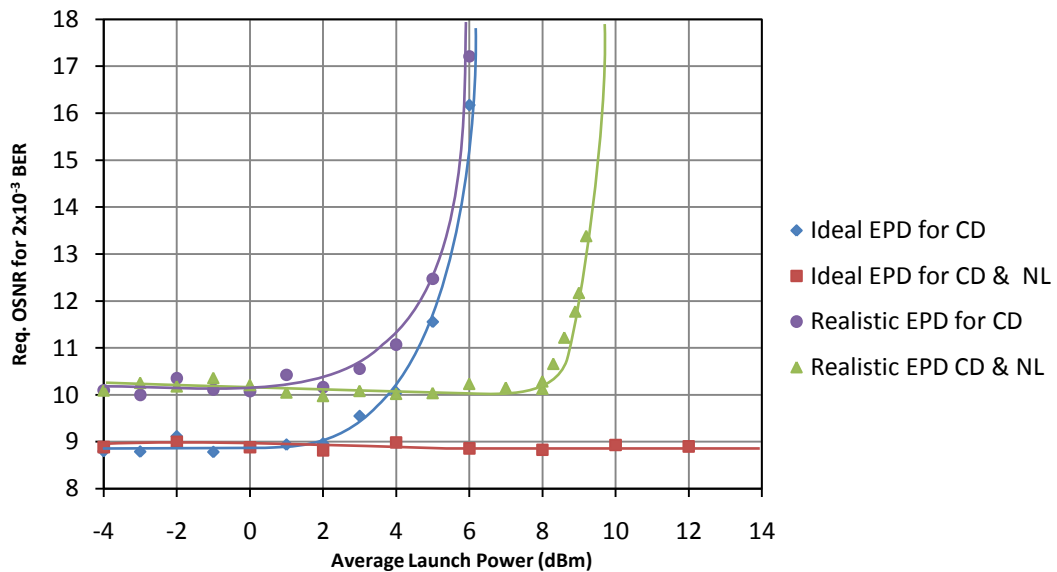


Figure 29: Simulation results of ideal and realistic EPD.
(5x90km transmission distance. Ideal: no digitalisation effects, Realistic: quantised signals and limited bandwidth of EPD transmitter)

We then applied limitations imposed by the EPD transmitter to the system, assuming that the EPD transmitter would be limited to 2 samples/bit, 64 signal levels and has a limited bandwidth. If we look at the purple curve in Figure 29 we see that this adds an OSNR penalty of 1 dB even at low launch powers. The launch powers at which NL effects start degrading the signal are at the same levels as ideal predistortion. The green curve is the one most closely related to this research because it shows performance of a practical transmitter as proposed here. We see that at low launch powers it works as well as CD only predistortion. It also shows that if we increase the launch power, a level is reached at which the effectiveness of the predistortion drops significantly (at approximately 9 dBm in the simulation). This 9 dBm is however 4 dB higher than the limit for a CD only system.

This difference is sufficiently large to suggest that we should be able to measure this difference in an experimental setup.

Another remark to make is that the drop in performance for realistic CD and NL predistorted signal is steep. When increasing the launch power by 2 dB (from 8 dBm to 10 dBm) it can be seen that the required OSNR drops from the maximal achievable 10 dB to over 20 dB. This is in contrast to the CD only simulation models in which this drop occurs over an increase in launch power of more than 5 dB.

4.3.3 Deviation in power to detect NL compensation

A method to show that NL effects are being compensated for is to transmit a predistorted signal at a particular launch power different from the value used in the calculation of that signal.

In Figure 30 we show the result of a model demonstrating this. We predistort a signal assuming it is to be sent across a link with a certain launch power (-2 dBm, +2 dBm and +6 dBm). We then send it across a link with a different actual launch power (so the back propagation Split Step NLSE and link simulation Split Step NLSE are done with different power levels). The actual power level is represented on the x-axis of the graph.

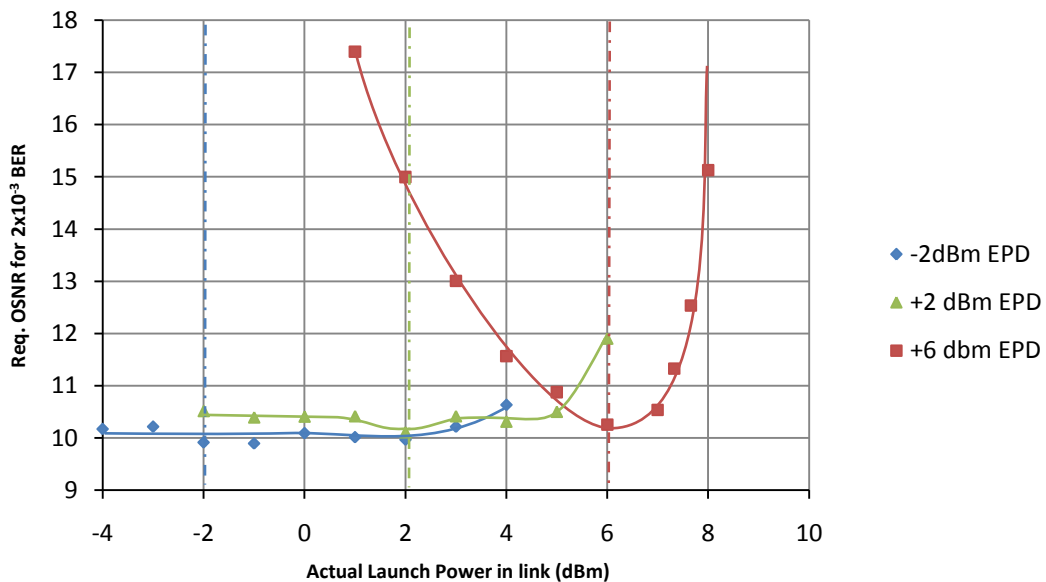


Figure 30: Simulation results of transmission at incorrect launch power.

CD is a distortion effect which is independent of the power of the signal. This means that if a signal is predistorted assuming a launch power A and it is transmitted with launch power

B then as long we ensure that we work in an area where the NL effects are negligible the predistortion should still achieve the same signal improvements. In our particular model this means maintaining A and B < 2 dBm. The blue curve in Figure 30 is an EPD signal calculated for a launch power of -2 dBm. Provided it is transmitted at under 2 dBm we see no change in required OSNR is observed.

NL is a distortion which is dependent on the power of the signal, so if we transmit a signal calculated for a particular launch power which includes significant NL distortion and transmit it at another launch power, a penalty will be observed. This is the red curve in Figure 30. The EPD signal is calculated for a launch power of +6 dBm. It can be seen that if the actual launch power is increased or reduced there is an OSNR penalty. We see in this simulation that the penalty curve is not symmetrical in relation to the optimal launch power (red dot-striped line) and notice an increase in the required OSNR by 4 dB for a 4 dB drop or 2 dB increase in launch power. These are values which we expect to be measurable in an experiment.

We can use this behaviour to confirm that we are compensating NL effects in a setup. If we decrease the power in a system, while keeping the same LUT entries, and the penalty increases, we confirm that we are compensating NL effects.

4.3.4 Influence of sampling method to calculate LUT

To assess the impact of the DAC sampling point on the performance, we constructed a quantization submodel that does not average but takes the instantaneous signal level at a certain offset from the start of the bit period as the level of the quantized sample. Simulations at 6 dBm launch power were carried out.

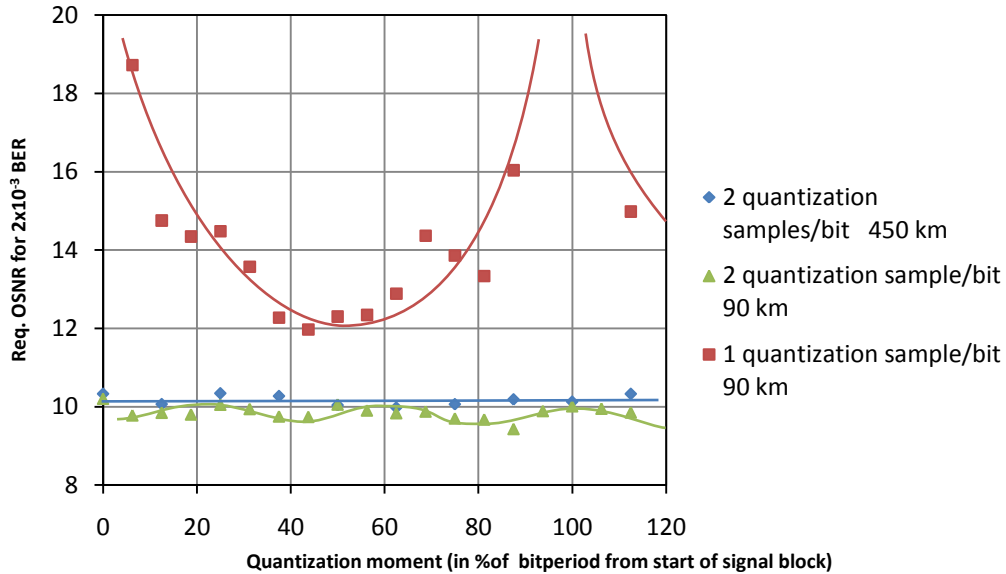


Figure 31: Impact of quantization method of EPD signal on performance.

Because the impact of varying the sampling moment is expected to be periodic with a period equal to the length of a quantization sample (so 100% of the bit period for 1 quantisation sample/bit curves and 50% of the bit period for 2 quantisation samples/bit in Figure 31) we can use this to discriminate between variation originating in the Monte Carlo approach (non periodic variation) and variation originating in the change of quantization moment (periodic variation).

We were unable to detect any periodic variation when using 2 quantization samples/bit and transmitting over 450 km. The noise varied over a range of 0.3 dB required OSNR. Because of this we expected that the impact of the different averaging methods used for creating the LUT in our setup would be even lower.

We could detect a periodic variation in the penalty when using a single span as transmission distance resulting in a variation of required OSNR on the order of 0.5 dB. To obtain a very significant impact on required OSNR it was required to drop the quantization rate to 1 quantization sample/bit over a single span. We could not run this simulation for single quantization sample per bit over 450 km because this makes the desired bit-error-rate of 2×10^{-3} unachievable. The performance flattens out at approximately 10^{-2} . This illustrates the previously described assessment of requiring at least 2 samples per bit for effective EPD.

From these results we concluded that running the setup with LUTs calculated without optimised quantisation moment and without averaging over the time period of the quanta was acceptable.

More details on issues with the sampling times on the back to back performance of NRZ can be found in 6.2 when the results with the experimental setup are presented.

4.4 Summary

With current simulation theory it is possible to simulate optical transmission accurately enough to make predictions on the expected results of a test setup.

From simulations of the envisioned transmitter, we conclude that the effects of predistortion on the penalty resulting from nonlinear distortion are on a measurable level. We expect to be able to show this by transmitting a signal at different launch powers than the assumed launch power in the calculation of the predistorted signal.

Chapter 5 has been removed from the published version of the thesis. This has been done to comply with none-disclosure agreements agreed on during the research related to this thesis.

6 Transmission results and analysis

6.1 Method

When carrying out a transmission experiment, except when explicitly mentioned, the following method is always used. First the length of the link is set by tapping off the signal at the desired EDFA in the link (the dotted drop points in the link shown in Figure 56). Then the corresponding code is loaded onto the FPGA. The FPGAs and DAC/MUXs are port synchronized followed by generation of a NRZ signal that is used to align the two arms of the transmitter and to optimize polarisation between the CW source and the modulator.

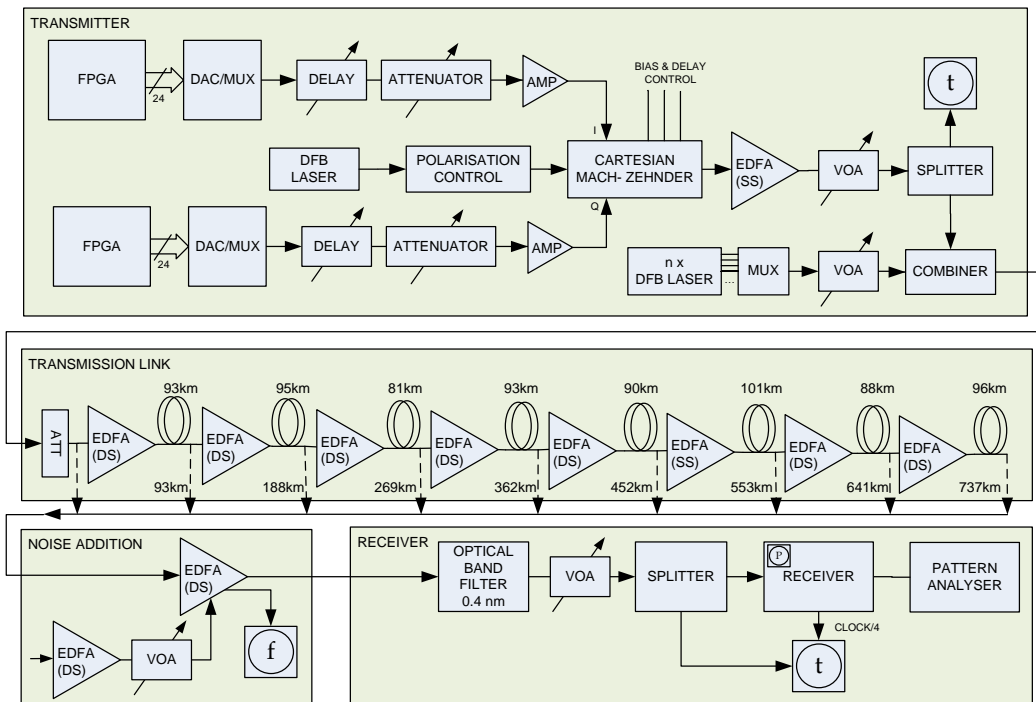


Figure 56: Diagram of transmission setup.

After arm alignment, we roughly set the analogue control signal and switch to the desired LUT table in the FPGA. We then iteratively adjust the analogue control levels in the transmitter (PkPk, Bias, $\pi/2$ delay), the receiver (decision threshold, sampling time), and the power settings of the EDFAs in the transmission link while adding sufficient noise to obtain a BER of approximately 10^{-6} and keeping the receiving power constant using the VOA in the receiver block, until further improvements in the BER are not possible. We then carry out BER measurements at multiple OSNR values by adding different amounts of

noise to the system by adjusting the VOA in the Noise Addition block and adjusting the final variable attenuator in the receiver to keep the Rx power constant and optimising the decision threshold at the receiver between the measurements with different noise levels.

The transmission link is constructed using commercial amplifier modules from an Ericsson long haul transmission product with integrated control algorithms and using fibre spools, (rather than installed fibre), as the transmission medium. The fibre is standard non-dispersion shifted fibre (NDSF) with estimated chromatic dispersion (D) of 17.2 ps/(nm km), a dispersion slope (S) of 0.0572 ps/(nm² km) at the reference frequency 193.1 THz and a nonlinear coefficient (γ) of 1.36 (W km)⁻¹. The chromatic dispersion compensating fibres, normally present at the mid-stage of the dual-stage (DS) amplifiers are removed and replaced by attenuators.

At the mid-stage of the last dual stage amplifier, amplified spontaneous emission (ASE) white noise is added to enable the optical signal to noise ratio (OSNR) at the receiver to be controlled. An extra 36 channels of the DWDM signal are filled with non-modulated signals following a 100 GHz channel plan, but spaced by 200 GHz from the electronic predistorted (EPD) channel to improve the accuracy of the OSNR measurements.

When comparing results we target an error rate of 2×10^{-3} the pre-FEC error rate that following the ITU standard G.975 [191] using a standardised 7% OTN FEC in an OTU-2 format, would result in a post FEC BER of 10^{-13} , an acceptable operating point for modern telecommunication networks. An issue of targeting the 2×10^{-3} error rate is that this is at the limit of what can be counted by the BER test set used⁸¹ at this working point. The setup is also more sensitive to small changes in settings and variations of transmission conditions. Statistical curve fitting, taking into account all related measurement points, is used to limit these effects.

The measurement of the OSNR is carried out at the monitoring point of the second stage of the amplifier in the noise addition block. We use a bandwidth of 0.6 nm to measure the signal strength and measure the noise at 0.4 nm away from the central frequency, and normalise the measured value to 0.1 nm bandwidth.

⁸¹ Above an error rate of around 5×10^{-3} (the exact limit was dependent on the distribution of the errors), the test set would not synchronize with the transmitted test pattern.

6.2 Linear transmission

Figure 57 shows the results when operating with an average EPD channel launch power of 0 dBm at the start of each span and with an 11 bit LUT. The fitted curves are second degree polynomials.

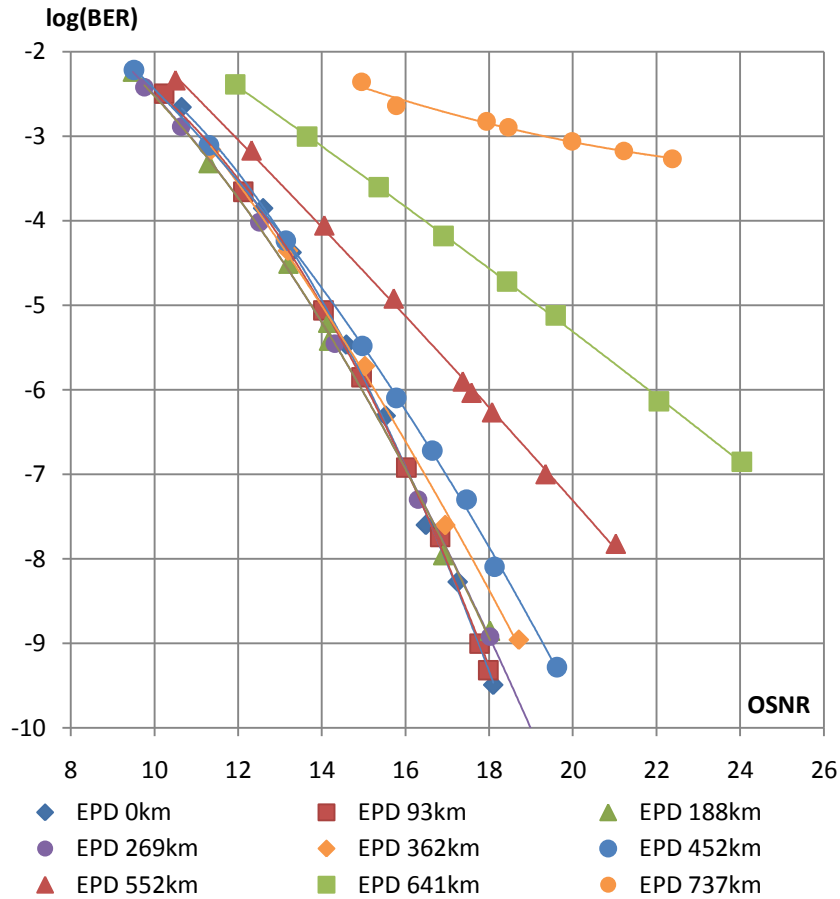


Figure 57: BER versus OSNR for an 11 bit LUT at 0 dBm launch power [1].

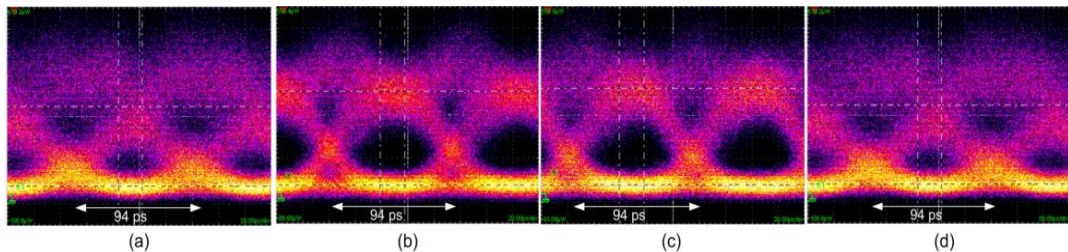


Figure 58: Eye diagrams of 11 bit LUT EPD with an OSNR of 18 dB at the receiver of (a) an uncompensated NRZ signal after 93 km transmission, compared to EPD NRZ after (b) 93 km, (c) 452 km and (d) 737 km transmission [1].

A BER $< 10^{-9}$ is achieved for transmission over 452 km, and BER $< 10^{-6}$ for distances up to 641 km. The eye diagrams presented in Figure 58 correspond to points on some of the

curves in Figure 57 at an OSNR of 18 dB. The eye diagrams are recorded by dividing the recovered clock by a factor of four to trigger the oscilloscope.

To achieve 7 bit LUT based EPD, we keep a LUT with 11 bit address size in the electronic design but load a table constructed taking only 7 bits into consideration. This gives identical entries in the table for memory addresses where the first 7 bits were identical. The results of this setup are presented in Figure 59.

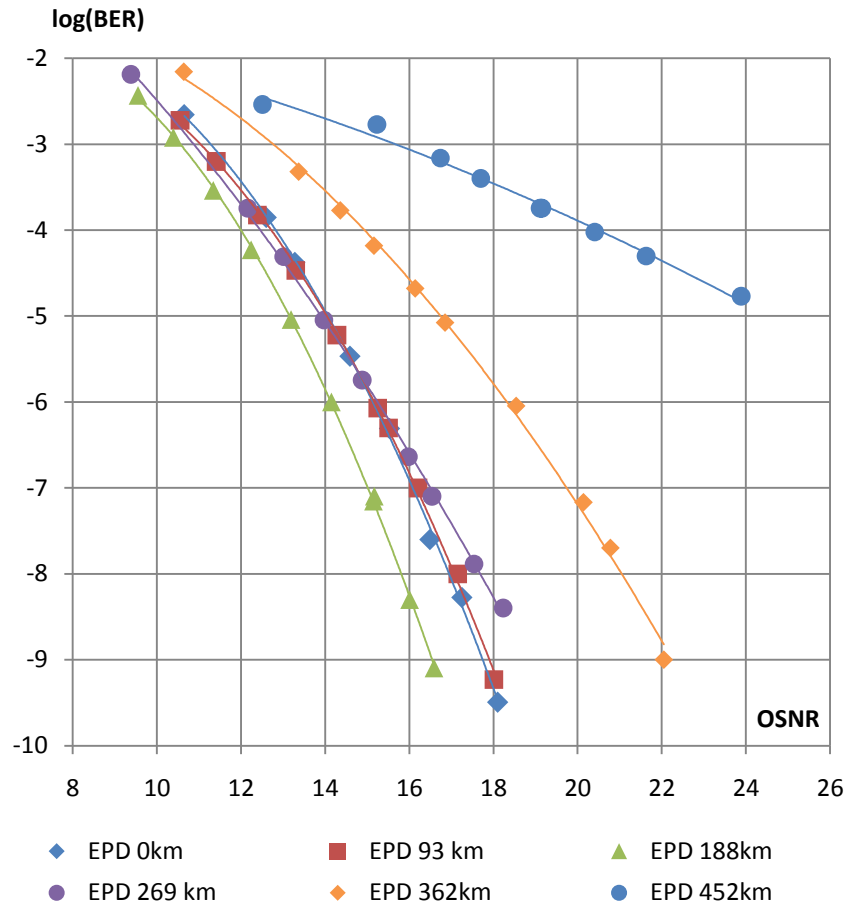


Figure 59: BER versus OSNR for a 7 bit LUT at 0 dBm launch power.

Figure 60 shows the comparison of the results with 7 bit LUT and 11 bit LUT based EPD, and also with NRZ without EPD. Only points for 0 and 93 km are present for NRZ without EPD, because at 188 km, locking of the clock recovery module to the received signal is not possible. Intermediate distances are not investigated because of the fixed length of the spans in the transmission setup.

The performance of the EPD signal shows a penalty of less than 1 dB (for $BER < 2 \times 10^{-3}$ and compared to the NRZ back-to-back performance) optimal performance up to 500 km.

When the LUT address size is reduced to 7 bits this limit is reduced to 300 km, showing that, at this operating point, the memory depth of the LUT table is the limiting factor. The dotted curves in Figure 60 are manually added and are not calculated using a curve fitting algorithm.

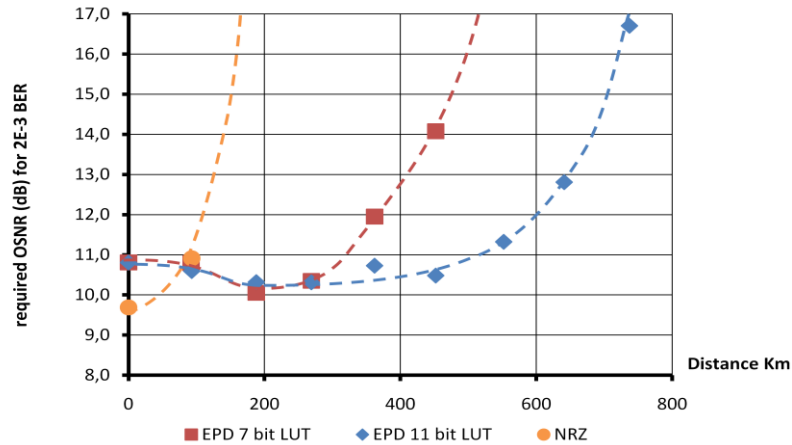


Figure 60: Performance comparison 7 bit, 11 bit LUT and uncompensated NRZ.

It can be seen that there is a penalty between the required OSNR using EPD at distances below the limit imposed by the size of the lookup table (e.g. below 500 km for 11 bit LUT) compared to back to back operation with NRZ. This penalty is present because of limited time and amplitude resolution when creating the transmitted signal by DACs and because of non-optimal LUT entries.

It can be seen that in back to back operation (0 km distance) our NRZ modulation table outperforms the table calculated for back to back operation by the EPD algorithm. So at short distance the measurements shows that NRZ outperforms EPD as implemented in this work.

To investigate the source of this, we compare the 11 bit LUT used to generate NRZ (Figure 61), EPD in BtoB operation (Figure 62) and EPD with +4 dBm launch power over 552 km (Figure 63). In all three figures the graphs (a) and (b) are based on the actual contents of the used LUTs, scaled in accordance to the settings of the analogue drive signals to the levels considered optimal by the simulation model used to generate the LUT entries.

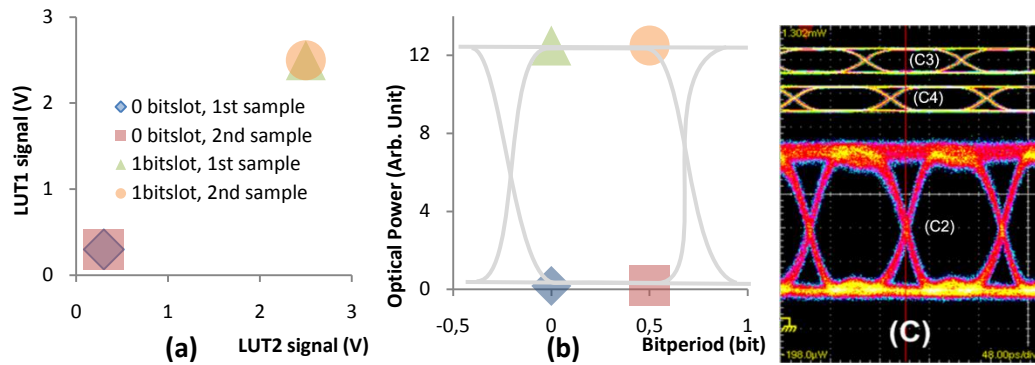


Figure 61: Analysis of NRZ LUT contents.

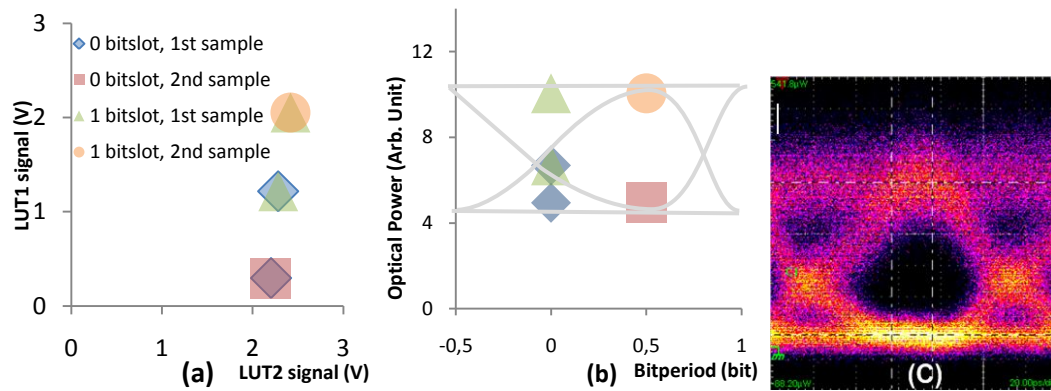


Figure 62: Analysis of EPD BtoB LUT contents.

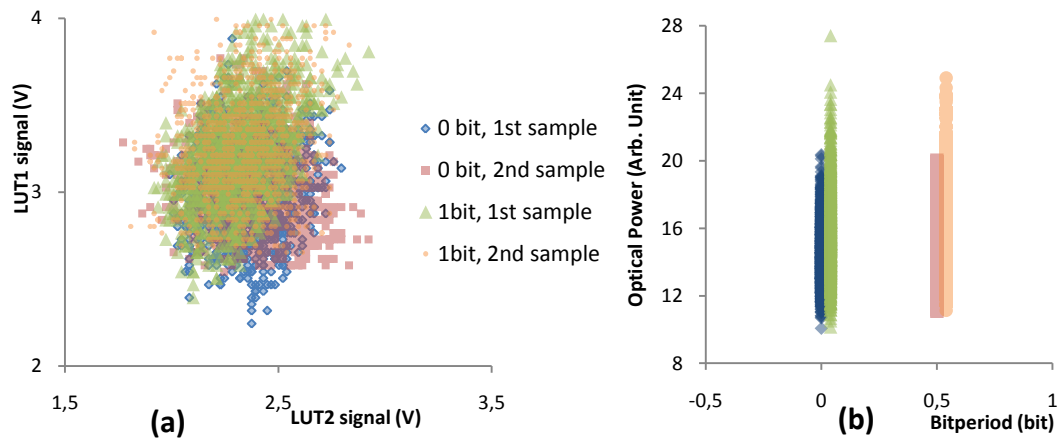


Figure 63: Analysis of EPD +4dBm 552km LUT contents.

We have grouped the 2x2048 entries in the LUT (2 samples for each possible 2^{11} bit sequences) in 4 groups: 1st and 2nd sample of a bit slot containing a 0 (blue diamonds and red squares) and 1st and 2nd sample of a bit slot containing a 1 (green triangles and orange circles).

Figure (a) represent the position of these 4096 points if we place the I and Q electrical drive signals on orthogonal axes. Hence the graph gives an indication of the position of these points in the optical IQ space after modulation by the MZ (it is not an absolute position because the analogue drive processing of the signals influences the absolute position). In graph b we have plotted the same four groups of points but now as power⁸² versus time (giving the classical eye diagram of the signal).

In Figure 61 and Figure 62 most points in graphs (a) and (b) of the same group overlap each other. Fig (c) shows the NRZ signals measured^{83 84} as generated and recorded by an oscilloscope. Trace C3 and C4 are the drive signals as generated by the DAC/MUXes and trace C2 is the optical signal generated by the MZ. It can be seen that the eye shape in trace (c) and graph (b) in Figure 63 are similar and so confirm that ignoring the influences of the analogue components is acceptable.

In Figure 62 the same graphs are presented but now for the BtoB LUT calculated as described in paragraph 5.8. Because there is 0 km length fibre present there is no signal distortion by fibre and hence there is no real predistortion effects added by the backpropagation algorithm. We see however that the signal waveform is more distorted than that of the NRZ in two major ways:

Firstly the maximum extinction ratio of the Cartesian MZ is not achieved by the BtoB LUT. The arm driven by LUT2 is only marginally contributing to the modulation depth. This is because the algorithm that calculates the LUT does not optimise for maximum modulation depth by rotating the signal by $\pi/4$ radians in IQ space, to optimally use the modulation of both arms. This effect was partly compensated by adjusting the PkPk level by using the stepped attenuators in the setup.

Secondly, it can be seen that the first sample of the bit is not at the maximal or minimal level during transitions from a logical 0 to 1, or 1 to 0. This is a consequence of sampling on the edge of the pulse when calculating the LUT. A proposed solution for this could be

⁸² Calculated from the drive signals.

⁸³ It is common to apply pulse shaping to optimise transmission in NRZ systems. We did not apply pulse shaping in our transmitter to avoid overcomplicating the design.

⁸⁴ Figure 61(c) and Figure 62 (c) were recorded with different noise levels. In Figure 61 no extra noise was added. In Figure 62 an OSNR of 18 dB was used by inserting additional noise as described in earlier chapters.

to take, rather than the 1st and 16th sample of a bit in the LUT calculation algorithm, the 8th and 24th sample or to use some kind of averaging or summation across multiple samples to calculate the LUT entry.

While these effects contribute to a measurable penalty in back-to-back operation, their negative influence on the performance becomes less when transmitting over a link where actual distortion is present and is compensated by the LUT. This is a consequence of intersymbol interference (which we compensate for by predistortion) resulting in the steep pulse edges of the bits no longer being present at the 1st sample in the bit slot but now becoming distributed across all samples. This lessens the second effect described above. In addition, the full modulation depth of both arms is used in this case. Both these effects are illustrated in Figure 63.

6.3 Effects of suboptimal control parameters

Figure 64 shows the degradation of the received signal when the bias voltages for the I and Q inputs of the MZ and the quadrature ($\pi/2$) control are adjusted away from the optimum values.

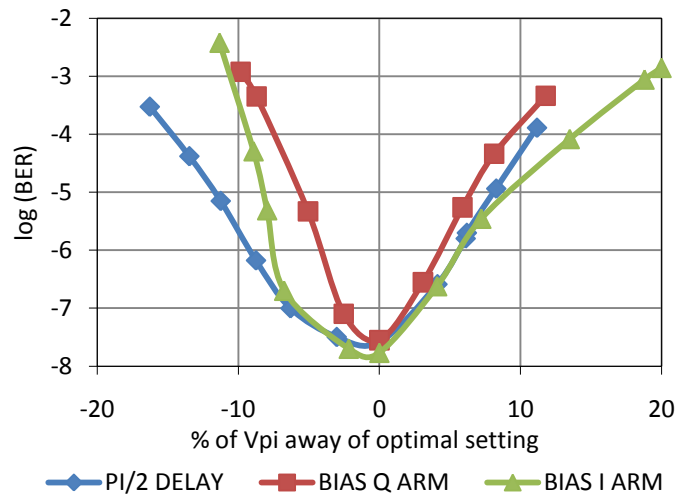


Figure 64: Influence of suboptimal control signals [1].

Figure 64 is for the case of transmission over 452 km with 0 dBm launch power and an OSNR of 17 dB at the receiver. Figure 64 shows that keeping the setting within $\pm 4\% V_{\pi}$ of the optimal value limits the penalty to less than a decade.

Dependence of the BER on the control signals has two sources. Firstly they each influence the transmission signal in different ways and some changes affect the BER more than

others. Secondly the analogue systems between the measured generated voltage value and the effect they create on the optical signal might not be identical. In particular the response curve of the MZ modulator for the different control signals are not 100% identical.

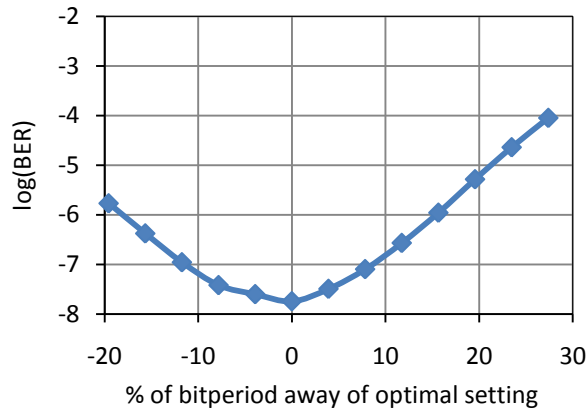


Figure 65: Influence of misalignment in time between I and Q arm [1].

In Figure 65 (also for transmission over 452 km) we show the effect of timing misalignment between the two arms driving the MZ. If the misalignment is kept below 12% of the bit period, the penalty on the BER is less than a decade. Two possible mechanisms can be the source for variations in the settings presented in both graphs: actual variation in the control voltages (because of imperfect DC sources), or changes in the transmission system (for example, temperature changes within the MZ) requiring adjustment of the optimal setting.

The influence of changing the PkPk levels of the signals driving the arms of the MZ away from the optimal setting is presented in Figure 66, the optimal setting being the point at which the combination of the control settings for the PkPk levels, the biases, quadrature delay and arm delays resulted in the minimal BER at the receiver. This graph is obtained for transmission over 552 km fiber, with 0 dBm launch power and an OSNR of 20 dB at the receiver. The graph is based on 26 measuring points inside the coloured area of the graph. A Kriging based algorithm with minimal smoothing was used for interpolating the points. The minimum achievable BER is 2.5×10^{-8} . It can be seen that keeping the PkPk level within 10% V_{π} of the optimal value limits the penalty to below one decade of BER.

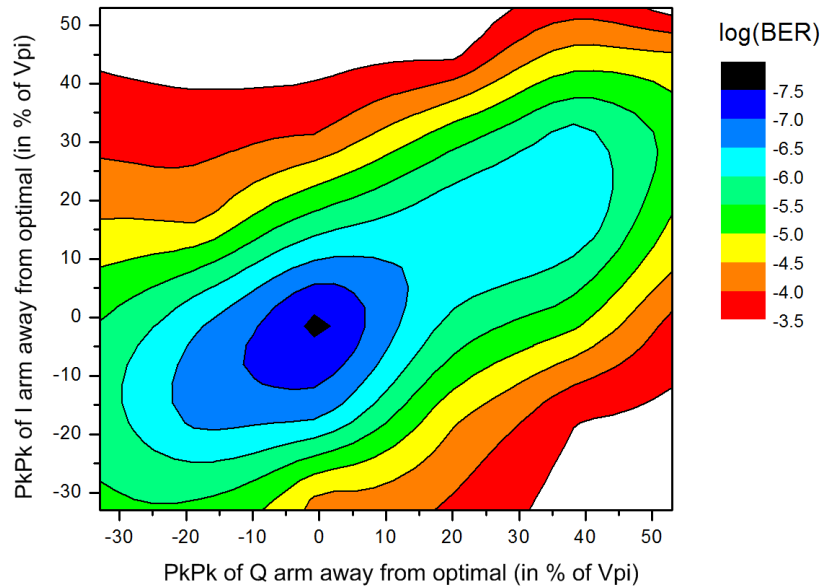


Figure 66: Effect of non-optimal PkPk levels of the signal driving the MZ arms [1].

As expected, within certain limits, an inaccuracy in the setting of the PkPk level of one arm can be compensated by optimizing the PkPk level of the other arm. This is indicated by the trough in the plot at an angle to the x and y axis. It is the ratio of the setting of the two arms that is important to maintain a good level of performance, rather than the absolute level of the settings of the arms.

If the components used to control both arms of the MZ modulator were to have identical characteristics then the trough in the plot would have a 45° angle to both axis of the graph. Because in practice the amplification factor of the electrical amplifiers in the arms, the modulation curve of each arm of the MZ, cable losses etc are slightly different, the angle of the trough is not exactly 45°

The optimal peak-to-peak voltages driving the MZ are found to correspond to 90% of V_π on the I input and 105% of V_π on the Q input. These values are actually larger than those assumed in the calculation of the LUT tables, in which a modulation PkPk value of 30% of V_π on the I input and 36% of V_π on the Q input are used. However, it can be seen from Fig. 8 that decreasing the PkPk values, while reoptimising all the other control setting to achieve minimal BER to operate at the PkPk levels used in the calculation of the LUT does not improve the achieved BER. We suggest that three elements can explain this. Firstly the value of V_π is measured on the DC ports of the MZ, and a greater V_π might be present on the RF ports. Secondly the extreme signal values at which the peak levels are reached and

which lie in the non-linear part of the modulation curve do not occur often in the drive signals. Hence, the majority of the samples lie within the linear part of the modulation curve. Thirdly there is a trade-off between maintaining linearity and achieving maximal extinction ratio.

6.4 Nonlinear transmission

Next, higher power transmission experiments are performed on the same link as in the previous paragraph, to show that effects of fibre nonlinearity (NL) are being compensated by LUT based EPD. We do not use clipping when constructing the LUT contents. However driving the signals at the higher than calculated PkPk levels, as already mentioned, introduces a form of clipping because of the saturation of the electrical amplifier and the nonlinear modulation characteristics of the MZ modulator. This occurred because we use feedback (end to end BER) of the overall link performance to optimise the settings instead of trying to generate a signal as close as possible to the one assumed in the simulations and calculations of the LUT.

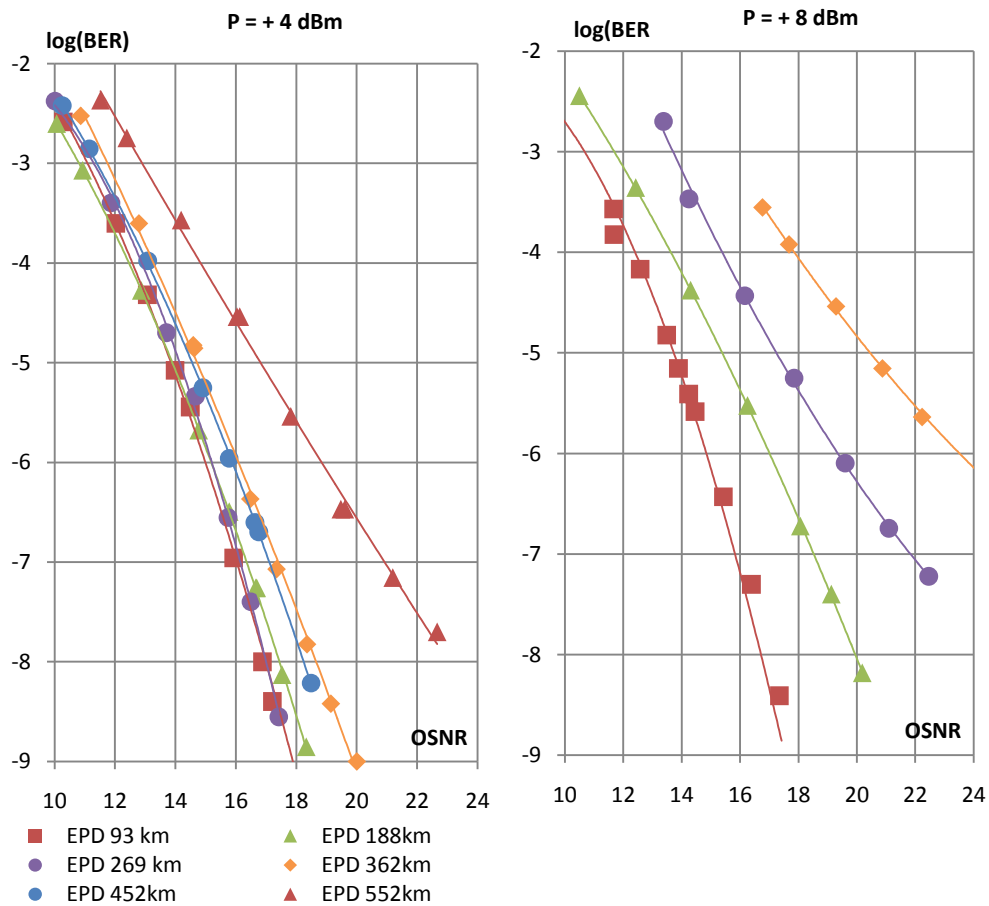


Figure 67: Performance at +4 dBm and +8 dBm launch power.

Figure 67 shows the results for LUT of +4 dBm and +8 dBm average launch power of the EPD modulated wavelength transmitted over different transmission lengths.

Figure 68 compares the results in Figure 67 with those presented in Figure 57 we plot the required OSNR for a BER of 2×10^{-3} versus length for EPD for all three launch powers and add the NRZ transmission as a reference.

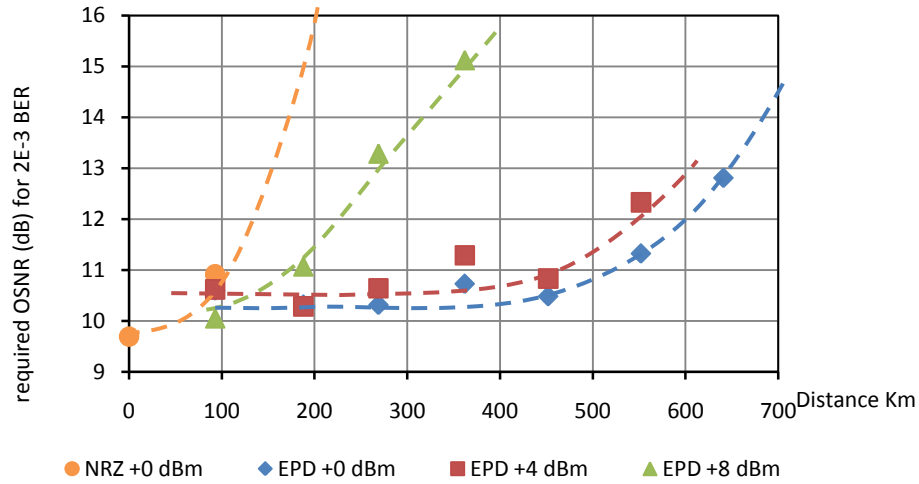


Figure 68: Performance for different launch powers.

There is a penalty of less than 1 dB when increasing the power of the EPD channel from 0 dBm to +4 dBm over distances up to 500 km. The transmitter is capable of predistorting the additional NL based signal distortions. When increasing the launch power of the EPD channel up to +8 dBm, the performance deteriorates (at 450 km the OSNR penalty compared to 0 dBm and +4 dBm launch power is greater than 10 dB).

Figure 69 shows the performance curves of LUT based EPD for the case where the entries in the LUT tables are calculated for a particular fixed launch power, while the actual launch power in the link is varied.

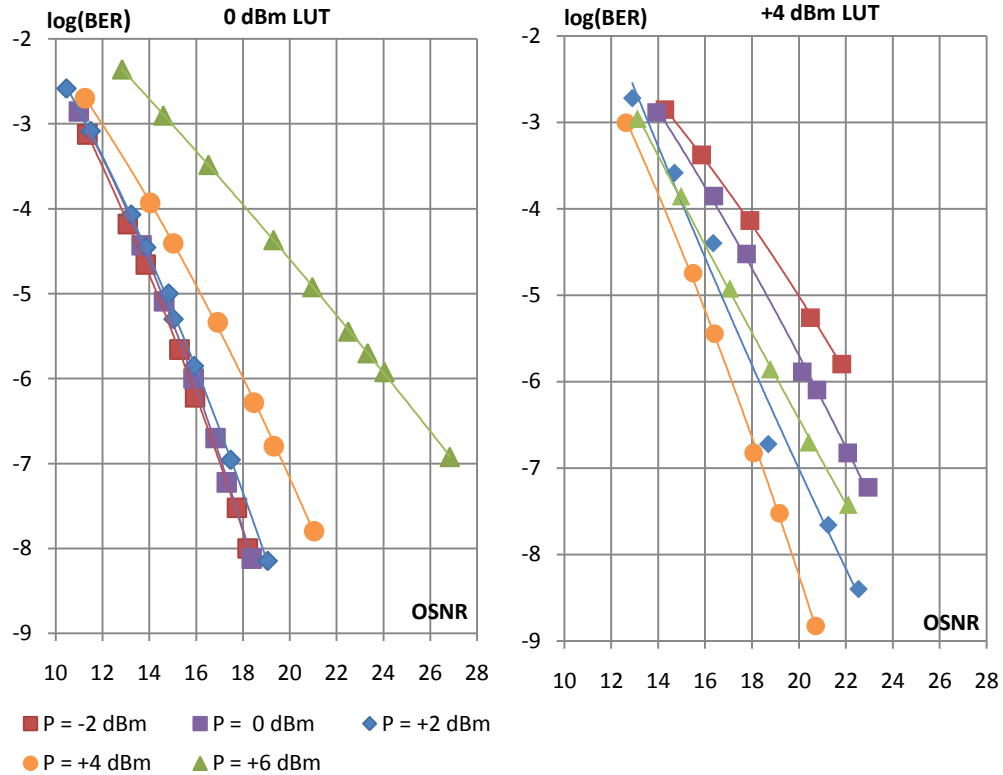


Figure 69: Performance of LUTs being used at different launch powers 0 dBm (left) and +4 dbm (right).

Because the added noise dominates the performance it is difficult to see the compensation of the much smaller NL effects at a BER of 2×10^{-3} . To show that NL effects are being effectively compensated, we will compare the performance to achieve a BER of 10^{-6} shown in Figure 70.

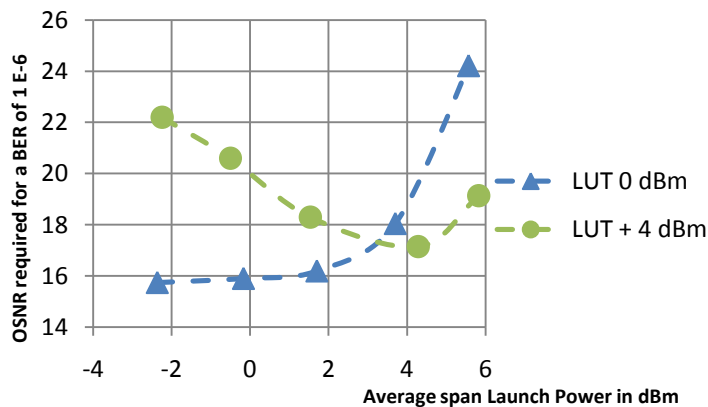


Figure 70: Transmission results showing compensation of nonlinear effects [1].

When acquiring the measurement points, we only adjust the launch power, the variable optical attenuators controlling the added noise, the received power and the decision threshold level. We keep the other control signals (PkPk levels, biases, quadrature ($\pi/2$))

control) at the values required when optimising at the normal operating point for that particular LUT. We only adjust these other controls when loading a new LUT for a different launch power.

In Figure 70 the blue markers show that a link in which the LUT entries are calculated for 0 dBm launch power suffers a decrease in performance when increasing the launch power, due to SPM, while there is no reduction in performance when reducing the power below 0 dBm. This indicates that it is mainly linear chromatic dispersion that is being corrected, and that there is no significant NL effects degrading the signal at 0 dBm. The green markers show the same measurements for the LUT entries calculated for +4 dBm launch power. In this case we observe a 2 dB reduction in the required OSNR at +4 dBm, and an increase in required OSNR when lowering the launch power, indicating that the effect of SPM in addition to CD is being effectively compensated for

6.5 Summary

The setup used to evaluate the transmitter presented in chapter 5 was a linear link equipped with components from a commercial telecommunication system. Experiments are carried out on a single channel with EPD.

We are able to increase transmission distances from less than 100 km to over 500 km without using other distortion combating techniques. This is mainly due to compensating chromatic distortion by the method applied.

Nonlinear effects can be compensated with this method and with the technology used in this setup. It is demonstrated that, increasing the launch powers from 0 to 4 dBm in a 450 km link, the OSNR penalty is reduced from 4 dB to 1 dB.

Imperfections in the analogue circuits part of the transmitter have a measurable effect on the overall performance of the signal and should not be ignored in the design of the transmitter.

In a detailed discussion we showed that algorithms giving good results for signals that experience significant distorting effects may not always find the optimal signal waveform in cases with only limited distortion.

7 Conclusions and future work

The main conclusion from this thesis is that it is possible to build an EPD transmitter compensating for chromatic dispersion and nonlinear effects with commercial off-the-shelf components including integrated digital to analogue converters and field programmable gate arrays (FPGA).

The transmitter constructed during this project was capable of transmitting 10.7 Gb/s NRZ modulated data with a pre-FEC BER of 2×10^{-3} at an OSNR of 13 dB with an 11 bit look-up table over 650 km (7 spans) of uncompensated non-dispersion shifted fibre (CD of 17 ps/nm/km) with 0 dBm launch power.

By implementing predistortion compensation for non-linearity in addition to chromatic dispersion effects, a penalty of less than 1 dB in required OSNR when the launch power was increased from 0 dBm to 4 dBm in experiments over 452 km was observed.

In doing so we showed that:

- Current FPGAs are sufficiently fast to apply LUT based filters on 20 Gsample/s digital signals. Filters sufficiently large for compensating the effects of >700 km of NDSF do however push the boundary of the available resources on the current (2008) generation of FPGAs.
- It is possible to overcome the issues related to non-synchronized different high speed output ports of an FPGA in a fully automated way. After synchronisation the system runs in a stable manner for a prolonged period of time (on the order of minutes to hours) but it can occasionally lose synchronisation. This results in the necessity to carry out periodic realignment if sustained transmission is needed.
- The use of memory resources on the FPGA leaves other resources (slices) available on the FPGA for other DSP algorithms. This has been verified by the usage numbers of an actual working design.
- The use of look-up table based predistortion, taking into account non-linear effects improves transmission performance in comparison to CD only compensation, in the case of significant levels of SPM distortion.

The optical measurements described in this thesis are directly relevant for intermediate length (100-700 km) 10 Gb/s per channel links. They show that the EPD technique makes it possible to extend these links from non-amplified spans (<100km) to amplified spans of 500-600 km, and that there are possibilities to extend the length of these links even further by optimizing the design presented in this thesis. Longer length links in EPD-only systems are possible by improving the digital filter design in the transmitter. This can be done by combining FIR and LUT filters while using the unmodified hardware as presented in this thesis.

To be able to apply EPD to higher speed links, higher speed electronics , e.g. DACs with increased sampling rates and bandwidths, than what is currently available on the market are needed. The period over which they will become available depends on the confidential business plans of IC manufacturers. The author expects that FPGAs and DACs with better performance will become available in the coming years.

The author, however, does not expect that the designers of these components will focus on EPD as a major market for FPGAs and DACs because other markets, e.g. packet processing, are more the focus of attention in FPGA development. As such, it will still be necessary to adapt non-ideal components to the needs of the research on EPD, especially because the expectations for predistortion methods will also be raised as time passes.

The fully documented transmitter constructed as part of this project makes it possible to assess and analyse EPD in many scenarios (such as DWDM, other fibre types, combination of EPD with DCF etc.) other than the one presented in this thesis. This would be possible without changing the design or physical build of the transmitter. Whether this will be done depends on the interest from and resources available to the research community and industry.

The experience of building the EPD transmitter has made clear that a significant amount of digital and analogue circuit development is needed in comparison to the amount of work required on the optical components. Hence we believe that progress in the area of realistic digital signal processing for optical communication will require more resources in these areas to achieve new products and novel optical transmission results.

There are still many technical challenges which could be addressed by future research to improve our knowledge of the fundamentals and implementation of EPD. The following can be mentioned:

- Optimisation of the methodology for calculating predistorted signals for all possible scenarios, especially addressing the issues with short (<100km) links as described in this thesis. This could be achieved by improving the algorithm used to reduce the sample rate in the calculation of the predistorted shape to the sample rate used in the hardware.
- Integration of LUT and FIR filters in the transmitter to further increase the amount of distortion that can be compensated. This combination of filters can be assessed by modelling and, in addition, implementation issues can be researched.
- Automating the synchronization procedure between the two parts of the transmitter each controlling one arm of the MZ modulator.
- Adding more performance tests in different scenarios and comparison with other distortion combating techniques.
- Implementing the filter in an ASIC instead of an FPGA.
- Optimising the filter models for different link parameters.

The author does not expect that the FPGAs and DACs currently available and expected in the coming years will be used in commercial implementations of EPD. The expected product makes the complexity of the transmitter too high. As demonstrated by other research groups transfer to ASIC of the same principle is a viable solution for this issue. The main issue, whether the cost of doing so makes an acceptable business proposal, has to be assessed within a particular system house and cannot be generalized. The author's opinion is that only when other DSP function are required in a transmitter/receiver (such as soft FEC or OFDM modulation) will it start making commercial sense to add EPD to the system by adding the EPD in the same IC as used for these other functions.

In addition, some of the issues addressed by EPD can be solved by already developed techniques such as DCM. Because of this, it is less likely that a system house will spend the research resources on EPD when it can already sell another solution to its customers. The issue of cost reduction could be an argument, but we cannot carry out this analysis without detailed market information, which is not available to academia. The author is aware that different system houses did make this analysis and have come to different conclusions.

The approach of using FPGA for building experimental transmitters to demonstrate and analyse optical transmission proposals is however a very realistic application. This is

clearly demonstrated by this project. It gives the research community the possibility to demonstrate theoretical principles in physical setups while only requiring limited resources. The big issue here is that it does require that optical research groups need to acquire (themselves or by outsourcing this to other parties) in-depth knowledge of digital design.

The design presented in this thesis has been left at the Ericsson research facilities in Backnang (GE) in Jan 2009 for research in DSP for other modulation formats. The author helped with adapting the synchronisation mechanism to work on sample instead of bit basis so it could be used for optical orthogonal frequency division multiplexing (OFDM) experiments. It is currently also being used for experiments with DQPSK signals, where the characteristics of this format are being used to expand the design with a fully automated arm synchronization mechanism.

At UCL the Optical Networks Group is continuing with research in this area. The experience of this project is being used by other researchers for work on predistortion for WDM systems and digitally generated OFDM.

Appendix A : An introduction to FPGAs

Field Programmable Gate Arrays (FPGA) are programmable logic circuits. On an FPGA a large number of interconnected standard blocks are present with different basic functionalities. The functionality of the blocks and the interconnections between them can be changed by programming the chip. This in contrast to Application Specific Integrated Circuits (ASIC) where the functionality of the chip is hardwired into the physical layers of the chip⁸⁵.

Because the same type of standard FPGA can be used for many applications, by reprogramming it, the advantages of mass production are introduced in components only needed in small quantities, such as our experimental transmitter. Also the capability to reprogram an FPGA means that a change in design can be implemented by changing the description of the functionality within the software tools and then downloading the design onto the chip. This process is much simpler than the development of an ASIC where a new design would require building a new chip in a clean room facility. A disadvantage of an FPGA is that an ASIC based on the same technology will in general outperform an FPGA in many domains (power consumption, speed of operation, size of the chip, etc.) For a more detailed review of FPGAs see [192] and for comparison with ASICs to section 2.5.7.3

Figure 71 represents a simplified block diagram of an imaginary basic FPGA (this one is so basic it would never be considered for production). The diagram can however be used to show the elementary components and the working principles of an FPGA. I will simplify many things (for example: I will not discuss power distribution. It can be seen that the example has no power supply pins. Any real working FPGA will of course need power).

⁸⁵ This is a very simplified view of digital components. It can be argued that certain ASICs can be considered programmable (like Central Processing units, CPUs, with microcode) and there exist other type of devices, such as Programmable Logic Devices (PLDs) which are programmable and are not considered to be FPGAs or ASICs and also components such as structured ASIC, in which only some mask layer are customised and others are generic to many chips.

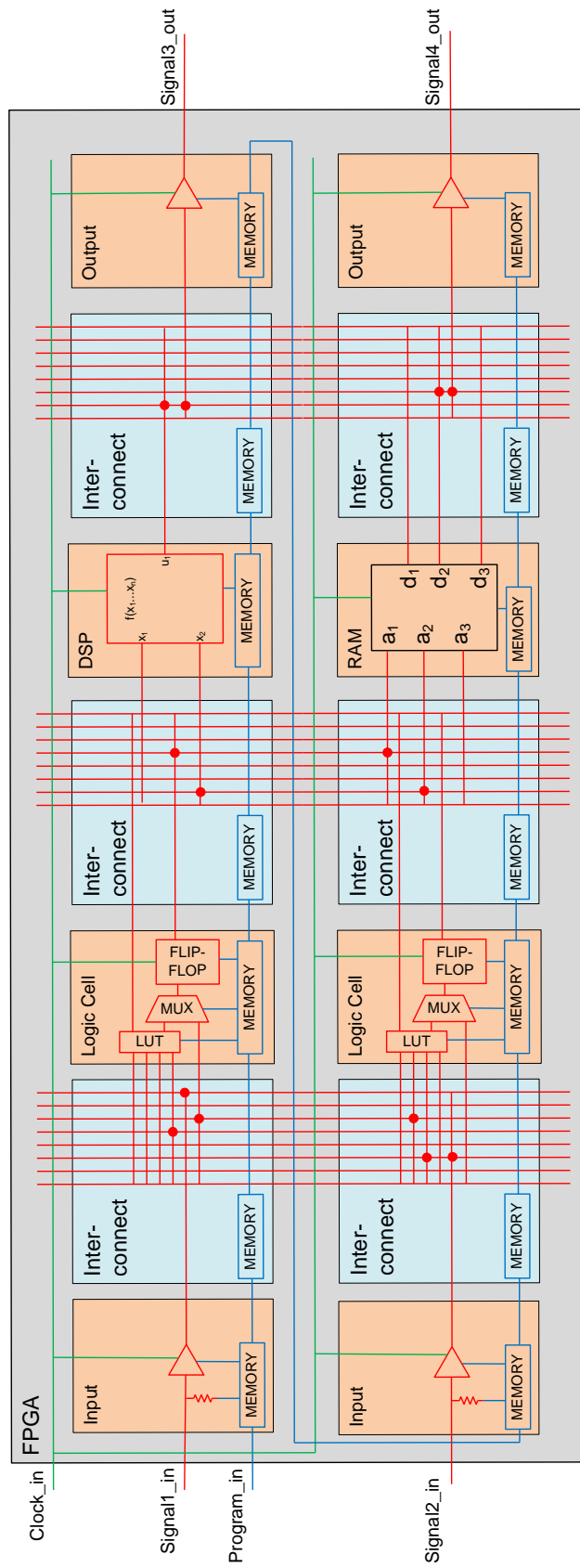


Figure 71 : A block diagram explaining basic principles of an FPGA.

The building blocks of the FPGA can be divided up into 2 main categories: programmable signal processing blocks (light orange in Figure 71) and programmable interconnects (light blue). In our case there are five types of signal processing blocks: Input, Logic Cell, DSP, RAM and Output. Real FPGAs will have many more types (some have even one or more blocks containing a complex CPU with all peripheral functions that make the FPGA useable for a 'system on chip' design). As an example the FPGA used in the transmitter we developed had 142128 Logic Cells compared to only 2 in the model in Figure 71.

We have three types of connections between them. Interconnections carrying the actual signals we want to be processed (red), a signal chain used to program the FPGA (blue) and clock distribution (green). The FPGA in this example has 6 external pins.

The most universal block is the general logic block. General logic blocks consist, in most cases, of a small Look Up Table (LUT) typical with a 4-8 bit width input address connected with a multiplexer and one or more flip-flops. This particular design for a logic block means that, depending on what is loaded onto the LUT table and how the mux and flip-flops are operating, this block can operate as many elementary digital circuits such as a logic port, a small memory, a signal adder, etc.

Xilinx groups 2 general logic cells together and calls this a 'slice'. Two logic blocks in a slice share some clock and reset signals.

Other blocks such as Input/Output allow internal signals to be related to external signals received or transmitted on pins. Often the interfacing standard used on the pin can be software controlled and is independent of the signal standard used internally in the FPGA.

The functionality of a DSP or Memory block could in principle be achieved by a large collection of general logic cells. Having blocks specially designed for a complex functionality can increase performance of an FPGA and lower the amount of chip space required to accomplish the same functionality. The disadvantage is a decrease in flexibility. For example a RAM cannot be used to achieve complex DSP functions while a general logic block would be capable of doing storage (RAM) or DSP depending on how it is configured.

The programmable interconnect block determines how the different processing blocks are connected to each other. This is accomplished by big databuses which run through the FPGA (in our example we have three of them, all vertically positioned in Figure 71). By

selecting to which wire in a bus a particular input/output of a processing block is connected (the red dots), signals are routed across the FPGA from processing block to processing block.

To make the FPGA carry out a given functionality it is necessary to program the interconnects and the different processing blocks. For this, each block contains a memory (blue rectangular symbol, some FPGAs use other technology than dynamic memory). The contents of the memory determines which interconnections are made in the interconnect blocks and how the functional block operates. We can envisage all these memories to be cascaded in one long chain representing a very long shift register. Via the pin Program_in a long program pattern is pushed through these shift registers configuring all the blocks of the FPGA⁸⁶.

Many blocks of the FPGA will work synchronously and hence will require a clock signal. In our example in Figure 71 a single clock is distributed across the FPGA (green network) to all components that need it. In reality an FPGA processing block can be programmed to use a particular clocksignal out of many different clocknets and the clocknets can be interconnected with the signalnet.

⁸⁶ Obviously this will require a clock and reset signals distributed into the 'blue' memory blocks containing the configuration. These signals are omitted from the diagram to keep it clear.

Appendix B : Introduction to FPGA design

As mentioned in Appendix A : An introduction to FPGAs we need to program an FPGA to define its functionality. This is done with the help of a collection of specialised software tools. There exist many tools on the market, some suitable for the entire design process, some focusing on specific steps in the process, some only supporting a particular vendor of FPGA, others supporting multiple vendors. There are similarities with computer programming but it would be a mistake to assume that it is identical. A major difference to illustrate this is that in an FPGA design, operation occurs in parallel while in most computer programming techniques they take place sequentially. There exist many books and courses focusing on digital design, and specifically digital design for FPGAs. [186] and [187] are standard texts for the VHDL language, and [193] and [194] explain the design process from a more Xilinx Inc. (the vendor of the tools and chips used in this work) focused view.

The main workflow for creating a digital design for an FPGA is represented in Figure 72 After defining the functionality and making a conceptual design we need to translate this into a format that will be understood by the software tools. There exist many possibilities. The most common way is to describe it in a Hardware Description Language (HDL). The three most used HDLs are: VHDL (Very high speed integrated circuits Hardware Language Description), Verilog and System C. We used VHDL to describe our entire design. For certain parts we used other tools to generate VHDL code⁸⁷ (an example is the use of a 'Wizard', supplied by Xilinx Inc., which can be used to generate the code that would interface with the high speed input output ports). The generated code was then integrated into the overall design. Another point to note is that HDLs are in most cases languages describing the design on RTL level. This means that everything has to be expressed in the form of digital signals, so while a signal bus could represent an abstract element like an integer in the design, it has to be handled as a parallel bus of logic signals (standardized libraries do exist to help with this). Once the total functionality is expressed in HDL we need to add some specific files: test benches and constraint files.

⁸⁷ This is a simplification. Some tools deliver their results in a non-HDL format (EDIF) which can bypass the synthesis step.

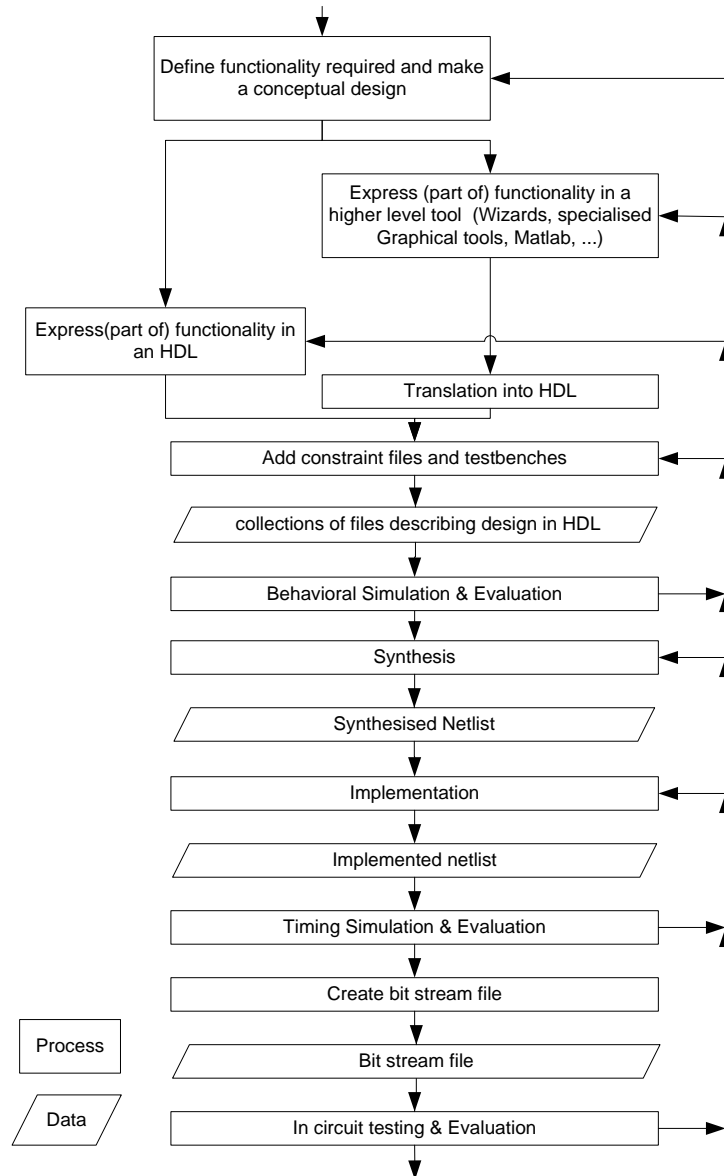


Figure 72 : Workflow for creating an FPGA design.

The constraints file applies two major constraints: location constraints and timing constraints. Location constraints tell the design that certain parts of the design have to be placed at specific positions on the chip. Most commonly this is saying that certain input/outputs have to be placed at specific pins and that the location cannot be chosen at random by the tools (because, for example, certain pins of the device are already wired up to other components and we do not want to change this every time we update our design). Timing constraints specify the required timings for certain nets on the design (nets: a term used in digital design to designate an interconnection between different blocks in a design), especially for clock pulses. With timing constraints you tell the design

tools that certain nets have to be operating at certain speeds (or within certain delays) to be accepted.

Testbenches are files used for simulating the design. The system built was connected to components outside the device (for example push buttons used to select certain settings in the device, LEDs connected to outputs to give feedback, and data ports connecting the IC to other components). In a testbench we describe all the incoming signals to the design in the time domain. During simulation a simulation package will apply these incoming signals to the design and calculate the output signal based on the design given to the simulator in a certain format. More complicated testbenches also describe the expected output signals and relations between input and output and by using the additional information can evaluate a design without an operator painstakingly analysing the output signals.

A first type of simulation is behavioural simulation⁸⁸. In this simulation the description in HDL is given to the simulator. The simulator compiles and simulates the code before it is translated into a design which can be programmed onto the FPGA. The main function of behavioural simulation is to check whether the description of the model created by the designer is correct, not if this design can actually be implemented in hardware. In the past this also meant that the behavioural simulation only gives you a feedback if the description of the design is acceptable assuming you have an 'ideal' FPGA, ideal meaning: no delays inside the components, infinitely fast response time of electronics, unlimited resources (logic blocks, interconnects, etc.) available on the FPGA. Current more advanced simulators attempt to estimate timings and resources used to confirm if the design is acceptable. Because the design is however not yet 'placed' onto the FPGA, it can only estimate these and cannot give accurate results concerning timings and resources used.

Once the design shows the expected behavioural simulation results, the next step is to synthesise it. Synthesis is the process in which all the constructs we used in the HDL language are translated into the blocks that are actually available on the FPGA. This is related to the fact that in VHDL (and also other HDL languages) we can have a behavioural

⁸⁸ Depending on the literature also known as functional simulation. Other literature uses the term functional simulation for what I term post-synthesis simulation. While there is a certain degree of standardisation in terminology there is no absolute reference and different vendors and their related 'followers' sometime use different terms.

description in addition to a structural description. In a structural description we only describe interconnections between already existing sub-blocks. If we assume we only use sub-blocks which are physically present on the FPGA and hierarchically build our design, the synthesis step is much simpler. If however we use sub-blocks representing complex functionality (such as adding two busses representing an integer) or we use behavioural style (we are expressing what we want to happen without limiting or breaking it down to components actually present on the FPGA) we need synthesis. Synthesis also includes optimisation algorithms which attempt to reduce the amount of resources used. It is possible to simulate the design after synthesis (not represented in Figure 72).

The synthesised netlist is then passed on to the implementation step. This step consists of three sub-steps: Translate, Map, Place & Route. The first step, Translate, has to do with the multiple standards used in representing the design at this stage and this step will convert it into a format accepted by the Map tool. Map will map the logical design (already broken down to elementary digital design blocks) onto the physical cells present on the specific physical FPGA. The output of the Map process is an NCD (Native Circuit Description) file. This file is passed on to the Place & Route routine which will place the different blocks onto specific physically positioned circuits on the FPGA and determine exactly which physical interconnects need to be made or broken. These steps also involve optimisation steps, because many layouts are possible for a specific design and some may result in better performance (better in this case mainly meaning having shorter or equal length interconnects on crucial paths leading to higher operating speeds for the design). This will give a placed and routed NCD.

Because of the detailed design information in the placed and routed NCD, it is possible to use this file to carry out accurate timing simulations.

The placed and routed NCD is now used to generate a file that can be used to program the FPGA (the 'Create bitstream file' block in Figure 72). Depending on how we interface the FPGA different file formats are used. An import detail is to know that the memory holding the functionality of the blocks in the FPGA is volatile memory. To be able to power the FPGA up and down the program is often stored in a flash memory connected to the FPGA with a controller circuit that will reload the program when the FPGA powers up.

In blocks representing simulation in Figure 72 the designer evaluates the results of the simulation. If they are not as expected it is necessary to redesign parts. It may be

necessary to go back multiple steps to correct the issue. So passing a certain evaluation/simulation step in the process does not mean that the work done up to that point is acceptable, only that at that point it cannot detect any more issues with the design.

Synthesis and implementation do not produce the best or even identical outputs if they are rerun with the same input files. In particular the implementation tools are tools that will first generate a failing solution for the design. They will then iteratively improve the solution until a solution is found that is acceptable within the constraints given or until a predetermined amount of effort is spend after which the design may work or not. Some of the iterative steps involve random changes which will only be accepted if they improve the solution for the given design. This means that better performing circuits can sometimes be found by allowing the same algorithms to spend more time on improving a solution.

Some VHDL terminology: to be able to understand Chapter 5, some basic knowledge of VHDL terminology is needed. Three terms are used regularly: entity, architecture and instance. An entity is a block defined within the VHDL environment that can be used to build a design (compare it to a function in a function library of a program language). The architecture is the code describing in a particular way what an entity does (compare it to the code of a function in the function library). An instance is using an entity in a design (compare it to calling the function from a program). An important difference between programming and digital design is that if we place two instances of an entity in a design we will need twice the amount of resources to create the entity. If we call a function in a computer program this is not needed because we can make use of stacks only storing the data for each time the function is called and only have one copy of the function code in computer memory.

References

1. R. Waegemans, S. Herbst, L. Holbein, P. Watts, P. Bayvel, C. Fürst and R.I. Killey "10.7 Gb/s electronic predistortion transmitter using commercial FPGAs and D/A converters implementing real-time DSP for chromatic dispersion and SPM compensation" *Optics Express* (2009), Vol.17 Iss.10 pp.8630-8640.
2. P. Watts, R. Waegemans, M. Glick, P. Bayvel and R. Killey "An FPGA-based Optical Transmitter Using Real-Time DSP for Implementation of Advanced Signal Formats and Signal Predisortion" in *Proc. of European Conference on Optical Communication* (2006) in Cannes, Vol.3 pp.315-316, We3_P_97.
3. M. Glick, P. Watts, R. Waegemans, P. Bayvel and R.I. Killey "Electronic Signal Processing to Improve System Performance of Optical Interconnects" in *Proc. of 9th International Conference on Transparent Optical Networks* (2007) in Rome, Vol.1 pp.298-301.
4. P. Watts, S. Savory, Y. Benlachtar, R. Waegemans, V. Mikhailov, R. Killey and P. Bayvel "Compensation of Chromatic Dispersion using Coherent Modulation and Demodulation" in *Proc. of European Conference on Optical Communication* (2007) in Berlin, Vol.1 pp.11, Workshop 5 Hall 4/5.
5. P. Watts, R. Waegemans, M. Glick, P. Bayvel and R. Killey "An FPGA-Based Optical Transmitter Design Using Real-Time DSP for Advanced Signal Formats and Electronic Predistortion" *Journal of Lightwave Technology* (2007), Vol.25 Iss.10 pp.3089-3099.
6. P. Watts, M. Glick, R. Waegemans, Y. Benlachtar, V. Mikhailov, S. Savory, P. Bayvel and R.I. Killey "Experimental demonstration of real-time DSP with FPGA-based optical transmitter" in *Proc. of 10th International Conference on Transparent Optical Networks* (2008) in Athens, Vol.1 pp.202-205.
7. P.M. Watts, R. Waegemans, Y. Benlachtar, V. Mikhailov, P. Bayvel and R.I. Killey "10.7 Gb/s transmission over 1200 km of standard single-mode fiber by electronic predistortion using FPGA-based real-time digital signal processing" *Optics Express* (2008), Vol.16 Iss.16 pp.12171-12180.
8. P.M. Watts, R. Waegemans, Y. Benlachtar, V. Mikhailov, M. Glick, P. Bayvel and R.I. Killey "10.7 Gb/s electronically predistorted transmission over 800 km standard single mode fibre using FPGA-based real-time processing" in *Proc. of European Conference on Optical Communication* (2008) in Brussels, Vol.3 pp.121-122.
9. P.M. Watts, R. Waegemans, Y. Benlachtar, P. Bayvel and R.I. Killey "Real-time FPGA Implementation of Transmitter Based DSP" in *Proc. of European Conference on Optical Communication* (2009) in Vienna, Vol.1 pp.449-452, 5.4.2.
10. K.C. Kao and G.A. Hockham "Dielectric-Fibre Surface Waveguides for Optical Frequencies" *Proceedings of the Institution of Electrical Engineers* (1966), Vol.113 Iss.7 pp.1151-.

11. A. Werts "Propagation de la lumière cohérente dans les fibres optiques" *L'onde électrique* (1966), Vol.47 pp.967-980.
12. *Bandwith demand driving FTTH in Europe* Lightwave Online (2007), PennWell [cited July 2007]; Available from:
http://lw.pennnet.com/articles/article_display.cfm?Section=ONART&C=NNEWS&ARTICLE_ID=297385&KEYWORDS=Frost%20%26%20Sullivan&p=13
13. C. Holliday *High Speed Access Report - Fourth Quarter 2006* (2006), Information Gatekeepers Inc. [cited Okt 2007]; Available from:
<http://www.igigroup.com/holliday/4Q06.pdf>.
14. Plunkett Research Ltd. *Plunkett's Telecommunications Industry Almanac 2007* (2007): Plunkett Research Ltd.
15. J. Mitchell, I. Darwazeh and D. Selviah *TTS Telecommunications Transmission Systems* (2002), London: University College London.
16. R. Killey, T. Kenyon and D. Selviah *EP78/G61 Optical Transmission and Networks* (2003), London: University College London.
17. G.E. Keiser *Optical Fibre Communications* 3th edition(2000): McGraw Hill
18. J. Hecht *Understanding Fiber Optics* 4th edition(2002), London, UK: Prentice Hall.
19. G.P. Agrawal *Nonlinear Fiber Optics* 3th edition Optics and Photonics, ed.: P.L. Kelley, I.P. Kaminow and G.P. Agrawal (2001), Rochester NY: Academic Press.
20. C. Soanes *Compact Oxford English dictionary* 2nd edition(2003), Oxford: Oxford University Press.
21. H. Newton *Newton's Telecom Dictionary* 17th edition(2001), New York: CMP Books.
22. F. Shimizu "Frequency Broadening in Liquids by a Short Light Pulse" *Physical Review Letters* (1967), Vol.19 Iss.19 pp.1097-.
23. R.J. Essiambre, B. Mikkelsen and G. Raybon "Intra-channel cross-phase modulation and four-wave mixing in high-speed TDM systems" *Electronics Letters* (1999), Vol.35 Iss.18 pp.1576-1578.
24. V.S.D. Appathurai *Investigation of the limiting fibre nonlinearities and there suppression in 40Gbit/s optical transmission systems* at Department of Electronic and Electrical Engineering (2005), London: University of London, Thesis for the degree of Ph. D.
25. H. Bülow, C.J. Xie, A. Klekamp, X.A. Liu and B. Franz "PMD Compensation/Mitigation Techniques for High-Speed Optical Transport" *Bell Labs Technical Journal* (2009), Vol.14 Iss.1 pp.105-124.
26. P.M. Krummrich, E.-D. Schmidt, W. Weierhausen and A. Mattheus "Field trial results on statistics of fast polarization changes in long haul WDM transmission systems" *at*

- Optical Fiber Communication and the National Fiber Optic Engineers Conference* (2005) in Anaheim CA, Vol.4 pp.3,OThT6.
27. H. Kogelnik and R.M. Logan "Polarization-Mode dispersion", in *Optical Fiber Telecommunications IVB: System and impairments*, Editors: I.P. Kaminow and T. Li (2002), Burlington MA: Academic Press pp. 725-861.
 28. J. Sinsky and P. Winzer "100-Gb/s optical communications" *IEEE Microwave Magazine* (2009), Vol.10 Iss.2 pp.44-57.
 29. B. Sklar *Digital Communications: Fundamentals and Applications* 2nd edition(2001), Upper Saddle River NJ: Prentice Hall.
 30. S.U.H. Qureshi "Adaptive Equalization" *Proceedings of the IEEE* (1985), Vol.73 Iss.9 pp.1349-1387.
 31. R.W. Lucky "The adaptive equalizer" *IEEE Signal Processing Magazine* (2006), Vol.23 Iss.3 pp.104-107.
 32. J.G. Proakis *Digital Communications* 4th edition(2001), New York: McGraw Hill.
 33. H. Moon and R. Sedaghat "FPGA-Based adaptive digital predistortion for radio-over-fiber links" *Microprocessors and Microsystems* (2006), Vol.30 Iss.3 pp.145-154.
 34. A.J. Cooper "Fiber Radio for the Provision of Cordless-Mobile Telephone Services in the Access Network" *Electronics Letters* (1990), Vol.26 Iss.24 pp.2054-2056.
 35. Hong Bong Kim *Radio over Fiber based Network Architecture* at Elektrotechnik und Informatik (2005), Berlin: Technischen Universität Berlin, Thesis for the degree of Dr. Ing.
 36. I.H. Choi, S.H. Lee, H.C. Kwon, Y.W. Choi and S.K. Han "Compensation of intermodulation distortion of laser diode by using opto electronically predistorted signals" *Microwave and Optical Technology Letters* (2006), Vol.48 Iss.6 pp.1144-1148.
 37. A. Gumaste and T. Antony *DWDM Network Designs and Engineering Solutions* (2003), Indianapolis IN: Cisco Press.
 38. I.B. Djordjevic, H.G. Batshon, M. Cvijetic, L. Xu and T. Wang "PMD Compensation by LDPC-Coded Turbo Equalization" *IEEE Photonics Technology Letters* (2007), Vol.19 Iss.15 pp.1163-.
 39. *Description of product portofolio*, Corning Inc. [cited 3 Jul 2007]; Available from: www.corning.com.
 40. M.-J. Li, X. Chen, D.A. Nolan, J. Wang, J.A. West and K.W. Koch "Speciality fibers for optical communication systems", in *Optical Fiber Telecommunications VA: Components and subsystems*, Editors: I.P. Kaminow, T. Li and A.E. Wilner (2008), Burlington MA: Academic Press.

41. P.J. Winzer and R.-J. Essiambre "Advanced optical modulation formats", in *Optical Fiber Telecommunications VB: Systems and Networks*, Editors: I.P. Kaminow, T. Li and A.E. Willner (2008), Burlington MA: Academic Press pp. 23-93.
42. G. Charlet "Progress in optical modulation formats for high-bit rate WDM transmissions" *IEEE Journal of Selected Topics in Quantum Electronics* (2006), Vol.12 Iss.4 pp.469-483.
43. L.N. Binh *Digital Optical Communications* (2009), Boca Raton FL: CRC Press.
44. P.M. Krummrich "Advanced modulation formats for more robust optical transmission systems" *AEÜ - International Journal of Electronics and Communications* (2007), Vol.61 Iss.3 pp.141-146.
45. T. Hills *Who Makes What: 40- & 100-Gbit/s Systems* Lightreading (2009), United Business Media Ltd. [cited 9 July 2009]; Available from: http://www.lightreading.com/document.asp?doc_id=177345.
46. Optical transport network physical layer interfaces G.959.1 (2008), Geneva: International Telecommunication Union.
47. T. Hills *40- & 100-Gbit/s Technology & Components* Lightreading (2008), United Business Media Ltd.; Available from: http://www.lightreading.com/document.asp?doc_id=161755.
48. J. Berthold, J. Hutchins, K. Gass, D.R. Stauffer, T. Schmidt, F. Caggioni and T. Wuth *100G Ultra Long Haul DWDM Framework Document* (2009), Optical Internetworking Forum [cited Okt 2009]; Available from: <http://www.oiforum.com/public/documents/OIF-FD-100G-DWDM-01.0.pdf>.
49. S. Hardy *Nortel unveils DP-BPSK modulation format for 40G ultra long haul* Lightwave Online (2009), PennWell Corp. [cited Okt 2009]; Available from: <http://www.lightwaveonline.com/general/nortel-unveils-dp-bpsk-modulation-format-for-40g-ultra-long-haul-54896022.html>.
50. L. Illing and M.B. Kennel "Shaping current waveforms for direct modulation of semiconductor lasers" *IEEE Journal of Quantum Electronics* (2004), Vol.40 Iss.5 pp.445-452.
51. N. Dokhane and G.L. Lippi "Improved direct modulation technique for faster switching of diode lasers" *IEE Proceedings-Optoelectronics* (2002), Vol.149 Iss.1 pp.7-16.
52. E. Säckinger *Broadband Circuits for Optical Fiber Communication* (2004), Hoboken NJ: Wiley-Interscience.
53. J.D. Ralston, J.M. Kahn and K.P. Ho "Advanced modulation and signal processing techniques for 40 Gb/s optical transmission systems" in *Proc. of Conference on Active and Passive Optical Components for WDM Communications II* (2002) in Boston MA, Vol.4870 pp.600-607.

54. S. Bigo "Multiterabit/s DWDM terrestrial transmission with bandwidth-limiting optical filtering" *IEEE Journal of Selected Topics in Quantum Electronics* (2004), Vol.10 Iss.2 pp.329-340.
55. P.M. Watts, V. Mikhailov, M. Glick, P. Bayvel and R.I. Killey "Single sideband optical signal generation and chromatic dispersion compensation using digital filters" *Electronics Letters* (2004), Vol.40 Iss.15 pp.958-960.
56. Y. Miyamoto, K. Yonenaga and S. Kuwahara "Dispersion-tolerant RZ signal transmission using baseband differential code and carrier suppressed modulation" in *Proc. of European Conference on Optical Communication* (1998) in Madrid pp.351-352.
57. T. Ono, Y. Yano, K. Fukuchi, T. Ito, H. Yamazaki, M. Yamaguchi and K. Emura "Characteristics of optical duobinary signals in terabit/s capacity, high-spectral efficiency WDM systems" *Journal of Lightwave Technology* (1998), Vol.16 Iss.5 pp.788-797.
58. K. Yonenaga and S. Kuwano "Dispersion-tolerant optical transmission system using duobinary transmitter and binary receiver" *Journal of Lightwave Technology* (1997), Vol.15 Iss.8 pp.1530-1537.
59. F. Buchali, R. Dischler and X.A. Liu "Optical OFDM: A Promising High-Speed Optical Transport Technology" *Bell Labs Technical Journal* (2009), Vol.14 Iss.1 pp.125-146.
60. A. Hasegawa "Soliton-based ultra-high speed optical communications" *Pramana-Journal of Physics* (2001), Vol.57 Iss.5-6 pp.1097-1127.
61. A.R. Pratt, P. Harper, S.B. Alleston, P. Bontemps, B. Charbonnier, W. Forsysiak, L. Gleeson, D.S. Govan, G.L. Jones, et al. "5,745 km DWDM transcontinental field trial using 10 Gbit/s dispersion managed solitons and dynamic gain equalization" in *Proc. of Optical Fiber Communication and the National Fiber Optic Engineers Conference* (2003) in Atlanta GA, Vol.3, PD26-P1-3.
62. J. Onishi, S. Kojima and T. Numai "Effects of Frequency Allocations and Zero-Dispersion Frequencies on FDM Lightwave Transmission Systems" *Journal of Lightwave Technology* (2007), Vol.25 Iss.7 pp.1719-.
63. G.694.1 Spectral grids for WDM applications: DWDM frequency grid (2002), Geneva: International Telecommunication Union.
64. C. Lin, H. Kogelnik and L.G. Cohen "Optical-Pulse Equalization of Low-Dispersion Transmission in Single-Mode Fibers in the 1.3-1.7-Mu-M Spectral Region" *Optics Letters* (1980), Vol.5 Iss.11 pp.476-478.
65. L. Gruner-Nielsen, M. Wandel, P. Kristensen, C. Jorgensen, L.V. Jorgensen, B. Edvold, B. Palsdottir and D. Jakobsen "Dispersion-compensating fibers" *Journal of Lightwave Technology* (2005), Vol.23 Iss.11 pp.3566-3579.
66. T. Nielsen and S. Chandrasekhar "OFC 2004 Workshop on Optical and Electronic Mitigation of Impairments" *Journal of Lightwave Technology* (2005), Vol.23 Iss.1 pp.131-142.

67. F. Ouellette, J.F. Cliche and S. Gagnon "All-Fiber Devices for Chromatic Dispersion Compensation Based on Chirped Distributed Resonant Coupling" *Journal of Lightwave Technology* (1994), Vol.12 Iss.10 pp.1728-1738.
68. C.R. Doerr and K. Okamoto "Planar lightwave circuits in fiber-optic communications", in *Optical Fiber Telecommunications VA: Components and subsystems*, Editors: I.P. Kaminow, T. Li and A.E. Wilner (2008), Burlington MA: Academic Press pp. 269-341.
69. O. Leclerc, B. Lavigne, D. Chiaroni and E. Desurvire "All-Optical Regeneration: Principles and WDM Implementation", in *Optical Fiber Telecommunications IVA: Components*, Editors: I. Kaminow and T. Li (2002), Burlington MA: Academic Press pp. 732-783.
70. D. Welch, C. Joyner, D. Lambert, P.W. Evans and M. Raburn "III-V photonic integrated circuits and their impact on optical network architectures", in *Optical Fiber Telecommunications VA: Components and subsystems*, Editors: I.P. Kaminow, T. Li and A.E. Willner (2008), Burlington MA: Academic Press pp. 343-379.
71. A. Yariv, D. Fekete and D.M. Pepper "Compensation for Channel Dispersion by Non-Linear Optical Phase Conjugation" *Optics Letters* (1979), Vol.4 Iss.2 pp.52-54.
72. S.L. Jansen, D. van den Borne, P.M. Krummrich, S. Spalter, G.D. Khoe and H. de Waardt "Long-haul DWDM transmission systems employing optical phase conjugation" *IEEE Journal of Selected Topics in Quantum Electronics* (2006), Vol.12 Iss.4 pp.505-520.
73. S. Watanabe and M. Shirasaki "Exact compensation for both chromatic dispersion and Kerr effect in a transmission fiber using optical phase conjugation" *Journal of Lightwave Technology* (1996), Vol.14 Iss.3 pp.243-248.
74. S.D. Personick "Receiver Design for Digital Fiber Optic Communication Systems .1." *Bell System Technical Journal* (1973), Vol.52 Iss.6 pp.843-874.
75. J.H. Winters and R.D. Gitlin "Electrical Signal-Processing Techniques in Long-Haul Fiberoptic Systems" *IEEE Transactions on Communications* (1990), Vol.38 Iss.9 pp.1439-1453.
76. P. Murphy CoreOptics and Marconi Unveil Industry's First Adaptive Distortion Tolerant Transponder Platform (2004), Nurnberg (GE): CoreOptics.
77. A. Shanbhag, Q. Yu and J. choma "Electronic signal processing for dispersion compensation and error mitigation in optical transmission networks", in *Optical Fiber Telecommunications VA: Components and subsystems*, Editors: I.P. Kaminow, T. Li and A.E. willner (2008), Burlington MA: Academic Press.
78. H. Bülow, F. Buchali and A. Klekamp "Electronic dispersion compensation" *Journal of Lightwave Technology* (2008), Vol.26 Iss.1-4 pp.158-167.
79. S.J. Savory "Digital signal processing options in long haul transmission" in *Proc. of Optical Fiber Communication and the National Fiber Optic Engineers Conference* (2008) in San Diego CA pp.2508-2510.

80. D. McGhan, M. O'Sullivan, M. Sotoodeh, A. Savchenko, C. Bontu, M. Belanger and K. Roberts "Electronic Dispersion Compensation" at *Optical Fiber Communication and the National Fiber Optic Engineers Conference* (2006) in Anaheim CA,OWK1.
81. J. Sitch "High-speed digital signal processing for optical communications" in *Proc. of European Conference on Optical Communication* (2008) in Brussels,Vol.6 pp.123-143,TH.1.A.1.
82. L. Thylén, U. Westergren, P. Holmström, R. Schatz and P. Jänes "Recent development in high-speed optical modulators", in *Optical Fiber Telecommunications VA: Components and subsystems*, Editors: I.P. Kaminow, T. Li and A.E. Willner (2008), Burlington MA: Academic Press.
83. T. Kawanishi, T. Sakamoto and M. Izutsu "High-speed control of lightwave amplitude, phase, and frequency by use of electrooptic effect" *IEEE Journal of Selected Topics in Quantum Electronics* (2007), Vol.13 Iss.1 pp.79-91.
84. Y. Akage, K. Kawano, S. Oku, R. Iga, H. Okamoto, Y. Miyamoto and H. Takeuchi "Wide bandwidth of over 50GHz travelling-wave electrode electroabsorption modulator integrated DFB lasers" *Electronics Letters* (2001), Vol.37 Iss.5 pp.299-300.
85. A. Mahapatra and E.J. Murphy "Electrooptic Modulators", in *Optical Fiber Telecommunications IVA: Components* (2002), Burlington MA: Academic Press pp. 258-294.
86. E.L. Wooten, K.M. Kissa, A. Yi-Yan, E.J. Murphy, D.A. Lafaw, P.F. Hallemeier, D. Maack, D.V. Attanasio, D.J. Fritz, et al. "A review of lithium niobate modulators for fiber-optic communications systems" *IEEE Journal of Selected Topics in Quantum Electronics* (2000), Vol.6 Iss.1 pp.69-82.
87. K. Kikuchi "Coherent optical communication systems", in *Optical Fiber Telecommunications VB: systems and networks*, Editors: I.P. Kaminow, T. Li and A.E. Willner (2008), Burlington MA: Academic Press.
88. S.J. Savory "Digital filters for coherent optical receivers" *Optics Express* (2008), Vol.16 Iss.2 pp.804-817.
89. A.D. Ellis and M.E. McCharthy "Receiver side electronic dispersion compensation using passive field detection for low cost 10 Gb/s 600km reach applications" in *Proc. of Optical Fiber Communication and the National Fiber Optic Engineers Conference* (2005) in Anaheim, CA.
90. N. Takachio and K. Iwashita "Compensation of Fiber Chromatic Dispersion in Optical Heterodyne-Detection" *Electronics Letters* (1988), Vol.24 Iss.2 pp.108-109.
91. B. Wedding, W. Pohlmann, D. Schlump, E. Schlag and R. Ballentin "SiGe circuits for high bit-rate optical transmission systems" in *Proc. of IEEE International Symposium on Circuits and Systems* (1999),Vol.2 pp.492-495, 717.
92. H. Jiang, R. Saunders and S. Colaco "SiGe Equalizer IC for PMD Mitigation and Signal Optimization of 40Gbits/s Transmission" in *Proc. of Optical Fiber Communication and the National Fiber Optic Engineers Conference* (2005) in Anaheim CA,OWO2.

93. R.G. Lyons *Understanding Digital Signal Processing* 2th rev edition(2004), Upper Saddle River, NJ: Prentice Hall.
94. P. Schvan, D. Pollex and T. Bellingrath "A 22GS/s 6b DAC with integrated digital ramp generator" in *Proc. of IEEE International Solid-State Circuits Conference* (2005) pp.122-588 Vol. 1.
95. P. Schvan, J. Bach, C. Fait, P. Flemke, R. Gibbins, Y. Greshishchev, N. Ben-Hamida, D. Pollex, J. Sitch, et al. "A 24GS/s 6b ADC in 90nm CMOS" in *Proc. of IEEE International Solid-State Circuits Conference* (2008) pp.544-634.
96. GigOptix's 100G Mach Zehnder Modulator Enables 110GHz Time Stretched Analog to Digital Conversions at UCLA (2009), Gigoptix;Available from: www.gigoptix.com.
97. J. Chou, J. Conway, G. Seffler, G. Valley, B. Jalali and Ieee "150 GS/s Real-Time Oscilloscope Using a Photonic Front End" in *Proc. of International Topical Meeting on Microwave Photonics/ Asia-Pacific Microwave Photonics Conference* (2008) in Gold Coast pp.35-38.
98. T. Ellermeyer *VEGA Phase Align Info* (2008), Bochum: MICRAM Microelectronics GmbH.
99. *B7HF200 200 GHz SiGe Technology* (2007), Infineon Technologies AG, [cited Okt 2009];Available from: <http://www.infineon.com/dgdl/B7HF200-br-2007.pdf?folderId=db3a30431355314001136803c84101e1&fileId=db3a304314dca38901154117421f1616>.
100. *Services & Products: Data Converter Modules* Maxtek [cited Aug 2009]; Available from: <http://www.maxtek.com/services6.html>.
101. R. Wilson *FPGA vs. ASIC battle gets refought once again at Globalpress Forum* (2009), Electronics, Design, Strateg and News;Available from: <http://www.edn.com/blog/1690000169/post/1460042746.html>.
102. F.J. Bartos *ASICs Versus FPGAs* Control Engineering (2005), CE International [cited Okt 2009];Available from: http://www.controleng.com/article/270095-ASICs_Versus_FPGAs.php.
103. P. Aycinena *ASICs versus FPGAs* (2003) [cited Okt 2009];Available from: http://www10.edacafe.com/nbc/articles/view_weekly.php?articleid=209273&page_no=1.
104. J. Kriegbaum *FPGA's vs. ASIC's* EE Times (2004) [cited 21 Aug 2009];Available from: <http://www.design-reuse.com/exit/?url=http://www.eetimes.com/showArticle.jhtml;jsessionid=1M025IY0CYDV4QSNDBCSKHSCJUMKJVN?articleID=47101995>.
105. T. Danzer *Low-Cost ASIC Conversion Targets Consumer Success* FPGA and structured ASIC journal (2006) [cited Okt 2009];Available from: http://www.fpgajournal.com/articles_2006/20061107_ami.htm.
106. *Online Pricelist Avnet* (2009), www.avnet.com.

107. *EasyPath FPGAs FAQ* (2008), Xilinx Inc. [cited Feb 2008]; Available from: www.xilinx.com.
108. J.L. Turley *The essential guide to semiconductors* (2003), Upper Saddle River NJ: Prentice Hall pp.217.
109. X. Li, X. Chen, G. Goldfarb, E. Mateo, I. Kim, F. Yaman and G. Li "Electronic post-compensation of WDM transmission impairments using coherent detection and digital signal processing" *Optics Express* (2008), Vol.16 Iss.2 pp.880-888.
110. P.M. Watts *Chromatic Dispersion Compensation using Electrical Signal Processing in High Speed Optical Communications* at Department of Electronic and Electrical Engineering (2008), London (UK): University College London, Thesis for the degree of Doctor of Philosophy.
111. P. Poggiolini, G. Bosco, M. Visintin, S.J. Savory, Y. Benlachar, P. Bayvel and R.I. Killey "MLSE-EDC versus optical dispersion compensation in a single-channel SPM-limited 800 km link at 10 Gbit/s" in *Proc. of European Conference on Optical Communication* (2007) in Berlin, Vol.4 pp.27-28, 9.1.3.
112. K. Roberts "Electronic dispersion compensation beyond 10Gb/s" at *IEEE Leos Summer Topical Meetings* (2007) in Portland OR.
113. A. Färbert "Application of digital equalization in optical transmission systems" in *Proc. of Optical Fiber Communication and the National Fiber Optic Engineers Conference* (2006) in Anaheim CA, OTuE5.
114. W. Rosenkranz and C.M. Xia "Electrical equalization for advanced optical communication systems" *AEÜ - International Journal of Electronics and Communications* (2007), Vol.61 Iss.3 pp.153-157.
115. D. Fonseca, A.V.T. Cartaxo and P. Monteiro "On the use of electrical precompensation of dispersion in optical single-sideband transmission systems" *IEEE Journal of Selected Topics in Quantum Electronics* (2006), Vol.12 Iss.4 pp.603-614.
116. M. Sieben, J. Conradi and D.E. Dodds "Optical single sideband transmission at 10 Gb/s using only electrical dispersion compensation" *Journal of Lightwave Technology* (1999), Vol.17 Iss.10 pp.1742-1749.
117. M. Birk, X. Zhou, M. Boroditsky, S.H. Foo, D. Bownass, M. Moyer and M. O'Sullivan "WDM technical trial with complete electronic dispersion compensation" in *Proc. of European Conference on Optical Communication* (2006) in Cannes pp.1-2.
118. D. McGhan, C. Laperle, A. Savchenko, C. Li, G. Mak and M. O'Sullivan "5120 km RZ-DPSK Transmission over G652 Fiber at 10 Gb/s with No Optical Dispersion Compensation" in *Proc. of Optical Fiber Communication and The National Fiber Optic Engineers Conference* (2005) in Anaheim CA, PDP27.
119. B. Franz, F. Buchali, D. Rösener and H. Bülow "Adaptation Techniques for Electronic Equalizers for the Mitigation of Time-Variant Distortions in 43 Gbit/s Optical

- Transmission Systems" in *Proc. of Optical Fiber Communication and the National Fiber Optic Engineers Conference* (2007) in Anaheim CA,OMG1.
120. M. Bertelsmeier and W. Zschunke "Linearization of Broad-Band Optical-Transmission Systems by Adaptive Predistortion" *Frequenz* (1984), Vol.38 Iss.9 pp.206-212.
 121. T.L. Koch and R.C. Alferness "Dispersion Compensation by Active Predistorted Signal Synthesis" *Journal of Lightwave Technology* (1985), Vol.3 Iss.4 pp.800-805.
 122. M.M. El Said, J. Sitch and M.I. Elmasry "An electrically pre-equalized 10-Gb/s duobinary transmission system" *Journal of Lightwave Technology* (2005), Vol.23 Iss.1 pp.388-400.
 123. R.I. Killey, P. Watts, V. Mikhailov, M. Glick and P. Bayvel "Electronic dispersion compensation by signal predistortion using digital processing and a dual-drive Mach-Zehnder modulator" *IEEE Photonics Technology Letters* (2005), Vol.17 Iss.3 pp.714-716.
 124. R.I. Killey, P.M. Watts, V. Mikhailov, M. Glick and P. Bayvel "Electronic dispersion compensation by signal predistortion using a dual-drive Mach-Zehnder modulator" in *Proc. of Optical Fiber Communication and the National Fiber Optic Engineers Conference* (2005) in Anaheim CA,Vol.4 pp.3,OTHJ2.
 125. J. McNicol, M. O'Sullivan, K. Roberts, A. Comeau, D. McGhan and L. Strawczynski "Electrical Domain Compensation of Optical Dispersion" in *Proc. of Optical Fiber Communication and the National Fiber Optic Engineers Conference* (2005) in Anaheim CA,OTHJ3.
 126. M.S. O'Sullivan, K. Roberts and C. Bontu "Electronic Dispersion Compensation Techniques for Optical Communication Systems" in *Proc. of European Conference on Optical Communication* (2005),Tu3.2.1.
 127. D. McGhan, C. Laperle, A. Savchenko, C.D. Li, G. Mak and M. O'Sullivan "5120-km RZ-DPSK transmission over G.652 fiber at 10 Gb/s without optical dispersion compensation" *IEEE Photonics Technology Letters* (2006), Vol.18 Iss.1-4 pp.400-402.
 128. R.I. Killey, P.M. Watts, M. Glick and P. Bayvel "Electronic precompensation techniques to combat dispersion and nonlinearities in optical transmission" in *Proc. of European Conference on Optical Communication* (2005) in Glasgow,Vol.2 pp.251-254,Tu 4.2.1.
 129. P.J. Winzer and R.-J. Essiambre "Electronic pre-distortion for advanced modulation formats " in *Proc. of European Conference on Optical Communication* (2005) in Glasgow,Tu 4.2.2.
 130. R.-J. Essiambre and P.J. Winzer "Fibre Nonlinearities in Electronically Pre-Distorted Transmission" in *Proc. of European Conference on Optical Communication* (2005) in Glasgow,Tu3.2.2.
 131. P. Watts, P. Bayvel, R. Killey and M. Glick "Techniques for long haul transmission without optical dispersion compensation" in *Proc. of The IEE Seminar on Optical*

- Fibre Communications and Electronic Signal Processing* (2005) in London pp.7.1-7.6,IEEE 1588583.
132. D. Walker, H. Sun, C. Laperle, A. Comeau and M. O'Sullivan "960-km transmission over G.652 fiber at 10 Gb/s with a laser/electroabsorption modulator and no optical dispersion compensation" *IEEE Photonics Technology Letters* (2005), Vol.17 Iss.12 pp.2751-2753.
 133. K. Roberts, C.D. Li, L. Strawczynski, M. O'Sullivan and I. Hardcastle "Electronic precompensation of optical nonlinearity" *IEEE Photonics Technology Letters* (2006), Vol.18 Iss.1-4 pp.403-405.
 134. R.J. Essiambre and P.J. Winzer "Impact of fiber nonlinearities on advanced modulation formats using electronic pre-distortion" in *Proc. of Optical Fiber Communication and the National Fiber Optic Engineers Conference* (2006) in Anaheim CA pp.413-415.
 135. A. Klekamp, F. Buchali, M. Audoin and H. Bulow "Nonlinear limitations of electronic dispersion pre-compensation by intrachannel effects" in *Proc. of Optical Fiber Communication and the National Fiber Optic Engineers Conference* (2006) in Anaheim CA pp.1017-1019.
 136. R.I. Killey, P.M. Watts, M. Glick and P. Bayvel "Electronic dispersion compensation by signal predistortion" in *Proc. of Optical Fiber Communication and the National Fiber Optic Engineers Conference* (2006) in Anaheim CA pp.3.
 137. X. Liu, X. Wei, S. Chandrasekhar and A.H. Gnauck "Increased OSNR gains of forward-error correction in nonlinear optical transmissions" *IEEE Photonics Technology Letters* (2003), Vol.15 Iss.7 pp.999-1001.
 138. C. Weber, J.K. Fischer, C.A. Bunge and K. Petermann "Electronic precompensation of intrachannel nonlinearities at 40 Gb/s" *IEEE Photonics Technology Letters* (2006), Vol.18 Iss.13-16 pp.1759-1761.
 139. R.J. Essiambre, P.J. Winzer, X.Q. Wang, W. Lee, C.A. White and E.C. Burrows "Electronic predistortion and fiber nonlinearity" *IEEE Photonics Technology Letters* (2006), Vol.18 Iss.17-20 pp.1804-1806.
 140. A.J. Lowery "Fiber nonlinearity pre- and post-compensation for long-haul optical links using OFDM" *Optics Express* (2007), Vol.15 Iss.20 pp.12965-12970.
 141. R.S. Luís, D. Fonseca, A.L.J. Teixeira and P. Monteiro "Dispersion Management of Electrically Precompensated RZ Single-Sideband Signals at 10 Gb/s Without Inline Dispersion Compensation" *IEEE Photonics Technology Letters* (2007), Vol.19 Iss.14.
 142. R.S. Luís, A. Teixeira and P. Monteiro "XPM degradation of dispersion-precompensated intensity modulation direct-detection systems without inline dispersion compensation" *IEEE Photonics Technology Letters* (2008), Vol.20 Iss.9-12 pp.736-738.

143. C. Weber and K. Petermann "Impact of fibre nonlinearities in electronic dispersion compensation systems at 40 Gb/s" in *Proc. of European Conference on Optical Communication* (2008) in Brussels, Vol.5 pp.151-152, P.4.10.
144. Y. Konishi, T. Sugihara and T. Mizuochi "A novel flip-flop based look-up table in digital signal processing for optical communications" in *Proc. of International Conference on Optical Internet* (2008) pp.1-2.
145. T. Sugihara and Ieee "Practical Implementation of Precoding Technologies in High-speed Optical Transmission" in *Proc. of 7th International Conference on the Optical Internet* (2008) in Tokyo, JAPAN pp.153-154.
146. D.J. Geisler, N.K. Fontaine, R.P. Scott, J.P. Heritage, K. Okamoto and S. Yoo "360 Gb/s data modulation with dispersion precompensation using optical arbitrary waveform generation" in *Proc. of Annual Meeting of the IEEE Lasers and Electro-Optics Society* (2008) pp.822-823.
147. D.J. Geisler, N.K. Fontaine, R.P. Scott, J.P. Heritage, K. Okamoto and S.J.B. Yoo "360-Gb/s Optical Transmitter With Arbitrary Modulation Format and Dispersion Precompensation" *IEEE Photonics Technology Letters* (2009), Vol.21 Iss.7 pp.489-491.
148. C. Weber, C.A. Bunge, M. Winter and K. Petermann "Fibre Nonlinearities in 10 and 40 Gb/s Electronically Dispersion Precompensated WDM Transmission" in *Proc. of Optical Fiber Communication and the National Fiber Optic Engineers Conference* (2009) in San Diego CA, OTuD2.
149. T. Sugihara, K. Goto, Y. Konishi and T. Mizuochi "Electronic Predistortion by Polar Coordinate Transformation Using the CORDIC Algorithm" *Journal of Lightwave Technology* (2009), Vol.27 Iss.16 pp.3607-3613.
150. M. Brodsky, N.J. Frigo and M. Tur "Polarization mode dispersion", in *Optical Fiber Telecommunications VA: Components and subsystems*, Editors: I.P. Kaminow, T. Li and A.E. Willner (2008), Burlington MA: Academic press pp. 605-669.
151. X. Liu and D.A. Fishman "A fast and reliable algorithm for electronic pre-equalization of SPM and chromatic dispersion" in *Proc. of Optical Fiber Communication and the National Fiber Optic Engineers Conference* (2006) in Anaheim CA, OThD4.
152. E. Ip and J.M. Kahn "Compensation of Dispersion and Nonlinear Impairments Using Digital Backpropagation" *Journal of Lightwave Technology* (2008), Vol.26 Iss.20 pp.3416-3425.
153. G. Goldfarb and G.F. Li "Chromatic dispersion compensation using digital IIR filtering with coherent detection" *IEEE Photonics Technology Letters* (2007), Vol.19 Iss.13-16 pp.969-971.
154. D. McGhan, M. O'Sullivan and Y. Beaulieu *Optical E-field modulation using a Mach-Zehnder Interferometer* (2005) Filed at United States.
155. S. Chandrasekhar, C.R. Doerr and L.L. Buhl "Demonstration of 100% precompensated DWDM transmission over 1280 km of SSMF with no inline

- dispersion compensation using interconnected recirculating loops" *IEEE Photonics Technology Letters* (2006), Vol.18 Iss.1-4 pp.256-258.
156. S.L. Jansen, I. Morita, D. van den Borne, G.D. Khoe, H. de Waardt and P.M. Krummrich "Experimental study of XPM in 10-Gb/s NRZ pre-compensated transmission systems" in *Proc. of Optical Fiber Communication and the National Fiber Optic Engineers Conference* (2007) in Anaheim CA pp.1-3.
 157. M.C. Jeruchim, P. Balaban and K.S. shanmugan *Simulation of Communication Systems* 2Rev edition Application of communication theory, ed.: R.W. Lucky (2000), New York, USA: Kluwer Academic / Plenum Publishers.
 158. I.P. Kaminow and T. Li *Optical Fiber Telecommunications IVB: System and impairments* 4th edition, ed.: I.P. Kaminow and T. Li (2002), San Diego, CA, USA: Academic Press.
 159. *ONG-Simulator* (2007), London: University College London Optical Networks Group.
 160. *Matlab & Simulink* (2009) TheMathworks Inc,.
 161. A.J. Lowery "Photonic Simulation Tools", in *Optical Fiber Telecommunications IVB: System and impairments*, Editors: I.P. Kaminow and T. Li (2002), San Diego CA: Academic Press.
 162. R. Waegemans *Advanced signal processing techniques for optical communications* (2007), London: University College London, Thesis for the degree of transfer from MPhil to PhD.
 163. *DS112 Virtex-4 Family Overview (v3.0)* (2007) Xilinx Inc.; Available from: www.xilinx.com.
 164. *UG070 Virtex-4 User Guide (v2.3)* (2007) Xilinx Inc.; Available from: www.xilinx.com.
 165. J. Edwards *No room for Second Place*, Electronics Design Strategy News, Electronic Business [cited Jul 2009]; Available from: <http://www.edn.com/article/CA6339519.html>.
 166. *CS90 Configurable Switch Array Family*, Cswitch Inc. [cited Jul 2009]; Available from: <http://www.cswitch.com/www/Products/devices.htm>.
 167. *Introducing Stratix IV GT FPGAs: The only FPGAs with Integrated 11.3-Gbps Transceivers*, Altera Corporation, [cited Jul 2009]; Available from: <http://www.altera.com/b/stratix-iv-gt-transceiver.html>.
 168. G. Knipper *System ACE Configuration Solution for Xilinx FPGAs* (2007) Xilinx Inc., Vol.WP151 (v3.0.1); Available from: www.xilinx.com.
 169. *DS080 System ACE CompactFlash Solution Advance Product Specification (v1.5)* (2002) Xilinx Inc. [cited Dec 2008]; Available from: www.xilinx.com.
 170. *VEGA Signal Convertors*, VEGA Signal Converters, MICRAM Microelectronics GmbH 2009; Available from: <http://www.micram.com/index.php/products/vega>.

171. S. Schmid *SD40-DP Customer Product Specification* (2008), Avanex Corporation.
172. *Details for LS-P140-KFKM*, Spectrum Elektrotechnik GmbH [cited Mar 2008]; Available from: www.spectrum-et.org.
173. *Thumb Wheel and Panel Mount Step Attenuators* (2008), Narda East [cited Mar 2008]; Available from: www.nardamicrowave.com.
174. *Datasheet SHF 810 Broadband Amplifier V002* (2007), SHF Communication Technologies AG. [cited Jul 2008]; Available from: www.shf.de.
175. *Agilent 81663A DFB Laser 8165xA Fabry-Perot Lasers Data Sheet* (2008), Agilent Technologies Inc.; Available from: www.agilent.com.
176. *Datasheet Tunable Optical Drop Unit Xtract* (2008), Anritsu Corporation; Available from: www.anritsu.com.
177. J. Uniphase *RX10 Receiver User's Manual* (2002), JDS Uniphase [cited Aug 2008]; Available from: www.jdsu.com.
178. J. Uniphase *MAP Multi-Rate Clock and Data Recovery Cassette User's Manual* (2003), JDS Uniphase [cited Aug 2008]; Available from: www.jdsu.com.
179. MP1764A Error Detector Operation Manual in Document No.: M-W0887Ae-16.0 (2002) Anritsu Corporation.
180. T.L. Floyd *Digital Fundamentals with VHDL* (2002), Upper Saddle River NJ: Prentice Hall.
181. J.F. Wakerly *Digital Design, Principles and Practices* 4th edition (2006), Upper Saddle River NJ: Prentice Hall.
182. R. Whatcott *Timing Closure 6.1i* (2008), Xilinx Inc.; Available from: www.xilinx.com.
183. R. Waegemans *Procedures for EPD transmitter* (2008), Backnang: Ericsson EPD project.
184. P.J. Winzer, C. Woodworth, F. Fidler, P.K. Reddy, H. Song and A. Adamiecki "Temporal alignment of high-speed transmit channels of FPGA" *Electronics Letters* (2008), Vol.44 Iss.2 pp.113-115.
185. *Std 1076/INT-1991 IEEE Standard Interpretations VHDL Language Reference Manual* (1991) Design Automation, Technical Committee of the IEEE Computer Society, Vol.1076/INT-1991.
186. *Std 1076-2002 Standard VHDL Language reference Manual* (2002) IEEE, Vol.1076-2002.
187. P.J. Ashenden *The designer's guide to vhdl* 2nd edition (2002), San Francisco CA: Morgan Kaufmann Publishers Inc.
188. K.L. Short *VHDL for engineers* (2009), Upper Saddle River NJ: Pearson Higher Education.

189. J. Lenge *Photoss Application Manual v4.5* (2008), Bergkamen: I.T. Systems.
190. J. Lenge *Photoss Component Manual v4.5* (2008), Bergkamen: I.T. Systems.
191. G.975.1 Forward Error correction for high bit rate DWDM submarine systems (2006), Geneva: International Telecommunication Union.
192. C. Maxfield *The Design Warrior's Guide to FPGAs* (2004), Burlington MA: Elsevier.
193. *Programmable Logic Design Quick Start Handbook* (2006) Xilinx Inc.; Available from: www.xilinx.com.
194. *ISE 9.2i Development System Reference Guide* (2007) Xilinx Inc.; Available from: www.xilinx.com.